Doctoral Dissertation

# Minimizing methods and related topics for twist maps and the $n$-body problem

Yuika Kajihara

Department of Applied Mathematics and Physics
Graduate School of Informatics
Kyoto University

Supervisor: Associate Professor Mitsuru Shibayama

# Contents

# Chapter 1

# Introduction

This thesis relates *dynamical systems* and *variational problems*. The field of dynamical systems, broadly speaking, studies time evolutions of systems formulated as differential equations or mappings. Henri Poincaré originated the field in the 1890s. Variational problems also have a long history, beginning with the brachistochrone curve problem presented by Johann Bernoulli in the 1690s. Classically speaking, the calculus of variations involves calculating differentiation in a functional space, and *minimizing methods* are a standard way to obtain critical points of a functional. For some ordinary or partial differential equations, there are functionals whose critical points correspond to their solutions. Variational problems can be formulated for symplectic mappings through Poincaré's lemma. Therefore we expect to obtain solutions of differential equations or orbits of mappings by finding critical points of the corresponding functionals.

Our purpose is to show the existence of topologically or geometrically characteristic solutions or orbits in chaotic dynamics by using minimizing methods and to study their properties. This thesis mainly deals with twist maps and the $n$-body problem, especially the restricted three-body problem, which is a special case of the three-body problem. *Twist maps* are a class of area-preserving maps on the annulus satisfying twist condition and *the $n$-body problem* is the problem of studying the individual behaviors of a group of particles interacting with each other gravitationally and represented by a system of ordinary differential equations. Both of them are parts of important subjects for dynamical systems and have variational structures.

Area-preserving maps are two-dimensional symplectic mappings and they contain a lot of significant maps, such as standard maps [4, 9] and billiard maps [34, 57]. In particular, twist maps have been studied vigorously [3, 29, 32]. Based on [5], Mather [35] considered a variational problem for twist maps to show the existence of periodic or quasi-periodic orbits, and his ideas led to Aubry-Mather theory, as seen later. By applying Mather's approach, Yu [66] recently have shown the existence of infinitely many heteroclinic and homoclinic orbits of twist maps between a pair of two periodic orbits called the neighboring, which implies chaotic dynamics.

In addition, it is well-known that the $n$-body problem, including the restricted three-body problem, is non-integrable when $n \geq 3$ [31, 47, 61]. Whereas, beginning with the figure-eight by Chenciner and Montgomery [18], a lot of periodic solutions of the full $n$-body problem have been shown to exist by using variational approaches [13, 15, 53]. The restricted three-body problem is also an important research area that deals with significant issues in celestial mechanics, such as analyzing asteroid movement behavior and orbit design for space probes. However, there are fewer studies on variational problems for the restricted three-body problem compared with the full $n$-body problem, because the corresponding action functional is more complicated [39].

What properties of dynamical systems does the existence of various periodic solutions indicate in the $n$-body problem? To consider this issue, we can define braids for periodic solutions in the $n$-body problem that are shown to exist by using minimizing methods. This study of braids is motivated by the fact that braid theory is closely associated with low-dimensional dynamical systems through mapping class groups [10]. Although the $n$-body problem is not a low-dimensional dynamical system, our viewpoint sheds some new light on the relationship between dynamical systems, variational analysis, and braid theory.

In the rest of this chapter, we first review several basic terminologies for dynamical systems and basic concepts of variational problems for ordinary differential equations including the $n$-body problem, and area-preserving maps through previous research. Additionally, we describe $n$-braids for periodic solutions of the planar $n$-body problem.

## 1.1 Variational structures for ordinary differential equations

For $t \in \mathbb{R}$ and $x \in \mathbb{R}^n$, we set

$$\dot{x} = F(t, x) \tag{1.1.1}$$

where $\dot{x} = dx/dt$ and $F\colon \mathbb{R} \times \mathbb{R}^n \to \mathbb{R}^n$ is a smooth vector field. There are three key types of time-global solutions for (1.1.1): *periodic, heteroclinic*, and *homoclinic solutions*.

**Definition 1.1.1** (periodic, heteroclinic, and homoclinic solutions)**.** *Let $x = x(t)$ be a solution of* (1.1.1)*. Then*

*(i) For $T > 0$, $x(t)$ is said to be $T$-periodic if $x(t) = x(t+T)$ for all $t \in \mathbb{R}$. Moreover, if a constant vector $e$ satisfies $F(t, e) = 0$ for all $t \in \mathbb{R}$, then we call $e$ an equilibrium point. If $e$ is an equilibrium point, then $x(t) \equiv e$ is called a stationary solution.*

*(ii) The solution $x(t)$ is said to be heteroclinic if there are two distinct equilibrium points $e_1$ and $e_2$ with $x(t) \not\equiv e_i$ $(i = 1, 2)$ such that $|x(t) - e_1| \to 0$ as $t \to -\infty$ and $|x(t) - e_2| \to 0$ as $t \to \infty$.*

*(iii) The solution $x$ is said to be homoclinic if there is an equilibrium point $e$ with $x(t) \not\equiv e$ such that $|x(t) - e| \to 0$ as $|t| \to \infty$.*

What kinds of solutions appear in ordinary differential equations? This question is extremely difficult to answer in general. However, we can often obtain a time-global solution with interesting geometric or topological behaviors by replacing the original system with a *variational problem*.

We say '(1.1.1) has a variational structure' when there is a functional $\mathcal{A}\colon X \to \mathbb{R}$ such that if $x \in X$ satisfies $\mathcal{A}'(x) = 0$, then $x$ is a weak solution of (1.1.1). Here, $X$

is a functional space. A typical example is a potential system, which has a function $V\colon \mathbb{R} \times \mathbb{R}^n \to \mathbb{R}$ such that:

$$\ddot{x} = \frac{\partial V}{\partial x}(t, x). \tag{1.1.2}$$

We set $W^{1,2}([a, b]) := \{x\colon [a, b] \to \mathbb{R}^n \mid \|x\|^2_{W^{1,2}} < \infty\}$, where $a < b$ and:

$$\|x\|^2_{W^{1,2}([a,b])} = \int_a^b (|\dot{x}|^2 + |x|^2)dt.$$

A function $L\colon \mathbb{R}^n \times \mathbb{R}^n \to \mathbb{R}$ is given by:

$$L(x, \dot{x}) := \frac{1}{2}|\dot{x}|^2 + V(t, x).$$

For the described system, consider a functional $\mathcal{A}\colon W^{1,2}([a, b]) \to \mathbb{R}$ given by:

$$\mathcal{A}_{[a,b]}(x) = \int_a^b L(x, \dot{x})dt. \tag{1.1.3}$$

For simplicity, suppose that $V$ is smooth and $n = 1$. To obtain a periodic solution, we consider when both $t$ and $x$ are 1-periodic. We set:

$$X := W^{1,2}(\mathbb{T}^1) = \{x\colon \mathbb{T}^1 \to \mathbb{R} \mid \|x\|_{W^{1,2}(\mathbb{T}^1)} < \infty\},$$

and

$$\mathcal{A}(x) := \mathcal{A}_{\mathbb{T}^1}(x).$$

Note that if $x \in X$, then $x$ is continuous. It is well-known that $x$ satisfying $\mathcal{A}'(x) = 0$ is a weak solution of (1.1.2), and also a classical solution if $V$ is smooth. Thus, the problem of finding a solution of (1.1.2) is replaced by the problem of finding a critical point of (1.1.3).

What kinds of critical points does the functional have? The standard approach is to find a minimum point of (1.1.3). Such methods are called *minimizing methods* or *direct methods*. If we obtain $x^*$ satisfying:

$$\mathcal{A}(x^*) = \inf_{x \in X} \mathcal{A}(x), \tag{1.1.4}$$

then it is a periodic solution of (1.1.2). (Note that the existence of $x^*$ is guaranteed in the weak closure $\bar{X}$ of $X$ in general.)

Now we consider heteroclinic and homoclinic solutions. Given two equilibrium points $e_1$ and $e_2$, let a functional $\mathcal{A}_\infty$ and a set $Y_1$ be defined by:

$$\mathcal{A}_\infty(x) = \int_{-\infty}^{\infty} \frac{1}{2}|\dot{x}|^2 + V(t, x)dt \tag{1.1.5}$$

and

$$Y_1 = \{x \in X_{\mathrm{loc}} \mid \|x - e_1\|_{L^2[i,i+1]} \to 0 \ (i \to -\infty),\ \|x - e_2\|_{L^2[i,i+1]} \to 0 \ (i \to \infty)\}, \tag{1.1.6}$$

where $X_{\text{loc}} = W^{1,2}_{\text{loc}}(\mathbb{R}, \mathbb{R})$. That is, $x \in X_{\text{loc}}$ implies $\|x\|_{W^{1,2}([a,b])} < \infty$ for any $a, b$ with $a < b$. Since the value of $\inf_{x \in Y} \mathcal{A}_\infty(x)$ can always be infinity, we need to normalize (1.1.5). We redefine $\mathcal{A}_\infty$ as:

$$\mathcal{A}_\infty(x) = \sum_{i \in \mathbb{Z}} a_i(x), \tag{1.1.7}$$

where:

$$a_i(x) = \int_{-\infty}^{\infty} \frac{1}{2}|\dot{x}|^2 + V(t, x)dt - c$$

and $c$ is a constant determined from the choice of $Y_1$. Since a minimizer converges to $e_1$ or $e_2$ if $a_i \geq 0$ for all $i \in \mathbb{Z}$, we can expect that $x$ that gives the minimum of the functional $\mathcal{A}_\infty$ is a heteroclinic solution if $x \in Y_1$. To obtain a homoclinic solution, we set:

$$Y_2 = \{x \in X_{\text{loc}} \mid \|x - e_1\|_{L^2[i,i+1]} \to 0 \ (|i| \to \infty)\}. \tag{1.1.8}$$

Note that this setting is not appropriate where $e_1 \in Y_2$ and can be a minimizer of (1.1.7). Therefore we need to assume some technical constraints on $Y_2$. However, adding constraints makes it more difficult to show that a minimizer is in $Y_2$, not in $\bar{Y_2} \backslash Y_2$. We omit the detailed argument here. The above discussion is based on [49].

Although we considered a potential system, a similar approach is valid for partial differential equations (e.g. see [50]). To delve deeper into the calculus of variations for multivariable functions, we recommend [25]. Furthermore, there are approaches other than minimizing methods to find critical points. For a well-known example, see [48] for a minimax method.

## 1.2 Variational structures for area-preserving maps

Let $f \colon \mathbb{R}^n \to \mathbb{R}^n$ be a smooth function and $f^{-1}$ be its inverse. Taking $x_0 \in \mathbb{R}^n$, we set $x = (x_i)_{i \in \mathbb{Z}}$ by $x_i = f^i(x_0)$ and call it an *orbit*. For a given orbit $x$, we define periodic, heteroclinic, and homoclinic orbits, relating to Definition 1.1.1.

**Definition 1.2.1** (periodic, heteroclinic, and homoclinic orbits)**.**

*(i) The orbit $x$ is said to be periodic if there is $m \in \mathbb{N}$ such that $x_{i+m} = x_i$ for all $i \in \mathbb{Z}$. Moreover if $x_0 = f(x_0)$, then we call $x_0$ a fixed point.*

*(ii) The orbit $x$ is said to be heteroclinic if there are two distinct fixed points $e_1$ and $e_2$, such that $x_i \neq e_j$ for all $i \in \mathbb{Z}$ and $j = 1, 2$, with $|x_i - e_1| \to 0$ as $i \to -\infty$ and $|x_i - e_2| \to 0$ as $i \to \infty$.*

*(iii) The orbit $x$ is said to be homoclinic if there is a fixed point $e$ such that $x_i \neq e$ for all $i \in \mathbb{Z}$ and $|x_i - e| \to 0$ as $|i| \to \infty$.*

Generally, we do not know whether (1.1.1) has a variational structure except in trivial cases such as potential systems. On the other hand, Poincare's lemma in the following shows what maps have a variational structure.

**Lemma 1.2.2** (Poincaré)**.** *If a $k$-form $\omega$ satisfies $d\omega = 0$ on a simply connected domain in $\mathbb{R}^n$, then for $1 \leq k \leq n$, there exists a $k-1$-form $\eta$ such that $\omega = d\eta$.*

We check the variational structure of area-preserving maps through Lemma 1.2.2. A map $f\colon \mathbb{R}^2 \to \mathbb{R}^2$ $((x,y) \mapsto (X,Y))$ is said to be *area-preserving* if $f$ satisfies:

$$dx \wedge dy = dX \wedge dY. \tag{1.2.1}$$

Assume $f \in C^1$ and is area-preserving. By simple calculation, (1.2.1) becomes:

$$d(YdX - ydx) = 0.$$

By Lemma 1.2.2, there is a function $h = h(x,X)$ satisfying:

$$dh = YdX - ydx.$$

For the above $h$, we define a function $H$ by:

$$H(x_j, \ldots, x_k) := \sum_{i=j}^{k-1} h(x_i, x_{i+1}) \tag{1.2.2}$$

Although the critical points of $H$ are not the orbits of $f$, the following discussion implies that if $f$ satisfies a twist condition, i.e., $\partial X/\partial y > 0$, then $f$ has a variational structure and $H$ is the corresponding function such as (1.1.3).

Let $x = (x_j, \ldots, x_k)$ be a critical point of (4.2.6). Clearly, $x$ satisfies:

$$\partial_2 h(x_{i-1}, x_i) + \partial_1 h(x_i, x_{i+1}) = 0,$$

where $\partial_1 = \partial/\partial x$ and $\partial_2 = \partial/\partial X$. We will show that $(x_i, y_i)$ $(i = 1, \cdots, n)$ is an orbit of $f$, where:

$$y_i = -\partial_1 h(x_i, x_{i+1}). \tag{1.2.3}$$

If $h$ is well-defined, then we obtain:

$$f(x_i, y_i) = f(x_i, -\partial_1 h(x_i, x_{i+1})) = (x_{i+1}, \partial_2 h(x_i, x_{i+1})) = (x_{i+1}, -\partial_1 h(x_{i+1}, x_{i+2})),$$

and $(x_i, y_i)_{i=1}^n$ is an orbit. Since $f \in C^1$, there is an inverse map and $y$ can be regarded as a map of $(x, X)$. The twist condition implies:

$$\frac{\partial y_i}{\partial X} = -\partial_2 \partial_1 h(x_i, x_{i+1}) > 0,$$

so $y_i$ is monotone and is not a multivalued function. Moreover, $y_i$ does not diverge because $h$ is of class $C^2$.

As in (1.1.7), we define the normalized function $H_\infty$ on $\mathbb{R}^{\mathbb{Z}}$ by:

$$H_\infty(x) = \sum_{i \in \mathbb{Z}} h(x_i, x_{i+1}) - c. \tag{1.2.4}$$

**Remark 1.2.3.** *For a $2n$-dimensional mapping $f\colon \mathbb{R}^{2n} \to \mathbb{R}^{2n}((x_1, y_1, \cdots, x_n, y_n) \mapsto (X_1, Y_1, \cdots, X_n, Y_n))$, (1.2.1) is replaced by a symplectic form, i.e.,*

$$\sum_{i=1}^n dx_i \wedge dy_i = \sum_{i=1}^n dX_i \wedge dY_i.$$

The above arguments relate to the Aubry-Mather theory, which was originated by [5] and further developed by Mather [36–38]. Whereas we discussed periodic solutions in a potential system, Mather [35] showed the existence of periodic or quasi-periodic orbits on twist maps. Moreover, Bangert [6] obtained good conditions of $h$ so that *minimal sets* contain interesting configurations. We provide further detail in Chapter 2.

## 1.3 Variational problems for the $n$-body problem

In this section, we introduce the $n$-body problem, which we will focus on in Chapters 3 and 4. The $n$-body problem, which is a potential system with singularities, is defined by:

$$m_i \ddot{\boldsymbol{q}}_i = -\sum_{j \neq i} \frac{m_i m_j}{|\boldsymbol{q}_i - \boldsymbol{q}_j|^3} (\boldsymbol{q}_i - \boldsymbol{q}_j) \ (i = 1, \cdots, n, \ \boldsymbol{q} \in \mathbb{R}^d), \tag{1.3.1}$$

and the corresponding potential $V$ is given by:

$$V(\boldsymbol{q}_1, \cdots, \boldsymbol{q}_n) = \sum_{i \neq j} \frac{m_i}{|\boldsymbol{q}_i - \boldsymbol{q}_j|} \ (\boldsymbol{q} \in \mathbb{R}^d). \tag{1.3.2}$$

It is well-known that (1.3.1) is integrable when $n = 2$ and non-integrable when $n \geq 3$. However, many works are proving periodic solutions of the $n$-body problem in the case of $n \geq 3$ by minimizing methods. Readers can see various figures of numerical periodic solutions of the $n$-body problem in [55].

Let an action functional $\mathcal{A}_T$ be given by:

$$\mathcal{A}_T(\boldsymbol{q}) = \int_0^T \sum_{i=1}^n \frac{m_i}{2} |\dot{\boldsymbol{q}}|^2 + \sum_{i<j} \frac{m_i m_j}{|\boldsymbol{q}_i - \boldsymbol{q}_j|} dt.$$

By considering the variational problem for (1.3.1), we can show the existence of periodic solutions. However, our proof differs from the method in Section 1.1 because (1.3.2) has singular points $\boldsymbol{q}_i = \boldsymbol{q}_j$.

We set:

$$\begin{aligned} \mathcal{X} &= \{\boldsymbol{q} = (\boldsymbol{q}_1, \cdots, \boldsymbol{q}_n) \in (\mathbb{R}^d)^n\}, \\ \Delta_{ij} &= \{\boldsymbol{q} \in \mathcal{X} \mid \boldsymbol{q}_i = \boldsymbol{q}_j\}, \\ \Delta &= \bigcup_{i<j} \Delta_{ij} \end{aligned}$$

and, by abuse of notation, can then define:

$$X = \{\boldsymbol{q} \colon [0,1] \to \mathcal{X} \mid \|\boldsymbol{q}\|_{W^{1,2}([0,1])} < \infty\}.$$

To prove that a minimizer is smooth, it suffices to show that it is not in $\Delta$, i.e., it has no collision. We explain the steps of the proof for showing periodic solutions as follows:

**Step 1** Impose some ‘good’ constraints or boundary conditions on $X$.

**Step 2** Show the existence of minimizers in the above set $X$.

**Step 3** Show that a minimizer is not a trivial solution.

**Step 4** Show that a minimizer has no collision.

Steps 1 and 4 are difficult. Although we show periodic solutions, we do not impose a periodic boundary condition in Step 1. As an example to demonstrate why not, we introduce the figure-eight.

**Example 1.3.1** (The figure-eight, [18])**.** *The figure-eight solution is periodic in the planar three-body problem with equal masses. Its existence was proved by Chenciner and Montgomery. The proof is based on minimizing methods. They used isosceles triangles and a linear configuration as the boundary conditions, as shown in Figure 1.1.*

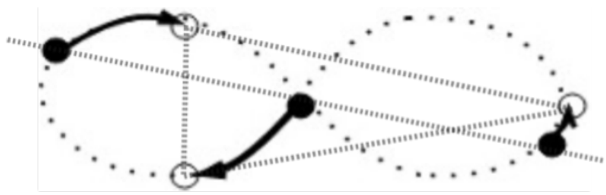

Figure 1.1: The figure-eight and its boundary conditions

In Step 4, we introduce two standard methods: *level estimate* and *local estimate.*

- Level estimate: Set
$$X_{\mathrm{col}} = \{\boldsymbol{q} \in X \mid \boldsymbol{q}(s) \in \Delta \text{ for some } s \in [0,1]\}.$$
We first estimate a constant $C$ so that the value of $\inf_{\boldsymbol{q}\in X_{\mathrm{col}}} \mathcal{A}_T(\boldsymbol{q})$ is bounded below. Next we construct a test path $\boldsymbol{q}_{\mathrm{test}} \in X$ satisfying $\mathcal{A}_T(\boldsymbol{q}_{\mathrm{test}}) \leq C$. Then we obtain:
$$\inf_{\boldsymbol{q}\in X_{\mathrm{col}}} \mathcal{A}_T(\boldsymbol{q}) > C \geq \mathcal{A}_T(\boldsymbol{q}_{\mathrm{test}}) \geq \inf_{\boldsymbol{q}\in X} \mathcal{A}_T(\boldsymbol{q})$$
and a minimizer has no collision. This method of proof is called a level estimate (or global estimate).
- Local estimate: Suppose that $\boldsymbol{q}_{\mathrm{col}}$ collides at $t = 0$. We first analyze the behavior of $\boldsymbol{q}_{\mathrm{col}}$ on $t \in [0, \varepsilon]$ for sufficiently small $\varepsilon > 0$ by using the blow-up technique. Moreover, taking another path $\boldsymbol{q}([0,\varepsilon])$ with $\boldsymbol{q}(\varepsilon) = \boldsymbol{q}_{\mathrm{col}}(\varepsilon)$, we show $\mathcal{A}_\varepsilon(\boldsymbol{q}) < \mathcal{A}_\varepsilon(\boldsymbol{q}_{\mathrm{col}})$. This approach is called a local estimate.

The existence of the figure-eight is shown by the level estimate. For other results using a level estimate, we refer to [11, 12]. Moreover, [53, 65] used a local estimate to show periodic solutions. Other methods to prove no collision include the averaging method [33] and rotating circle property [21], which we do not delve into in this thesis.

## 1.4 Braids and braid types of periodic solutions in the planar $n$-body problem

The figure-eight was first found by Moore, using numerical calculation. In [45], Moore classified numerical periodic solutions of the planar $n$-body problem with $n$-braids. In broad strokes, an $n$-braid is the suspension of an $n$-point set. The corresponding braid for a $T$-periodic solution, such as $(x(t), y(t))$, is determined by plotting $(x(t), y(t), t)$ in $t \in [0, T]$. Figure 1.2 (the same as Figure 5.7) illustrates the corresponding braid for the figure-eight in $t \in [0, T/3]$.

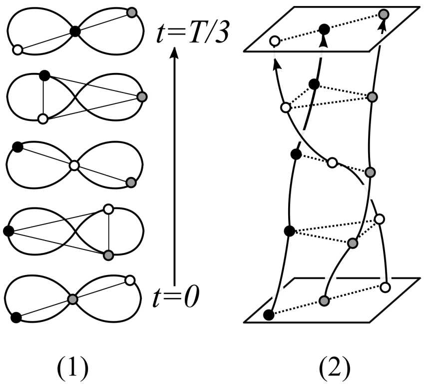


Figure 1.2: A figure-eight and its corresponding braid

However, because the corresponding braid can be changed if we see it from another direction, braids seem unsuitable for periodic orbits. For example, the braid in Figure 1.2 is different from the one made by turning it over. Therefore, we need to give some kind of equivalence classes. We consider using braid types as the equivalence class. We state precise definitions of braids and braid types in Chapter 5.

## 1.5 Outline of the thesis

This thesis is divided into two main parts. Chapters 2-4 deal with minimizing methods and Chapter 5 examines braid types for periodic solutions obtained by minimizing methods. More specifically, Chapter 2 consider twist maps and provides the variational structure for infinite transition orbits, which alternately passes the neighboring of two periodic or fixed points an infinite times. Chapter 3 and 4 are related to variational problems for the restricted three-body problem. In Chapter 3, we show the existence of several periodic solutions of the planar circular restricted three-body problem with the blow-up technique and a local estimate. Chapter 4 is devoted to the study of the special case. In the first half of this chapter, we use our methods in Chapter 3 to deal with the spacial Hill problem. The second half provides the existence proof of brake orbits in the two-center problem by using a level estimate. In Chapter 5, we study braid types for a family of periodic solutions in the planar $2n$-body problem and calculate the corresponding stretch factors with covering spaces.

# Chapter 2

# Infinite transition orbits for twist maps

## 2.1 Introduction

In this chapter, we consider chaotic dynamics and variational structures of area-preserving maps. The dynamics of such maps have been widely studied, with key findings by Poincaré and Birkhoff. To explore these variational structures, we define a special class of area-preserving maps called *monotone twist maps*:

**Definition 2.1.1** (monotone twist maps)**.** *Set a map $f\colon \mathbb{T}\times\mathbb{R}\to\mathbb{T}\times\mathbb{R}$ and assume that $f\in C^1$ and a lift $\tilde{f}$ of $f$ : $\mathbb{R}\times\mathbb{R}\to\mathbb{R}\times\mathbb{R}$, $(x,y)\mapsto(X,Y)$ satisfy the followings:*

*($f_1$) $\tilde{f}$ is area-preserving, i.e., $dx\wedge dy = dX\wedge dY$, and*

*($f_2$) $\partial X/\partial y > 0$ (twist condition)*

*Then $f$ is said to be a monotone twist map.*

By Poincaré's lemma, we get a generating function $h$ for a monotone twist map $f$ and it satisfies $dh = YdX - ydx$. That is,

$$y = \partial_1 h(x,X),\ Y = -\partial_2 h(x,X).$$

For the above $h$, by abuse of notation, we define $h\colon \mathbb{R}^{n+1}\to\mathbb{R}$ by

$$h(x_0,x_1,\cdots,x_n) = \sum_{i=1}^{n} h(x_i,x_{i+1}) \tag{2.1.1}$$

We can regard $h$ as a variational structure associated with $f$, because any critical point of (2.1.1), say $(x_0,\cdots,x_n)$, gives us an orbit of $\tilde{f}$ by $y_i = -\partial h_1(x_i,x_{i+1}) = \partial h_2(x_{i-1},x_i)$. This is known as the Aubry-Mather theory, which is so called because Aubry studied critical points of the action $h$ in [5] and Mather developed the idea (e.g. [35, 37]). We briefly summarize Bangert's investigation of good conditions of $h$ for study in minimal sets [6].

We consider the space of bi-finite sequences of real numbers and define convergence of a sequence $x^n \in \mathbb{R}^{\mathbb{Z}}$ to $x \in \mathbb{R}^{\mathbb{Z}}$ by

$$\lim_{n\to\infty} |x_i^n - x_i| = 0 \ ({}^{\forall} i \in \mathbb{Z}). \tag{2.1.2}$$

Assume that a Lipschitz continuous map $h\colon \mathbb{R}^2 \to \mathbb{R}$ satisfies $(h_1)$-$(h_4)$, where they are given by the followings:

$(h_1)$ For all $(\xi,\eta) \in \mathbb{R}^2$, $h(\xi,\eta) = h(\xi+1,\eta+1)$;

$(h_2)$ $\lim_{\eta\to\infty} h(\xi,\xi+\eta) \rightrightarrows \infty$;

$(h_3)$ If $\underline{\xi} < \bar{\xi}$ and $\underline{\eta} < \bar{\eta}$, then $h(\underline{\xi},\underline{\eta}) + h(\bar{\xi},\bar{\eta}) < h(\underline{\xi},\bar{\eta}) + h(\bar{\xi},\underline{\eta})$; and

$(h_4)$ If $(x,x_0,x_1)$ and $(\xi,x_0,\xi_1)$ are minimal and $(x,x_0,x_1) \neq (\xi,x_0,\xi_1)$, then $(x-\xi)(x_1-\xi_1) < 0$.

**Definition 2.1.2** (minimal configuration/stationary configuration). *A finite configuration $x = (x_i)_{n\le i\le m}$ is said to be minimal if, for any finite configuration $\{y_i\}_{i=n_0}^{n_1}$ with $y_{n_0} = x_{n_0}$ and $y_{n_1} = x_{n_1}$,*

$$h(x_{n_0}, x_{n_0+1}, \cdots, x_{n_1-1}, x_{n_1}) \le h(y_{n_0}, y_{n_0+1}, \cdots, y_{n_1-1}, y_{n_1}),$$

*where $n \le n_0 < n_1 \le m$. An infinite configuration $x = (x_i)_{i\in\mathbb{Z}}$ is called minimal if, for any $n < m$, we have $x = (x_i)_{i=n}^m$ is minimal. Moreover, a configuration $x$ is called locally minimal or a stationary configuration if for any $i \in \mathbb{Z}$, it holds that $\partial_2 h(x_{i-1},x_i) + \partial_1 h(x_i,x_{i+1}) = 0$.*

For $x = (x_i) \in \mathbb{R}^{\mathbb{Z}}$, we define

$$\alpha^+(x) := \lim_{i\to\infty} \frac{x_i}{i},\ \alpha^-(x) := \lim_{i\to-\infty} \frac{x_i}{i}.$$

**Definition 2.1.3** (rotation number). *If both $\alpha^+(x)$ and $\alpha^-(x)$ exist and $\alpha^+(x) = \alpha^-(x)(=: \alpha(x))$, then we call $\alpha(x)$ a rotation number of $x$.*

Let $\mathcal{M}_\alpha$ be a minimal set consisting of minimal configurations with rotation number $\alpha$. It is known that for any $\alpha \in \mathbb{R}$, the set $\mathcal{M}_\alpha$ is non-empty and compact (see [6] for the proof).

**Definition 2.1.4** (periodic orbits). *A configuration $x = (x_i)$ is said to be $(q,p)$-periodic if $x = (x_i) \in \mathbb{R}^{\mathbb{Z}}$ satisfies*

$$T_{p,q} x_i = x_{p+i} + q,$$

*for any $i \in \mathbb{Z}$.*

It is easily seen that if $x$ is $(q,p)$-periodic, then its rotation number is $p/q$. This chapter discusses the case where $\alpha \in \mathbb{Q}$. For $\alpha = p/q \in \mathbb{Q}$, we set

$$\mathcal{M}_\alpha^{\text{per}} := \{x \in \mathcal{M}_\alpha \mid x \text{ is } T_{(p,q)}\text{-periodic}\} \cap \mathcal{M}_\alpha.$$

**Definition 2.1.5** (neighboring)**.** *A pair of $(p,q)$-periodic minimal configurations $x^0, x^1$ with $x^0 \neq x^1$ is called neighboring if there is no other $x \in \mathcal{M}_\alpha^{\mathrm{per}}$ with $x^0 < x < x^1$*

Given a neighboring pair $(x^0, x^1)$, we define:

$\mathcal{M}_\alpha^+(x^0, x^1) = \{x \in \mathcal{M}_\alpha \mid |x_i - x^0| \to 0\ (i \to -\infty)\ \textit{and}\ |x_i - x^1| \to 0\ (i \to \infty)\}$ *and*
$\mathcal{M}_\alpha^-(x^0, x^1) = \{x \in \mathcal{M}_\alpha \mid |x_i - x^0| \to 0\ (i \to \infty)\ \textit{and}\ |x_i - x^1| \to 0\ (i \to -\infty)\}$.

Bangert [6] showed the following proposition.

**Proposition 2.1.6.** *Given $\alpha \in \mathbb{Q}$, if $\mathcal{M}_\alpha$ has a neighboring pair $(x^0, x^1)$, then $\mathcal{M}_\alpha^{\mathrm{per}}, \mathcal{M}_\alpha^+$ and $\mathcal{M}_\alpha^-$ are nonempty.*

Although we have discussed minimal configuration in the preceding paragraph, there are also interesting works that treat non-minimal orbits between periodic orbits, particularly, [49] and [66]. In [49], Rabinowitz used minimizing methods to prove the existence of three types of solutions-periodic, heteroclinic and homoclinic-in potential systems with reversibility for time, i.e. $V(t,x) = V(-t,x)$. Under an assumption called *gaps*, which is similar to neighboring, for periodic and heteroclinic solutions, each non-minimal heteroclinic and homoclinic orbit can be given as *$n$-transition orbits* ($n \geq 2$) between two periodic orbits.

**Definition 2.1.7** ($n$-transition orbits)**.** *An orbit is called an $n$ transition orbit if it passes between two periodic orbits, say $u^0$ and $u^1$, and alternately through a neighborhood of them, where 'n' means the number of times it changes from a neighborhood of $u^0$ to a neighborhood of $u^1$. When $n$ is odd, these are heteroclinic orbits; when $n$ is even, these are homoclinic orbits.*

**Remark 2.1.8.** *The existence of $1$-transition orbits ( i.e., minimal heteroclinic orbits) does not require gaps for heteroclinic orbits. We can see this by considering a simple pendulum system.*

Rabinowitz's approach can be applied to variational methods for area-preserving maps. Yu [66] added $h$ to the following assumption $(h_5) - (h_6)$ to $h$:

$(h_5)$ There exists a positive continuous function $p$ on $\mathbb{R}^2$ such that:

$$h(\xi, \eta') + h(\eta, \xi') - h(\xi, \xi') - h(\eta, \eta') > \int_\xi^\eta \int_{\xi'}^{\eta'} p$$

if $\xi < \eta$ and $\xi' < \eta'$.

$(h_6)$ There is a $\theta > 0$ satisfying the following conditions:

- $\xi \mapsto \theta\xi^2/2 - h(\xi, \xi')$ is convex for any $\xi'$, and
- $\xi \mapsto \theta\xi'^2/2 - h(\xi, \xi')$ is convex for any $\xi$.

**Remark 2.1.9.** *One of a sufficient conditions for $(h_2) - (h_5)$ is*

$$(\tilde{h})\ \partial_1\partial_2 h \leq -\delta < 0 \textit{ for some } \delta > 0.$$

*by taking a constant function $\rho = \delta$ as a positive function. If $f$ satisfies $\partial X/\partial y \geq \delta$ for some $\delta > 0$, a generating function $h$ for $f$ satisfies $(\tilde{h})$. However, $(\tilde{h})$ is not a necessary condition for satisfying $(h_2) - (h_5)$.*

Clearly, $(h_5)$ implies $(h_3)$. Mather [37] proved that if $h$ satisfies $(h_1)$-$(h_6)$, then $\partial_2 h(x_{i-1}, x_i)$ and $\partial_1 h(x_i, x_{i+1})$ exist in the meaning of the left-hand-side limit. In addition, he proved that if $x$ is a locally minimal configuration, then it satisfies:

$$\partial_2 h(x_{i-1}, x_i) + \partial_1 h(x_i, x_{i+1}) = 0.$$

Yu applied Rabinowitz's methods to twist maps to show finite transition orbits of monotone twist maps for all $\alpha \in \mathbb{Q}$. We will give a brief summary of his idea in the case of $\alpha = 0$ (i.e. $(p, q) = (1, 0)$ in Definition 2.1.4). Let $(u^0, u^1)$ be a neighboring pair with $\alpha = 0$. By abuse of notation, we then denote $u^j$ by the constant configuration $\{x_i = u^j\}_{i\in\mathbb{Z}}$. We set

$$c := \min_{x\in\mathbb{R}} h(x, x) (= h(u^0, u^0) = h(u^1, u^1)).$$

And:

$$I(x) = \sum_{i\in\mathbb{Z}} a_i(x), \tag{2.1.3}$$

where $a_i(x) = h(x_i, x_{i+1}) - c$.

Yu studied local minimizers of $I$ to show the existence of finite transition orbits. Given a rational number $\alpha \in \mathbb{Q}$ and a neighboring pair with $(x^0, x^1)$, we let:

$$I_\alpha^+(x^0, x^1) = \{x_0 \in \mathbb{R} \mid x \in \mathcal{M}_\alpha^+(u^0, u^1)\} \text{ and}$$
$$I_\alpha^-(x^0, x^1) = \{x_0 \in \mathbb{R} \mid x \in \mathcal{M}_\alpha^-(u^0, u^1)\}.$$

Under the above setting, he showed the following theorem.

**Theorem 2.1.10** (Theorem 1.7, [66])**.** *Given a rational number $\alpha \in \mathbb{Q}$, if*

$$I_\alpha^+(x^0, x^1) \neq (x_0^0, x_0^1) \text{ and } I_\alpha^-(x^0, x^1) \neq (x_0^0, x_0^1),$$

*then there exist infinite number of $2k$-transition heteroclinic orbits and $2k + 1$-transition homoclinic orbits which passes through the neighborhood of $x^0$ and $x^1$ alternately.*

Furthermore, [49] proved the existence of an infinite transition orbit as a limit of sequences of finite transition orbits. However, the variational structure of infinite transition orbits is an open question. To consider the question for twist maps, the following proposition is essential.

**Proposition 2.1.11** (Proposition 2.2, [66])**.** *If $I(x) < \infty$, then $|x_i - u^1| \to 0$ or $|x_i - u^0| \to 0$ as $|i| \to \infty$.*

Since this implies that $I(x) = \infty$ if $x$ is an infinite transition orbit, we need to fix the normalization of $I$. Therefore, we focus on giving the variational structure of infinite transition orbits of twist maps and discuss the conditions of $h$. Roughly speaking, our main theorem and the steps of the proof imply the following theorem.

**Theorem 2.1.12.** *The function $J$ defined in Section 2.3.1 gives us the variational structure of infinite transition orbits.*

This chapter is organized as follows. Section 2.2 deals with some results in [66] and remarks. In Section 2.3, our main results are stated and proved in the case of $\alpha = 0$.

## 2.2 Preliminary

In this section, we would like to introduce properties of (2.1.3) and minimal configurations using several useful results in [66]. Moreover, we study estimates of heteroclinic configurations.

### 2.2.1 Properties of minimal configurations

Let $(u^0, u^1)$ be a neighboring pair of $\mathcal{M}_0^{\mathrm{per}}$ and:

$$\begin{aligned} X = X(u^0, u^1) &= \{x = (x_i)_{i\in\mathbb{Z}} \mid u^0 \le x_i \le u^1 \ ({}^\forall i \in \mathbb{Z})\}, \\ X(n) = X(n; u^0, u^1) &= \{x = (x_i)_{i=0}^n \mid u^0 \le x_i \le u^1 \ ({}^\forall i \in \{0, \cdots, n\})\}, \mathit{and} \\ \hat{X}(n) = \hat{X}(n; u^0, u^1) &= \{x = (x_i)_{i=0}^n \mid x_0 = x_n,\ u^0 \le x_i \le u^1 \ ({}^\forall i \in \{0, \cdots, n\})\}. \end{aligned} \tag{2.2.1}$$

**Definition 2.2.1** ( [66])**.** *For $x \in X$, we set:*

$$d(x) := \max_{0 \le i \le n} \min_{j \in \{0,1\}} |x_i - u^j|.$$

*For any $\delta > 0$, let $C$ be a Lipschitz constant of $h$ and :*

$$\phi(\delta) := \inf_{n \in \mathbb{Z}^+} \inf \left\{ \sum_{i=0}^{n-1} a_i(x) \mid x \in \hat{X}(n) \text{ and } d(x) \ge \delta \right\}.$$

**Remark 2.2.2.** *(1)We can replace Lipschitz continuity with local Lipschitz continuity on $[u^0, u^1] \times [u^0, u^1]$. (2)The function $\phi(\delta)$ is positive for any $\delta > 0$ and $\phi(0) = 0$.*

**Lemma 2.2.3** (Lemma 2.7 and 2.8, [66])**.** *For any $n \in \mathbb{N}$ and $x \in \hat{X}(n)$ satisfying $\min |x_i - u^j| \ge \delta$,*

$$\sum_{i=0}^{n-1} a_i(x) \ge n\phi(\delta)$$

*and for any $n \in \mathbb{N}$ and $x \in X(n)$,*

$$\sum_{i=0}^{n-1} a_i(x) \ge -C|x_n - x_0|.$$

*Proof.* See [66]. This proof requires $(h_3)$. □

**Lemma 2.2.4** (Lemma 2.9, [66])**.** *If $x \in X$ satisfies $|x_i - u^0|$ as $|i| \to \infty$ and $x_i \ne u^0$ for some $i \in Z$, then $I(x) > 0$.*

We also need to check that each component of stationary configurations is not equal to $u^0$ or $u^1$. This follows from the next lemmas.

**Lemma 2.2.5** (Lemma 2.11, [66])**.** *For any $\delta \in (0, u^1 - u^0]$, if $(x_i)_{i=0}^2$ satisfies*

*(i) $x_i \in [u^0, u^1]$ for all $i = 0, 1, 2$;*

*(ii) $x_1 \in [u^1 - \delta, u^1]$, and $x_0 \ne u^1$ or $x_2 \ne u^1$; and*

*(iii)* $h(x_0, x_1, x_2) \leq h(x_0, \xi, x_2)$ *for all* $\xi \in [u^1 - \delta, u^1]$,

*then* $x_1 \neq u^1$. *This still holds if we replace every* $u^1$ *by* $u^0$ *and every* $[u^1 - \delta, u^1]$ *by* $[u^0, u^0 + \delta]$.

**Lemma 2.2.6** (Lemma 2.12, [66]). *If a finite configuration* $x = (x_i)_{i=n_0}^{n_1}$ *satisfies*

*(i)* $x_i \in [u^0, u^1]$ *for all* $i = n_0, \cdots, n_1$ *and*

*(ii) for any* $(y_i)_{i=n_0}^{n_1}$ *satisfying* $y_{n_0} = x_{n_0}$, $y_{n_1} = x_{n_1}$, *and* $y_i \in [u^0, u^1]$,

$$h(x_{n_1}, x_{n_1+1}, \cdots, x_{n_2-1}, x_{n_2}) \leq h(y_{n_1}, y_{n_1+1}, \cdots, y_{n_2-1}, y_{n_2}),$$

*then* $x$ *is a minimal configuration. Moreover, if* $x$ *also satisfies* $x_{n_0} \notin \{u^0, u^1\}$ *or* $x_{n_1} \notin \{u^0, u^1\}$, *then* $x_i \notin \{u^0, u^1\}$ *for all* $i = n_0 + 1, \cdots, n_1 - 1$.

*Proof of the two lemmas above.* See [66]. These proofs require $(h_4)$ and $(h_5)$. □

Moreover, we may replace $\alpha = 0$ with other rational numbers as seen below.

**Definition 2.2.7** (Definition 5.1, [66]). *For* $\alpha = p/q \in \mathbb{Q}\backslash\{0\}$, *we set:*

$$X_\alpha(x^-, x^+) := \{x = (x_i)_{i \in Z} \mid x_i^- \leq x_i \leq x_i^+ (i \in \mathbb{Z})\}.$$

*where* $x^-$ *and* $x^+$ *are* $(p, q)$*-periodic neighboring minimal configurations with* $x^- < x^+$.

**Definition 2.2.8** (Definition 5.2, [66]). *For* $h_1$ *and* $h_2$, *we define* $h_1 * h_2 \colon \mathbb{R}^2 \to \mathbb{R}$ *by*

$$h_1 * h_2(x_1, x_2) = \min_{\xi \in \mathbb{R}} (h_1(x_1, \xi) + h_2(\xi, x_2)).$$

*We call this the conjunction of* $h_1$ *and* $h_2$.

Using the conjunction, we denote $H \colon \mathbb{R}^2 \to \mathbb{R}$ for $\alpha = p/q$ by:

$$H(\xi, \xi') = h^{*q}(\xi, \xi' + p),$$

where $h^{*q}(x, y) = h_1 * h_2 * \cdots * h_q$ $(h_i = h)$.

**Definition 2.2.9** (Definition 5.5, [66]). *For any* $y = (y_i) \in X(x_0^-, x_0^+)$, *we define* $x = (x_i) \in X_\alpha(x^-, x^+)$ *as follows:*

*(i)* $x_{iq} = y_i + ip$ *and*

*(ii)* $(x_j)_{j=iq}^{(i+1)q}$ *satisfies*

$$h(x_{iq}, \cdots, x_{(i+1)q}) = H(x_{iq}, x_{(i+1)q}) = H(y_i, y_{i+1}),$$

*i.e.,* $(x_j)_{j=iq}^{(i+1)q}$ *is a minimal configuration of* $h$.

Although we focus on the case of rotation number $\alpha = 0$, we may apply our proof to all rational rotation numbers from the following.

**Proposition 2.2.10** (Proposition 5.6, [66]). *Let* $y \in X(x_0^-, x_0^+)$ *and* $x \in X_\alpha(x^-, x^+)$ *be defined as above. If* $y$ *is a stationary configuration of* $H$, *then* $x$ *must be a stationary configuration of* $h$.

### 2.2.2 Asymptotic behavior on $I$

Let $X^0$ and $X^1$ be given by:

$$X^0 = \{x \in X \mid |x_i - u^0| \to 0 \ (i \to \infty), |x_i - u^0| \to 0 \ (i \to -\infty)\} \ and$$
$$X^1 = \{x \in X \mid |x_i - u^0| \to 0 \ (i \to -\infty), |x_i - u^0| \to 0 \ (i \to \infty)\}.$$

By considering a local minimizer (precisely, a global minimizer in $X^0$ or $X^1$), Yu [66] proved the existence of heteroclinic configurations, which Bangert showed in [6], as per the following proposition.

**Proposition 2.2.11** (Theorem 3.4 and Proposition 3.5, [66]). *There exists a stationary configuration $x$ in $X^0$ (resp. $X^1$) satisfying $I(x) = c_0$ (resp. $I(x) = c_1$), where*

$$c_0 = \inf_{x \in X^0} I(x), \ c_1 = \inf_{x \in X^1} I(x)$$

*Moreover, $x$ is monotone, i.e., $x_i < x_{i+1}$ (resp. $x_i > x_{i+1}$) for all $i \in Z$.*

Let:

$$\mathcal{M}^0(u^0, u^1) = \{x \in X \mid c_0 = \inf_{x \in X^0} I(x)\} \ and$$
$$\mathcal{M}^1(u^0, u^1) = \{x \in X \mid c_1 = \inf_{x \in X^1} I(x)\}.$$

Set $c_* := I(x^0) + I(x^1)$, where $x^i \in \mathcal{M}^i$. From the above and Lemma 2.2.4, we immediately obtain the following corollary.

**Corollary 2.2.12.** $c_* > 0$

*Proof.* Choose $x^0 \in \mathcal{M}$ and $x^1 \in \mathcal{M}$ arbitrarily. From monotonicity, $x^0$ and $x^1$ intersect exactly once. We define $x^+$ and $x^-$ in $X$ by $x_i^+ := \max\{x_i^0, x_i^1\}$ and $x_i^- := \min\{x_i^0, x_i^1\}$. By $(h_3)$ and Lemma 2.2.3,

$$c_* = I(x^0) + I(x^-) \geq I(x^+) + I(x^-) > 0.$$

This completes the proof. □

Next, we consider a minimal configuration under fixed ends. Let:

$$Y^{*,0}(n, a, b) = X(n) \cap \{x_0 = u^0 + a\} \cap \{x_n = u^0 + b\} \ and$$
$$Y^{*,1}(n, a, b) = X(n) \cap \{x_0 = u^1 - a\} \cap \{x_n = u^1 - b\}$$

and $y^0(n, a, b) = (y_i^0) \in Y^{*,0}(n, a, b)$ be a finite configuration satisfying:

$$\sum_{i=0}^{n-1} a_i(y^0(n, a, b)) = \min_{x \in Y^{*,0}(n,a,b)} \sum_{i=0}^{n-1} a_i(x).$$

The assertion of the next lemma may appear confusing, but it is useful for our proof in Section 2.3.

**Lemma 2.2.13.** *For any $m_0, m_1 \in \mathbb{Z}_{\geq 0}(m_0 < m_1)$ and $\rho_0, \rho_1$, and $\delta$ with $\rho_0 + \rho_1 + 2\delta < c_*/2C$, there exists $n_0$ such that for all $n \geq n_0$, there exists $l \in [m_0, n - m_1] \cap \mathbb{Z}$ satisfying $|y^0_l(n, \rho_0, \rho_1) - u^0| \leq \delta$. A similar argument holds if $u^0$ and $y^0$ are replaced by $u^1$ and $y^1$.*

*Proof.* We first consider the case $m_0 = m_1 = 0$. Let $z = (z_i)_{i=0}^n$ be given by $z_0 = y^*_0$, $z_n = y^*_n$ and $z_i = u^0$ otherwise. Clearly, for any $n \in \mathbb{Z}_{>0}$,

$$\sum_{i=0}^{n} a_i(y^*_l(n, \rho_0, \rho_1)) \leq \sum_{i=0}^{n} a_i(z) \leq C(\rho_1 + \rho_2) < \frac{c_*}{2}.$$

On the other hand, Lemma 2.2.3 and the definition of $y^0$ imply that if $x \in X(n) \cap \{\min |x_i - u^j| \geq \delta\}$, then

$$\sum_{i=0}^{n} a_i(x) \geq n\phi(\delta) - C|\rho_1 - \rho_0|.$$

and $\sum_{i=0}^n a_i(x) > c_*/2$ for sufficiently large $n$, which is a contradiction. The above remark implies that for sufficiently large $n$, there exists $l \in [0, n] \cap \mathbb{Z}$ such that $|y_l(n, \rho_0, \rho_1) - u^0| \leq \delta$ or $|y_l(n, \rho_0, \rho_1) - u^1| \leq \delta$. That is, either of the following two conditions holds:

(a) There exists $l \in [0, n] \cap \mathbb{Z}$ such that $|x_l(n, \rho_0, \rho_1) - u^0| \leq \delta$ and $|x_i(n, \rho_0, \rho_1) - u^1| > \delta$ for all $i \in [0, n] \cap \mathbb{Z}$, or

(b) There exists $l \in [0, n] \cap \mathbb{Z}$ such that $|x_l(n, \rho_0, \rho_1) - u^1| \leq \delta$.

To prove our claim for $m_0 = m_1 = 0$, it suffices to show that the case of $(b)$ does not occur for sufficiently large $n$. If $(b)$ holds, then by Corollary 2.2.12,

$$\sum_i a_i(x) > c_* - C(\rho_1 + \rho_2) - 2C\delta > \frac{c_*}{2},$$

which is a contradiction. □

In fact, $y^i(n, a, b)$ can be asymptotic to $u^i$ any number of times, as per the following lemma.

**Lemma 2.2.14.** *For any $k$, $\rho_0, \rho_1$ and $\delta$ with $\rho_0 + \rho_1 + 2\delta < c_*/2C$, there exists $n_0$ such that for all $n \geq n_0$, there exist $l_1, \cdots, l_k \in [0, n] \cap \mathbb{Z}$ satisfying $|y^0_{l_i}(n, \rho_0, \rho_1) - u^0| \leq \delta$ for all $i = 1, \cdots, k$. A similar argument holds if $u^0$ and $y^0$ are replaced by $u^1$ and $y^1$.*

*Proof.* We only discuss the case where $k = 2$. If we assume the lemma is false, then we set $j_1 = \lfloor n/2 \rfloor$. For some $j_0 \in [0, n]$, there exists $x = (x_i)_{i=j_0}^{j_0+j_1}$ satisfying $|x_l(n, \rho_0, \rho_1) - u^0| > \delta$ for all $i \in [j_0, \cdots, j_0 + j_1] \cap \mathbb{Z}$. On the other hand, $(h_1)$ and Lemma 2.2.13 imply that for sufficiently large $j_1$, it holds that $\sum a_i(x) > c_*/2$, which is a contradiction. Other cases are shown in the same way. □

**Lemma 2.2.15.** *For any $\varepsilon > 0$, there exist $n_0 \in \mathbb{N}_{\geq 0}$ and $x \in \mathcal{M}^0(u^0, u^1)$ such that $\sum_{i=0}^{n-1} a_i(x) \in (c_0 - \varepsilon, c_0 + \varepsilon)$ for all $n \geq n_0$.*

*Proof.* For sufficiently large $n$, there exists $y \in \mathcal{M}^0$ such that:

$$y_0 - u^0 < \varepsilon/2C, \text{and } u^1 - y_n < \varepsilon/2C.$$

By Lemma 2.2.3 and the monotonicity of $y$,

$$\left|\sum_{i=0}^{n-1} a_i(y) - c_0\right| = \left|\sum_{i<0} a_i(y) + \sum_{i>n} a_i(y)\right| \leq C((y_0 - u^0) + (u^1 - y_n)) < \varepsilon$$

as desired. $\square$

Next, we assume a gap condition, i.e.,

$$(u_0, u_1)\backslash I_0 \text{ and } (u_0, u_1)\backslash I_1 \text{ are nonempty sets,} \tag{gap}$$

where $I_0 = I_0^+(u^0, u^1)$ and $I_1 = I_0^-(u^0, u^1)$. We will check the properties of the heteroclinic configurations. Under (gap), the following lemma holds.

**Lemma 2.2.16** (Proposition 4.1, [66])**.** *For any $\varepsilon > 0$, there exist $\delta_i$ $(i = 1, 2, 3, 4)$ and positive constants $e_0 = e_0(\delta_1, \delta_2)$ and $e_1 = e_1(\delta_3, \delta_4)$ satisfying*

$$\inf\{I(x) \mid x \in X^0, x_0 = u_0 + \delta_1 \textit{ or } x_0 = u_1 - \delta_2\} \geq c_0 + e_0 \textit{ and}$$
$$\inf\{I(x) \mid x \in X^1, x_0 = u_1 - \delta_3 \textit{ or } x_0 = u_0 + \delta_4\} \geq c_1 + e_1.$$

## 2.3 Statements and proofs of our main theorem

### 2.3.1 Variational settings and properties of action $J$

Let $(u^0, u^1)$ be a neighboring pair and set

$$\begin{aligned} K &= \{k = (k_i)_{i\in\mathbb{Z}} \subset \mathbb{Z} \mid k_0 = 0, k_i < k_{i+1}\} \textit{ and} \\ P &= \left\{\rho = (\rho_i)_{i\in\mathbb{Z}} \subset \mathbb{R}_{>0} \mid 0 < \rho_i < (u^1 - u^0)/2,\ \sum_{i\in\mathbb{Z}} \rho_i < \infty\right\}. \end{aligned} \tag{2.3.1}$$

For $k \in K$ and $\rho \in P$, the set $X_{k,\rho}$ is given by:

$$X_{k,\rho} = \left(\bigcap_{i\equiv 0,1} Y^0(k_i, \rho_i)\right) \cap \left(\bigcap_{i\equiv -1,2} Y^1(k_i, \rho_i)\right)$$

where

$$Y^j(l, p) = \{x \in X \mid |x_l - u^j| \leq p\} \ (j = 0, 1)$$

and $a \equiv b$ means $a \equiv b \pmod 4$. (See (2.2.1) for the definition of $X$.)

To ensure the topological property of $X_{k,\rho}$, we first show the following lemma.

**Lemma 2.3.1.** *The set $X$ is sequentially compact.*

*Proof.* By Tychonoff's theorem, $X$ is a compact set. It suffices to check that $X$ is metrizable. Let $d\colon X \times X \to \mathbb{R}$ be given by

$$d(x,y) = \sum_{i\in\mathbb{Z}} \frac{|x_i - y_i|}{2^{|i|}}.$$

Clearly, $d$ is a metric function. We show that convergence on $d$ and (2.1.2) is equivalent. Since for all $i \in \mathbb{Z}$

$$\frac{|x_i - y_i|}{2^{|i|}} \le d(x,y),$$

it is sufficient to show that for each $x, y \in X$, the function $d(x,y)$ goes to 0 if (2.1.2) holds. Let $(x^n)$ be a convergence sequence to $y$. There is a constant $M > 0$ such that for all $j \in \mathbb{Z}$

$$d(x^n, y) \le c(j,n) + \frac{M}{2^{|j|}}$$

where $c(j,n) = \sum_{i\le|j|} |x_i^n - y_i|/2^{|i|}$. Notice that for each $j \in \mathbb{Z}$, $c(j,n) \to 0$ as $n \to \infty$. Thus, for any $\varepsilon > 0$, we can take $i_0$ and $n_0$ such that $M/2^{|i_0|} < \varepsilon/2$ and $c(i_0, n_0) < \varepsilon/2$, thus completing the proof. □

Clearly, $X_{k,\rho}$ is a closed subset of $X$, so we find the following.

**Corollary 2.3.2.** *The set $X_{k,\rho}$ is sequentially compact.*

Now we define a renormalized action $J\colon \mathbb{R}^{\mathbb{Z}} \to \mathbb{R}$ on $X_{k,\rho}$ by:

$$J(x) := J_{k,\rho}(x) = \sum_{i\in\mathbb{Z}} A_i(x), \tag{2.3.2}$$

where

$$A_i(x) = \begin{cases} \{\sum_{j\in I_i} h(x_j, x_{j+1})\} - |I_i|c & i \equiv 0, 2 \\ \{\sum_{j\in I_i} h(x_j, x_{j+1})\} - c_i^+ & i \equiv 1 \\ \{\sum_{j\in I_i} h(x_j, x_{j+1})\} - c_i^- & i \equiv -1 \end{cases}, \tag{2.3.3}$$

$I_i = \{k_i, k_i + 1, \ldots, k_{i+1} - 1\}$ and $|I_i| = k_{i+1} - k_i$. The notations $c^+$ and $c^-$ represent

$$\begin{aligned} c_i^+ &= \min_{x\in Y^0(k_i,\rho_i)\cap Y^1(k_{i+1},\rho_{i+1})} \sum_{j\in I_i} h(x_j, x_{j+1}) \ \textit{and} \\ c_i^- &= \min_{x\in Y^1(k_i,\rho_i)\cap Y^0(k_{i+1},\rho_{i+1})} \sum_{j\in I_i} h(x_j, x_{j+1}). \end{aligned}$$

Clearly, $A_i(x) \ge 0$ for $i \equiv \pm 1$. Notice that $(h_1)$ implies that the values of $c_i^\pm$ depend on $\rho_i, \rho_{i+1}$ and $k_{i+1} - k_i$.

To check the basic properties of $J$ through the following discussion, we first show that for an infinite orbit, say $x$, $J(x)$ can be finite unlike $I(x)$.

**Lemma 2.3.3.** *If $\rho \in P$, then there exist $y \in X_{k,\rho}$ and a constant $M$ such that $J(y) \le M$ for all $k \in K$.*

*Proof.* For each $i \equiv 1$, choose some $z^{+i} = \{z_j^{+i}\}_{j \in I_i}$ satisfying $c_i^+ = \sum_{j \in I_i} h(z_j^{+i}, z_{j+1}^{+i})$. Define $z^{-i} = \{z_j^{-i}\}_{j \in I_i}$ for each $i \equiv -1$ in a similar way. We construct a test sequence $y = (y_i)_{i \in \mathbb{Z}}$ as follows:

$$y_j = \begin{cases} u^0 & \text{if } j \in I_i \backslash \{k_i\} \text{ and } i \equiv 0 \\ z_j^{+i} & \text{if } j \in I_i \cup \{k_{i+1}\} \text{ and } i \equiv 1 \\ u^i & \text{if } j \in I_i \backslash \{k_i\} \text{ and } i \equiv 2 \\ z_j^{-i} & \text{if } j \in I_i \cup \{k_{i+1}\} \text{ and } i \equiv -1 \end{cases}. \tag{2.3.4}$$

Since $A_i(y) = 0$ for $i \equiv \pm 1$:

$$J(y) = \sum_{i \in \mathbb{Z}} A_i(x) = \sum_{i \in 2\mathbb{Z}} A_i(x) \leq C \sum_{i \in \mathbb{Z}} \rho_i.$$

This completes the proof. □

The above lemma implies that $J$ overcomes the problem referred to in Proposition 2.1.11. Next, we show that $J$ is bounded below.

**Lemma 2.3.4.** *If $\rho \in P$, then $J(x) > -\infty$ for all $x \in X_{k,\rho}$.*

*Proof.* For $i \equiv 0, 2$, we see that $A_i(x) = a_i(x)$. By Lemma 2.2.3 and $A_i(x) \geq 0$ for $i \equiv \pm 1$,

$$J(x) \geq -C \sum_{i \in \mathbb{Z}} \max\{\rho_i, \rho_{i+1}\} \geq -2C \sum_{i \in \mathbb{Z}} \rho_i > -\infty.$$

By a similar argument, we obtain a constant $\gamma$ such that for any $n \in \mathbb{N}$,

$$\sum_{|i| \leq n} A_i(x) \geq \gamma,$$

thus completing the proof. □

To ensure that $J$ has a minimizer in $X_{k,\rho}$, we present the following lemma.

**Lemma 2.3.5.** *The function $J$ is well-defined on $\mathbb{R} \cup \{+\infty\}$, i.e.,*

$$\alpha := \liminf_{n \to \infty} \sum_{|i| \leq n} A_i(x) = \limsup_{n \to \infty} \sum_{|i| \leq n} A_i(x) =: \beta.$$

*Proof.* For the proof, we use a similar argument to Yu's proof of Lemma 6.1 and Proposition 2.9 in [66]. By contradiction, we assume $\alpha < \beta$. First, we consider the case where $\beta = +\infty$. For $\alpha < +\infty$, we take a constant $\tilde{\alpha}$ with $\tilde{\alpha} > \alpha + 1 - 2\gamma$. Then there are constants $n_0$ and $n_1$ such that $n_0 < n_1$ and:

$$\sum_{|i| \leq n_0} A_i(x) \geq \tilde{\alpha} \text{ and } \sum_{|i| \leq n_1} A_i(x) \leq \alpha + 1.$$

Then,

$$2\gamma > \alpha + 1 - \tilde{\alpha} \geq \sum_{|i| \leq n_1} A_i(x) - \sum_{|i| \leq n_0} A_i(x) = \sum_{i=-n_1}^{-n_0} A_i(x) + \sum_{i=n_0}^{n_1} A_i(x).$$

Combining the first term and end terms implies

$$\sum_{i=-n_1}^{-n_0} A_i(x) < \gamma \text{ or } \sum_{i=-n_1}^{-n_0} A_i(x) < \gamma.$$

This contradicts Lemma 2.3.4.

Next, we assume $\beta < +\infty$. Since $\alpha < \beta$, there are two sequences of positive integers $\{m_j \to \infty\}_{j\in\mathbb{N}}$ and $\{l_j \to \infty\}_{j\in\mathbb{N}}$ satisfying $m_j < m_{j+1}$, $l_j < l_{j+1}$ and $m_j + 1 < l_j < m_{j+1} - 1$ for all $j \in \mathbb{Z}_{>0}$, and:

$$\beta = \lim_{j\to\infty} \sum_{i\le|m_j|} A_i(x) > \lim_{j\to\infty} \sum_{i\le|l_j|} A_i(x) = \alpha.$$

Then we can find $j \gg 0$ such that

$$\sum_{i\le|l_j|} A_i(x) - \sum_{i\le|m_j|} A_i(x) = \sum_{i=-l_j}^{-m_j} A_i(x) + \sum_{i=m_j}^{l_j} A_i(x) < \frac{\alpha-\beta}{2}.$$

Since $|l_j|$ and $|m_j|$ are finite for fixed $j$, the above calculation does not depend on the order of the sums. Thus, we obtain:

$$\begin{aligned}\sum_{i=-l_j}^{-m_j} A_i(x) + \sum_{i=m_j}^{l_j} A_i(x) &\ge \sum_{i\in[-l_j,-m_j]\cap 2\mathbb{Z}} A_i(x) + \sum_{i\in[m_j,l_j]\cap 2\mathbb{Z}} A_i(x) \\ &= \sum_{i\in[-l_j,-m_j]\cap 2\mathbb{Z}} a_i(x) + \sum_{i\in[-l_j,-m_j]\cap 2\mathbb{Z}} a_i(x)\end{aligned}$$

For sufficiently large $j$, we have

$$\sum_{i\in[-l_j,-m_j]\cap 2\mathbb{Z}} a_i(x) \ge -C\sum_i |x_{-m_j} - x_{-l_j}| > \frac{\alpha-\beta}{4}$$

and

$$\sum_{i\in[-l_j,-m_j]\cap 2\mathbb{Z}} a_i(x) \ge -C\sum_i |x_{-m_j} - x_{-l_j}| > \frac{\alpha-\beta}{4}$$

because $\rho \in P$ implies

$$\sum_{|i|>n} \rho_i \to 0 \ (n \to \infty).$$

Therefore

$$\sum_{i=-l_j}^{-m_j} A_i(x) + \sum_{i=m_j}^{l_j} A_i(x) > \frac{\alpha-\beta}{2},$$

which is a contradiction. □

**Proposition 2.3.6.** *For all $k \in K$ and $\rho \in P$, there exists a minimizer of $J$ in $X_{k,\rho}$.*

*Proof.* By Lemmas 2.3.3 and 2.3.4, we can take a minimizing sequence $x = (x^n)_{n\in\mathbb{N}}$ of $J$ in $X_{k,\rho}$. Since $X_{k,\rho}$ is sequentially compact, there exists $\tilde{x} \in X_{k,\rho}$ with $x_{n_k} \to \tilde{x}$. It is enough to show that for any $\varepsilon > 0$, there exists $j_0$ and $n_0 \in \mathbb{N}$ such that:

$$\sum_{|i|>j_0} A_i(x^n) > -\varepsilon \text{ (for all } n \geq n_0) \text{ and } \sum_{|i|>j_0} A_i(\tilde{x}) < \varepsilon. \tag{2.3.5}$$

because if the above inequalities hold, we obtain:

$$\begin{aligned} J(\tilde{x}) &= \sum_{|i|\leq j_0} A_i(x) + \sum_{|i|>i_0} A_i(x) \\ &\leq \lim_{n\to\infty} \sum_{|i|\leq j_0} A_i(x^n) + \varepsilon = \lim_{n\to\infty} (\sum_{i\in\mathbb{Z}} A_i(x^n) - \sum_{|i|>j_0} A_i(x^n)) + \varepsilon \\ &\leq \lim_{n\to\infty} \sum_{i\in\mathbb{Z}} A_i(x^n) + 2\varepsilon. \end{aligned}$$

Using an arbitrary value of $\varepsilon$, we have $J(\tilde{x}) \leq \lim_{n\to\infty} \sum_{i\in\mathbb{Z}} A_i(x^n)$ and $\tilde{x}$ is the infimum (or greatest lower bound) of $J$.

We now show the first inequality of (2.3.5). Lemma 2.2.3 implies that for any $n \in \mathbb{N}$ and $j \in \mathbb{N}$:

$$\sum_{|i|>j} A_i(x^n) \geq -C \sum_{|i|>j} \max\{\rho_{2i}, \rho_{2i+1}\} \geq -C \sum_{|i|>j} \rho_i. \tag{2.3.6}$$

Note that $A_i \geq 0$ for $i \equiv 1, 2$. Since $\sum_{i\in\mathbb{Z}} \rho_i$ is finite, we have $\sum_{|i|>j} \rho_i < \varepsilon/C$ for sufficiently large $j$. Hence, the first inequality holds.

To check the second inequality, it suffices to show that $\sum_{i\in Z} J_i(\tilde{x})$ is finite. If $\sum_{i\in Z} J_i(y)$ is infinite, then for any $M > 0$, there is a $j_0$ such that:

$$M \leq \sum_{|i|\leq j_0} A_i(\tilde{x}) = \sum_{|i|\leq j_0} A_i(\lim_{n\to\infty} x^n) = \lim_{n\to\infty} \sum_{|i|\leq j_0} A_i(x^n),$$

since a finite sum $\sum_{|i|\leq j_0} A_i(x)$ is continuous. On the other hand, for any $\delta > 0$, there exists $n_0$ such that if $n \geq n_0$, then (2.3.6) gives:

$$\begin{aligned} \sum_{|i|\leq j_0} A_i(x^n) &= J(x^n) - \sum_{|i|>j_0} A_i(x^n) \\ &< \inf_{x\in X_{k,\rho}} J(x) + \delta + C \sum_{|i|>j_0} \rho_i, \end{aligned}$$

so $\sum_{|i|\leq j_0} A_i(x^n)$ is finite, which is a contradiction.

These results and the continuity of the finite sum of $A_i$ imply that, for any $\varepsilon > 0$,

$$J(\tilde{y}) = \sum_{|i|\leq i_0} A_i(y) + \sum_{|i|>i_0} A_i(y) \leq \lim_{n\to\infty} \sum_{|i|\leq i_0} A_i(y^n) + \varepsilon \leq \lim_{n\to\infty} \sum_{i\in\mathbb{Z}} A_i(y^n) + 2\varepsilon.$$

By using an arbitrary value of $\varepsilon$, we have $J(\tilde{y}) \leq \lim_{n\to\infty} \sum_{i\in\mathbb{Z}} A_i(y^n)$. □

### 2.3.2 Properties of the minimizer

Let $x^* = (x_i^*)_{i\in Z}$ be a minimizer in Proposition 2.3.6. First, we show the properties of $A_i$ for $i \equiv 0, 2$ if $\rho_i$'s are sufficiently small.

**Proposition 2.3.7.** *For any $\rho \in P$ and a positive sequence $\delta = (\delta_i)_{i\in\mathbb{Z}}$, if $\delta$ satisfies*

$$\rho_{2i} + \rho_{2i+1} + 2\max\{\delta_{2i}, \delta_{2i+1}\} < c_*/2C,$$

*then there exists a sequence $k = (k_i)_{i\in Z}$ that satisfies the following: there is a sequence $l = (l_i)_{i\in\mathbb{Z}}$ satisfying*

($l_1$) *$l_{2i}, l_{2i+1} \in (k_{2i}, k_{2i+1}) \cap \mathbb{Z}$ with $l_{2i} < l_{2i+1}$ and*

($l_2$) *$|x^*_{l_i} - x^j| < \delta_i$, where $j = 0$ if $i \equiv 0, 1$ and $j = 1$ if $i \equiv -1, 2$.*

*Proof.* It is immediately shown from ($h_1$), Lemmas 2.2.13 and 2.2.14. □

To see that $x^*$ is an infinite transition orbit, it suffices to show that $x^*$ is not on the boundary of $X_{k,\rho}$. We set $\tilde{I}_0 := (u_0, u_1)\backslash I_0$ and $\tilde{I}_1 := (u_0, u_1)\backslash I_1$. We assume a gap condition for periodic and heteroclinic configurations, i.e., $\tilde{I}_0$ and $\tilde{I}_1$ are nonempty sets.

**Remark 2.3.8.** *Notice that $\rho \in \tilde{I}_i$ can be chosen as arbitrarily small.*

We choose $\rho$ and $k$ in the following steps:

Step 1 First we take $\rho \in P$ so that:

(p1) $u^0 + \rho_i \in \tilde{I}_0$ for all $i \equiv 1, 2$ and $u^1 - \rho_i \in \tilde{I}_1$ for all $i \equiv -1, 0$ and

(p2) For any $i \in \mathbb{Z}$, $\rho_{2i} + \rho_{2i+1} < c_*/2C$

Step 2 To determine $|k_{2i} - k_{2i+1}|$, we define a positive sequence $(e^i)_{i\in\mathbb{Z}}$ by:

$$e^i = \begin{cases} e_0(\rho_{2i+1}, \rho_{2(i+1)}) & (i : even) \\ e_1(\rho_{2i+1}, \rho_{2(i+1)}) & (i : odd) \end{cases}.$$

Choose a positive sequence $(\delta_i)_{i\in\mathbb{Z}}$ so that:

(d) $2\max\{\delta_{2i}, \delta_{2i+1}\} < c^*/2C - (\rho_{2i} + \rho_{2i+1})$

Then, through Proposition 2.3.7 for $(\rho_i)$ and $(\delta_i)$, we can obtain $|k_{2i} - k_{2i+1}|$ and $l_i$ for each $i \in \mathbb{Z}$ such that ($l_1$) and ($l_2$) in Proposition 2.3.7 hold.

Step 3 For $\delta$ in Step 2, choose $(\varepsilon_i)_{i\in\mathbb{Z}}$ so that:

(e1) $\varepsilon_i + 2C(\delta_{2i+1} + \delta_{2(i+1)}) < e^i/2$ and

(e2) $\varepsilon_i/2C < \min\{\delta_{2i+1}, \delta_{2(i+1)}\}$.

For each $\varepsilon_i$, Lemma 2.2.15 gives $n_i$ and $x^i \in \mathcal{M}^i(u^0, u^1)$ such that $\sum_{i=0}^{n-1} a_i(x) \le c_0 + \varepsilon$ for all $n \ge n_i$. For $(n_i)_{i\in\mathbb{Z}}$ and $(x^i)_{i\in\mathbb{Z}}$, we choose $|k_{2i+1} - k_{2(i+1)}|$ satisfying

(k1) $|k_{2i+1} - k_{2(i+1)}| \ge n_i$ and (k2) $x^i \in \mathcal{M}_0 \cap Y^0(0, \rho_{2i}) \cap Y^1(|k_{2i-1} - k_{2i}|, \rho_{2i+1})$ when $i$ is even and $x^i \in \mathcal{M}_1 \cap Y^1(0, \rho_{2i}) \cap Y^0(|k_{2i-1} - k_{2i}|, \rho_{2i+1})$ when $i$ is odd.

Step 4 By the above steps and $k_0 = 0$, the sequence $k = (k_i)_{i\in\mathbb{Z}}$ is determined.

Now we are ready to state our main theorem when the rotation number $\alpha$ is zero.

**Theorem 2.3.9.** *For any $\rho = (\rho_i) \in P$ and $k = (k_i)$ chosen in the above steps, there exists a stationary configuration $x^*$ in $X_{k,\rho}$ with rotation number $\alpha = 0$.*

*Proof.* Lemmas 2.2.5 and 2.2.6 implies that $x_i^* \notin \{u^0, u^1\}$ for all $i \in \mathbb{Z}$. For a contradiction argument, we assume $x_{k_1}^* = u^0 + \rho_1$.

Hereafter, $x_i^*$ will be written simply as $x_i$ unless there is potential for confusion. Let $y$ be:

$$y_i = \begin{cases} x_i & i \in [k_1 - l_1, k_2 + l_2] \cap \mathbb{Z} \\ u^1 & i > k_2 + l_2 \\ u^0 & i < k_1 - l_1 \end{cases}.$$

Since $y \in X^0$, Lemma 2.2.16 and $(h_1)$ yield:

$$\begin{aligned} c_o + e^0 &\le I(y) \\ &= \sum_{i\in[k_1-l_1,k_2+l_2-1]\cap\mathbb{Z}} a_i(x) + \sum_{i<k_1-l_1} a_i(x) + \sum_{i>k_2+l_2} a_i(x) \\ &\le \sum_{i\in[k_1-l_1,k_2+l_2-1]\cap\mathbb{Z}} a_i(x) + C(\delta_1 + \delta_2) \end{aligned}$$

By the above remark and $a_i = A_i$ for $i \equiv 0, 2$,

$$\begin{aligned} &\sum_{i=k_1-l_1}^{k_1-1} (h(x_i, x_{i+1}) - c) + A_1(x) + \sum_{i=k_2}^{k_2+l_2-1} (h(x_i, x_{i+1}) - c) \\ &\quad > c_0 + e^0 - C(\delta_1 + \delta_2) + (|I_1|c - c_1^+). \end{aligned}$$

On the other hand, $(h_1)$ implies that $x^0 \in \mathcal{M}^0$ in Step 3 satisfies:

$$\sum_{i=k_1-l_1}^{k_1-1} (h(x_i^0, x_{i+1}^0) - c) + A_1(x^0) + \sum_{i=k_2}^{k_2+l_2-1} (h(x_i^0, x_{i+1}^0) - c) \ < c_0 + \varepsilon_0 + (|I_1|c - c_1^+)$$

We define a test sequence $z = (z_i)_{i\in\mathbb{Z}}$ by

$$z_i = \begin{cases} x_{i-k_1}^0 & i \in [k_1 - l_1, k_2 + l_2] \cap \mathbb{Z} \\ x_i & \text{otherwise} \end{cases}.$$

By Lipschitz continuity, the monotonicity of $x^0$ and (e2), we find:

$$\begin{aligned} &|h(x_{k_1+l_1-1}, x_{k_1-l_1}^0) - h(x_{k_1+l_1-1}, x_{k_1+l_1})| \le C|x_{k_1-l_1}^0 - x_{k_1-l_1}| < C\delta_1 \textit{ and} \\ &|h(x_{k_2+l_2}^0, x_{k_2+l_2+1}) - h(x_{k_2+l_2}, x_{k_2+l_2+1})| \le C|x_{k_2+l_2}^0 - x_{k_2+l_2}| < C\delta_2. \end{aligned}$$

Hence

$$\begin{aligned} J(z) - J(x^*) &< c_0 + \varepsilon_0 + C(\delta_1 + \delta_2) - (c_0 + e^0 - C(\delta_1 + \delta_2)) \\ &= 2(\delta_1 + \delta_2) + \varepsilon_0 - e_0 < -\frac{e^0}{2} < 0, \end{aligned}$$

which is a contradiction. The same proof works for the remaining cases. For example, if $x^*_{k_i} = u^0 + \rho_i$ or $x^*_{k_i} = u^1 - \rho_i$ for all $i \in \mathbb{Z}$, a similar argument yields:

$$J(\hat{z}) - J(x^*) < \sum_{i\in\mathbb{Z}} 2(\delta_{2i+1} + \delta_{2(i+1)}) + \varepsilon_i - e_i < -\sum_{i\in\mathbb{Z}} \frac{e^i}{2} < 0,$$

where $\hat{z} = (\hat{z}_i)_{i\in\mathbb{Z}}$ is given by:

$$\hat{z}_i = \begin{cases} x^j_{i-k_{2j+1}} & i \in [k_{2j+1} - l_{2j+1}, k_{2(j+1)} + l_{2(j+1)}] \cap \mathbb{Z} \text{ and } \ j : \textit{even} \\ x^j_{i-k_{2j+1}} & i \in [k_{2j+1} - l_{2j+1}, k_{2(j+1)} + l_{2(j+1)}] \cap \mathbb{Z} \text{ and } \ j : \textit{odd} \\ x_i & \text{otherwise} \end{cases}.$$

This completes the proof. □

Moreover, we immediately obtain the following corollary.

**Corollary 2.3.10.** *Given $\alpha \in \mathbb{Q}$, if*

$$I^+_\alpha(x^0, x^1) \neq (x^0_0, x^1_0) \textit{ and } I^-_\alpha(x^0, x^1) \neq (x^0_0, x^1_0),$$

*there exists a stationary configuration $x^*$ of $J$ with infinite transitions and rotation number $\alpha$.*

*Proof.* This follows from Proposition 2.2.10 and Theorem 2.3.9. □

# Chapter 3

# Periodic solutions in the planar restricted three-body problem

## 3.1 Introduction

The restricted three-body problem has long been studied. It is a special case of the three-body problem and is known to be non-integrable. It deals with significant issues in celestial mechanics, such as analyzing asteroid movement behavior and orbit designing for space probes (see [56] for more details). This chapter aims to show the existence of multiple periodic orbits in the planar circular restricted three-body problem (R3BP).

Chenciner and Montgomery successfully applied a variational method to the three-body problem. They showed the existence of a remarkable periodic orbit called the figure-eight orbit (see [18]), which has led to many works on the $n$-body problem. As a recent result in this field, we refer the reader to [65]. Compared with the $n$-body problem, there are few results on the restricted three-body problem using the variational methods because the technical parts of the level estimates for the restricted three-body problem are more difficult. In [39], Moeckel showed the existence of the transit orbit in the R3BP for regions from around the earth to around the moon. The result in [54] yields the existence of orbits realizing symbolic sequences in the Sitnikov problem. Arioli *et al.* showed the existence of periodic orbits revolving around Jupiter in [1]. Chen proved the existence of the orbits moving away from the center in [14].

The R3BP is defined by

$$\ddot{\boldsymbol{x}} = \nabla V(\boldsymbol{x}) \quad (\boldsymbol{x} \in \mathbb{C}), \tag{3.1.1}$$

where

$$V(\boldsymbol{x}, t; \mu) = \frac{1-\mu}{|\boldsymbol{x} + \mu e^{it}|} + \frac{\mu}{|\boldsymbol{x} - (1-\mu)e^{it}|} \tag{3.1.2}$$

and $\mu \in (0,1)$ is a parameter. Here $\mathbb{C}$ is regarded as $\mathbb{R}^2$. In the rotating coordinate system, the equations are represented by

$$\begin{aligned} \ddot{x} &= x + 2\dot{y} + \frac{\partial U}{\partial x} \\ \ddot{y} &= y - 2\dot{x} + \frac{\partial U}{\partial y}, \end{aligned} \tag{R3BP$_\mu$}$$

where

$$U(\boldsymbol{x};\mu) = \frac{1-\mu}{\sqrt{(x+\mu)^2+y^2}} + \frac{\mu}{\sqrt{(x-(1-\mu))^2+y^2}}.$$

Here $\boldsymbol{x} = x + iy$ and $i = \sqrt{-1}$.

We aim to show the existence of periodic orbits under several boundary conditions in the R3BP. Our proof will use an elementary minimization argument and a level estimate of the action functional in the R3BP. The steps of our proof give a new method for a level estimate in the rotating coordinate system.

The result of this chapter is organized as follows. Section 3.2 states our main theorems. Section 3.3 contains preliminaries for our proof including basic facts on variational methods. Section 3.4 provides the proofs of the main theorems. In Section 3.5, we discuss how the obtained periodic orbits behave and state open problems.

## 3.2 Main results

We define $X^o$, $X^-$, $X^+$, and $Y$ as follows:

$$\begin{aligned}
X^o &:= \{(x,0) \mid -\mu \le x \le 1-\mu\},\\
X^- &:= \{(x,0) \mid x < -\mu\},\\
X^+ &:= \{(x,0) \mid 1-\mu < x\} \text{ and}\\
Y &:= \{(0,y) \mid -\infty < y < \infty\}.
\end{aligned}$$

Set $\mathcal{X} = \{X^o, X^-, X^+\}$.

We state our main theorems. Each set $\mathcal{T}(A,B)(\subset \mathbb{R})$ in the following theorems is defined in Section 3.4.

**Theorem 3.2.1.** *For any $A, B \in \mathcal{X}$ and $T \in \mathcal{T}(A,B)$, there is a $2T$-periodic orbit $(x(t), y(t))$ of* (R3BP$_\mu$) *such that $x(2(k-1)T) \in A$, $x((2k-1)T) \in B$ and $\dot{x}(2(k-1)T) = y(2(k-1)T) = y((2k-1)T) = \dot{x}((2k-1)T) = 0$ for $k \in \mathbb{Z}$.*

This theorem shows the existence of periodic orbits that are orthogonal to the $x$-axis for $\mu \in (0,1)$. In the case of $\mu = 1/2$, we can show the existence of more symmetric periodic orbits that are orthogonal to the $x$-axis and $y$-axis.

**Theorem 3.2.2.** *Set $\mu = 1/2$. For any $A \in \mathcal{X}$ and $T \in \mathcal{T}(A,Y)$, there exists a $4T$-periodic orbit $(x(t), y(t))$ of* (R3BP$_\mu$) *that satisfies $x(2(k-1)T) \in A$ and $\dot{x}(2(k-1)T) = y(2(k-1)T) = \dot{y}((2k-1)T) = x((2k-1)T) = 0$ for $k \in \mathbb{Z}$.*

**Remark 3.2.3.** *Figures* 3.1 *and* 3.2 *may show the outlines of the given periodic orbits obtained from Theorems* 3.2.1 *and* 3.2.2 *respectively. As a result, the shape of the obtained orbits is symmetric about the $x$-axis. Moreover, the orbits from Theorem* 3.2.2 *are symmetric about the $y$-axis. Note that 'may' indicates we do not know their detailed global behavior, as will be discussed in Section 3.5.*

**Remark 3.2.4.** *The word 'periodic' in this chapter is used in reference to the rotating coordinate system. Therefore, in the stationary coordinate system, '$T$-periodic' orbits are periodic if $T/2\pi \in \mathbb{Q}$ and quasi-periodic if $T/2\pi \notin \mathbb{Q}$.*

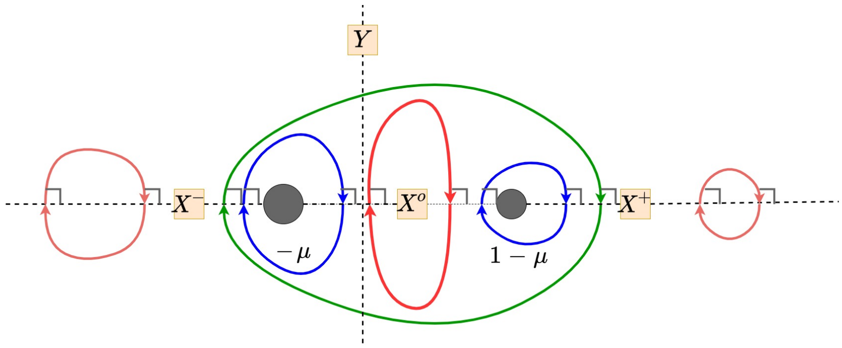


Figure 3.1: Periodic solutions in Theorem 3.2.1

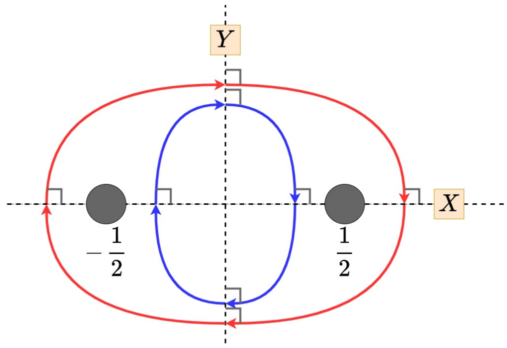


Figure 3.2: Periodic solutions in Theorem 3.2.2

## 3.3 Preliminaries

### 3.3.1 Lagrangians in the stationary and rotating coordinates

We use two different Lagrangian functions in this chapter. One is the original Lagrangian which is time-periodic:

$$L(\boldsymbol{x}, \dot{\boldsymbol{x}}, t; \mu) = \frac{1}{2}(\dot{x}^2 + \dot{y}^2) + V(\boldsymbol{x}, t; \mu), \tag{3.3.1}$$

where $V$ is introduced in (3.1.2) in Section 3.1. The other Lagrangian is in rotating coordinates and is time-independent:

$$L_{\text{R3BP}}(\boldsymbol{x}, \dot{\boldsymbol{x}}; \mu) = \frac{1}{2}(\dot{x}^2 + \dot{y}^2) + x\dot{y} - y\dot{x} + \frac{1}{2}(x^2 + y^2) + U(\boldsymbol{x}; \mu). \tag{3.3.2}$$

We will check that, up to a variable change, the two Lagrangian functions coincide. Indeed, using $z = x + iy \in \mathbb{C}$, we can write (3.3.1) as

$$L(z, \dot{z}, t; \mu) = \frac{1}{2}\dot{z}\dot{\bar{z}} + \frac{1-\mu}{|z + \mu e^{it}|} + \frac{\mu}{|z - (1-\mu)e^{it}|}.$$

Similarly, using $w = x + iy \in \mathbb{C}$, we can write (3.3.2) as

$$L_{\text{R3BP}}(w, \dot{w}; \mu) = \frac{1}{2}(w + i\dot{w})(\bar{w} - i\dot{\bar{w}}) + \frac{1-\mu}{|w - \mu|} + \frac{\mu}{|w - (1-\mu)|}.$$

Substituting $z(t) = w(t)e^{it}$ in the above, we have

$$\begin{aligned}
&\frac{1}{2}\dot{z}\dot{\bar{z}} + \frac{1-\mu}{|z+\mu e^{it}|} + \frac{\mu}{|z-(1-\mu)e^{it}|} \\
&= \frac{1}{2}(\dot{w}e^{it} + iwe^{it})(\dot{\bar{w}}e^{-it} - iwe^{-it}) + \frac{1-\mu}{|we^{it}+\mu e^{it}|} + \frac{\mu}{|we^{it}-(1-\mu)e^{it}|} \\
&= \frac{1}{2}(\dot{w}+iw)(\dot{\bar{w}}-iw) + \frac{1-\mu}{|w+\mu|} + \frac{\mu}{|w-(1-\mu)|}.
\end{aligned}$$

Hence, the values of the two Lagrangian functions are the same, so switching between them does not affect our results.

### 3.3.2 Some well-known facts in variational problems

Let $\mathcal{D}$ be an open set in $\mathbb{R}^n$, and $A,\ B \subset \mathcal{D}$ be nonempty subsets of affine subspaces in $\mathbb{R}^n$, for example, a line segment or a half-line. Consider

$$\Omega(A,B) = \{\boldsymbol{x} \in H^1([0,T],\mathcal{D}) \mid \boldsymbol{x}(0) \in A, \boldsymbol{x}(T) \in B\}$$

where the norm is defined by

$$\|\boldsymbol{x}\|_{H^1} = \left(\int_0^T |\boldsymbol{x}|^2 dt + \int_0^T |\dot{\boldsymbol{x}}|^2 dt\right)^{1/2}.$$

The action functional $\mathcal{A}_T(\boldsymbol{x};\mu)$ is given by

$$\mathcal{A}_T(\boldsymbol{x};\mu) = \int_0^T L(\boldsymbol{x},\dot{\boldsymbol{x}},t;\mu)dt, \tag{3.3.3}$$

where $T > 0$ is constant and $L$ is defined by (3.3.1).

We consider a minimizer of $\mathcal{A}_T$, say $\boldsymbol{x}^*$, i.e., $\boldsymbol{x}^*$ satisfying

$$\mathcal{A}_T(\boldsymbol{x}^*;\mu) = \inf_{\boldsymbol{x}\in\Omega(A,B)} \mathcal{A}_T(\boldsymbol{x};\mu).$$

The existence is ensured under some boundary conditions. To show the existence, we can use some useful lemmata. We first define coercivity.

**Definition 3.3.1** (coercivity)**.** *The action functional $\mathcal{A}_T$ is said to be coercive if it satisfies $\mathcal{A}_T(\boldsymbol{x};\mu) \to \infty$ as $\|\boldsymbol{x}\|_{H^1} \to \infty$.*

Hereinafter, $\Omega(A,B)$ is denoted to $\Omega$. The following lemma results from Tonelli's theorem [60].

**Lemma 3.3.2.** *Assume that $\mathcal{A}_T$ is weakly lower semi-continuous. If $\mathcal{A}_T|_\Omega$ is coercive, then there exists a minimizer $\boldsymbol{x}^*$ of $\mathcal{A}_T$ in the weak closure $\bar{\Omega}$ of $\Omega$.*

It is well-known that action functionals for potential systems are weakly semi-continuous (see for example [27]). We state some sufficient conditions for coercivity in the next three lemmata.

**Lemma 3.3.3.** *Let $A$ and $B$ be nonempty sets. If at least one of $A$ and $B$ is bounded, then $\mathcal{A}_T|_\Omega$ is coercive.*

**Lemma 3.3.4.** *Let $A$ and $B$ be nonempty sets. Suppose there is a constant $|C_0| < 1$ such that for any $\boldsymbol{a} \in A$ and $\boldsymbol{b} \in B$, it holds that $\boldsymbol{a} \cdot \boldsymbol{b} \leq C_0|\boldsymbol{a}||\boldsymbol{b}|$. Then, $\mathcal{A}_T|_\Omega$ is coercive.*

See [12] for proofs of the above two lemmata.

**Lemma 3.3.5.** *Let $A$ and $B$ be unbounded sets. Set $A_d := \{\boldsymbol{a} \in A \mid |\boldsymbol{a}| \leq d\}$ and $B_d := \{\boldsymbol{b} \in B \mid |\boldsymbol{b}| \leq d\}$. Suppose there is a constant $M > 0$ such that for any $\boldsymbol{a} \in A\backslash A_M$ and $\boldsymbol{b} \in B\backslash B_M$, it holds that $\boldsymbol{a} \cdot \boldsymbol{b} \leq C_1|\boldsymbol{a}||\boldsymbol{b}|$, where $C_1 \in [-1, 1)$. Then, $\mathcal{A}_T|_\Omega$ is coercive.*

*Proof.* Set $\Omega(A, B) = \bigcup_{i=1}^n \bigcup_{j=1}^m \Omega(A_i, B_j)$ such that $A = \bigcup_{i=1}^n A_i$ and $B = \bigcup_{j=1}^m B_j$. It is easily seen that if $\mathcal{A}|_{\Omega(A_i,B_j)}$ is coercive for each $i \in \{1, .., n\}$ and $j \in \{1, .., m\}$, then so is $\mathcal{A}|_{\Omega(A,B)}$. Under the assumption, we divide $\Omega(A, B)$ into the following:

$$\Omega(A, B) = \Omega(A_M, B_M) \cup \Omega(A\backslash A_M, B_M) \cup \Omega(A_M, B\backslash B_M) \cup \Omega(A\backslash A_M, B\backslash B_M).$$

Applying Lemma 3.3.3 yields that $\mathcal{A}|_{\Omega(A_M,B_M)}$, $\mathcal{A}|_{\Omega(A\backslash A_M,B_M)}$, and $\mathcal{A}|_{\Omega(A_M,B\backslash B_M)}$ are coercive. In the case $C_1 \in (-1, 1)$, Lemma 3.3.4 gives coercivity of $\mathcal{A}|_{\Omega(A\backslash A_M,B\backslash B_M)}$. Hence, it suffices to consider the case $C_1 = -1$. Then, $\boldsymbol{x}(T) = -C_2\boldsymbol{x}(0)$ $(C_2 > 0)$. It is clear that $|\boldsymbol{x}(0) - \boldsymbol{x}(T)| = (1 + C_2)|\boldsymbol{x}(0)|$. The rest of the proof is the same as that of Lemma 3.3.3. □

From the calculation in Section 3.3.1, if $\mathcal{A}_T(\boldsymbol{x}; \mu)$ is coercive, then so is the action functional corresponding to the Lagrangian (3.3.2) instead of (3.3.1).

### 3.3.3 Reversibility

Consider the following ordinary differential equations:

$$\dot{\boldsymbol{q}} = F(\boldsymbol{q}) \quad (\boldsymbol{q} \in \mathbb{R}^n). \tag{3.3.4}$$

**Definition 3.3.6** (Reversibility)**.** *Let $R$ be an involutory linear map from $\mathbb{R}^n$ to $\mathbb{R}^n$, i.e., $R^2 = \mathrm{Id}$. If* (4.2.3) *satisfies $FR + RF = 0$, then* (4.2.3) *is said to be reversible with respect to $R$.*

It is easy to show the following lemma.

**Lemma 3.3.7.** *Assume that* (4.2.3) *satisfies reversibility with respect to $R$. Then if $\boldsymbol{q}(t)$ is a solution of* (4.2.3)*, so is $R\boldsymbol{q}(-t)$.*

Set $\mathrm{Fix}(R) = \{\boldsymbol{q} \in \mathbb{R}^n \mid R\boldsymbol{q} = \boldsymbol{q}\}$. Assume that (4.2.3) is reversible with respect to $R$ and let $\boldsymbol{q}$ be a solution for (4.2.3). Then,

$$\boldsymbol{q}(s) \in \mathrm{Fix}(R) \Longleftrightarrow \boldsymbol{q}(s + t) = R\boldsymbol{q}(s - t).$$

See [51] for a more detailed explanation of reversible systems.

Moreover (R3BP$_\mu$) can be represented by

$$\frac{d}{dt}\begin{pmatrix} x \\ y \\ v_x \\ v_y \end{pmatrix} = \begin{pmatrix} v_x \\ v_y \\ x + 2v_y + \frac{\partial U}{\partial x} \\ y - 2v_x + \frac{\partial U}{\partial y} \end{pmatrix} \left( =: F\begin{pmatrix} x \\ y \\ v_x \\ v_y \end{pmatrix}\right)$$

and the system is reversible with respect to

$$R := \begin{pmatrix} 1 & 0 & 0 & 0 \\ 0 & -1 & 0 & 0 \\ 0 & 0 & -1 & 0 \\ 0 & 0 & 0 & 1 \end{pmatrix}. \tag{3.3.5}$$

Indeed

$$FR\begin{pmatrix} x \\ y \\ v_x \\ v_y \end{pmatrix} + RF\begin{pmatrix} x \\ y \\ v_x \\ v_y \end{pmatrix} = F\begin{pmatrix} x \\ -y \\ -v_x \\ v_y \end{pmatrix} + R\begin{pmatrix} v_x \\ v_y \\ x + 2v_y + \frac{\partial U}{\partial x} \\ y - 2v_x + \frac{\partial U}{\partial y} \end{pmatrix} = \mathbf{0}.$$

If $\mu = 1/2$, then (R3BP$_\mu$) is reversible with respect to $-R$. By the above remarks, we obtain the following proposition.

**Proposition 3.3.8.** *The system of* (R3BP$_\mu$) *has reversibility with respect to $R$ defined by* (3.3.5)*. Moreover, it is also reversible with respect to $-R$ if $\mu = 1/2$.*

### 3.3.4 Sundman's estimate

In the case that some particles collide at $t = 0$ in the $n$-body problem, the asymptotic behavior of each particle $\boldsymbol{x}_i(t)$ is represented by $\boldsymbol{x}_i(t) \sim \boldsymbol{c} + \boldsymbol{a}_i t^{2/3} + o(t)$ as $t \to 0^+$. This estimate is called *Sundman's estimate*. From [7], there is a wide class in which Sundman's estimate holds, including the classical $n$-body problems with Newtonian, quasi-homogeneous, and logarithmic potentials.

We prove that this asymptoticity holds for (R3BP$_\mu$). We analyze the singular points in (R3BP$_\mu$) using the Levi-Civita regularization. Consider the following transformation to study the singular point at $(1-\mu, 0)$:

$$(x - (1-\mu),\, y) \mapsto \left(\xi_1^2 - \xi_2^2,\, 2\xi_1\xi_2\right)$$

To construct canonical transformation, we set

$$(p_x,\, p_y) \mapsto \left(\frac{\xi_1\eta_1 - \xi_2\eta_2}{2(\xi_1^2+\xi_2^2)}, \frac{\xi_2\eta_1 + \xi_1\eta_2}{2(\xi_1^2+\xi_2^2)}\right). \tag{3.3.6}$$

The potential part becomes

$$\begin{aligned} \tilde{U}(\xi_1, \xi_2; \mu) &= \frac{1-\mu}{\sqrt{(\xi_1^2+\xi_2^2)^2 + 2(\xi_1^2-\xi_2^2) + 2\mu - 1}} + \frac{\mu}{\sqrt{(\xi_1^2+\xi_2^2)^2}} \\ &= \frac{1}{\xi_1^2+\xi_2^2}\left(\frac{(1-\mu)(\xi_1^2+\xi_2^2)}{\sqrt{(\xi_1^2+\xi_2^2)^2 + 2(\xi_1^2-\xi_2^2) + 2\mu - 1}} + \mu\right). \end{aligned}$$

Thus, we obtain

$$\begin{aligned}\tilde{H}(\xi_1,\xi_2,\eta_1,\eta_2;\mu) = &\frac{\|\boldsymbol{\eta}\|^2}{8\|\boldsymbol{\xi}\|^2} - (1-\mu)\frac{\xi_1\eta_2+\xi_2\eta_1}{2\|\boldsymbol{\xi}\|^2} + \frac{1}{2}(\xi_2\eta_1-\xi_1\eta_2)\\ &+\frac{1}{\|\boldsymbol{\xi}\|^2}\left(\mu+\frac{(1-\mu)\|\boldsymbol{\xi}\|^2}{\sqrt{\|\boldsymbol{\xi}\|^4+2(\xi_1^2-\xi_2^2)+2\mu-1}}\right),\end{aligned}$$

where $\boldsymbol{\xi}=(\xi_1,\xi_2)$ and $\boldsymbol{\eta}=(\eta_1,\eta_2)$. If $(x(t),y(t))$ is a solution of (R3BP$_\mu$), $\tilde{H}$ is conserved along each solution, say $\tilde{H}=h$. Set $\Gamma := \|\boldsymbol{\xi}\|^2(\tilde{H}-h)$. The canonical equations with respect to $\Gamma$ become

$$\begin{aligned}\frac{d\xi_1}{d\tau} &= \|\boldsymbol{\xi}\|^2\tilde{H}_{\eta_1} = \eta_1-(1-\mu)\xi_2+o(|\boldsymbol{\xi}|^2+|\boldsymbol{\eta}|^2)\\ \frac{d\xi_2}{d\tau} &= \|\boldsymbol{\xi}\|^2\tilde{H}_{\eta_2} = \eta_2-(1-\mu)\xi_1+o(|\boldsymbol{\xi}|^2+|\boldsymbol{\eta}|^2)\\ \frac{d\eta_1}{d\tau} &= -\|\boldsymbol{\xi}\|^2\tilde{H}_{\xi_1} = (1-\mu)\eta_2-2(1-\mu-h)\xi_1+o(|\boldsymbol{\xi}|^2+|\boldsymbol{\eta}|^2)\\ \frac{d\eta_2}{d\tau} &= -\|\boldsymbol{\xi}\|^2\tilde{H}_{\xi_2} = (1-\mu)\eta_1-2(1-\mu-h)\xi_2+o(|\boldsymbol{\xi}|^2+|\boldsymbol{\eta}|^2).\end{aligned} \tag{3.3.7}$$

The solutions $\boldsymbol{\xi}(\tau)$ of (3.3.7) imply the solutions $\boldsymbol{\xi}(\tau(t))$ of the canonical equation for Hamiltonian $\tilde{H}$ by changing the time variable according to $\dfrac{d\tau}{dt}=\dfrac{1}{\|\boldsymbol{\xi}\|^2}$. Note that since the right hand sides of (3.3.7) are analytic at $(\xi_1,\xi_2)=(0,0)$, the solutions are also analytic.

Considering $(\xi_1,\xi_2)=(0,0)$ and the Taylor expansion at $\tau=0$, we obtain

$$\xi_1(\tau)=\sum_{i=1}^{\infty}a_i\tau^i,\ \xi_2(\tau)=\sum_{i=1}^{\infty}b_i\tau^i,\ \eta_1(\tau)=\sum_{i=0}^{\infty}c_i\tau^i,\ \eta_2(\tau)=\sum_{i=0}^{\infty}d_i\tau^i. \tag{3.3.8}$$

Substituting (3.3.8) into (3.3.7), we can determine the coefficients. The relation between $t$ and $\boldsymbol{\xi}$ yields

$$\begin{aligned}t &= \int\|\boldsymbol{\xi}\|^2d\tau\\ &= \int(a_1\tau+a_2\tau^2+\cdots)^2+(b_1\tau+b_2\tau^2+\cdots)^2d\tau\\ &= (a_1^2+b_1^2)\int\tau^2d\tau+o(\tau^4)\\ &= \frac{1}{3}(a_1^2+b_1^2)\tau^3+o(\tau^4).\end{aligned}$$

This implies that $x(t)$ and $y(t)$ are represented by the forms $x(t)=(1-\mu)+\sum_{i=2}^{\infty}\tilde{a}_it^{i/3}$ and $y(t)=\sum_{i=2}^{\infty}\tilde{b}_it^{i/3}$.

# 3.4 Proofs of the main theorems

## 3.4.1 Variational settings

As observed in Section 3.3.2, we can consider the action functional with Lagrangian (3.3.2) as having the same property of the one associated with (3.3.1). Define the action functional $\mathcal{B}_T$ by

$$\mathcal{B}_T(\boldsymbol{x};\mu) = \int_0^T L_{\mathrm{R3BP}}(\boldsymbol{x},\dot{\boldsymbol{x}};\mu)dt, \tag{3.4.1}$$

where $\boldsymbol{x} = (x, y)$ and $L_{\mathrm{R3BP}}$ is given by (3.3.2). The Euler-Lagrange equation of (3.3.2) is equivalent to (R3BP$_\mu$). We consider six types of boundary conditions. Denote $\Omega_i$ by $\Omega_i = \{\boldsymbol{x} \in H^1([0,T],\mathcal{D}) \mid \boldsymbol{x}(0) \in A_i, \boldsymbol{x}(T) \in B_i\}$ for each $i = 1, ..6$, where

**Case 1:** $A_1 = X^o$ and $B_1 = X^o$;

**Case 2:** $A_2 = X^o$ and $B_2 = X^+$;

**Case 3:** $A_3 = X^+$ and $B_3 = X^+$;

**Case 4:** $A_4 = X^-$ and $B_4 = X^+$;

**Case 5:** $A_5 = X^o$ and $B_5 = Y$;

**Case 6:** $A_6 = X^+$ and $B_6 = Y$.

We summarize our variational settings in the table below.

| Case | $A_i \to B_i$ | $\mu$ | Period | Region of time $\mathcal{T}(A,B)$ |
|---|---|---|---|---|
| Case 1 | $X^o \to X^o$ | $\mu \in (0,1)$ | 4T | $T > T_{L_1}(\mu)$ |
| Case 2 | $X^o \to X^+$ | $\mu \in (0,1)$ | 4T | $T > 0$ |
| Case 3 | $X^+ \to X^+$ | $\mu \in (0,1)$ | 4T | $T > T_{L_2}(\mu)$ and $T \neq 2n\pi$ $(n \in \mathbb{Z}_+)$ |
| Case 4 | $X^- \to X^+$ | $\mu \in (0,1)$ | 4T | $T > 0$ and $T \neq (2n-1)\pi$ $(n \in \mathbb{Z}_+)$ |
| Case 5 | $X^o \to Y$ | $\mu = 1/2$ | 2T | $2T > T_{L_1}(1/2)$ |
| Case 6 | $X^+ \to Y$ | $\mu = 1/2$ | 2T | $T > 0$ and $T \neq (n-\frac{1}{2})\pi$ $(n \in \mathbb{Z}_+)$ |

Table 3.1: Variational settings

Here, $T_{L_i}, i = 1, 2$, are defined in section 3.4.2. Now, we can define the time interval $\mathcal{T}(A,B)$ in Theorems 3.2.1 and 3.2.2. For example, following Table 3.1, we have:

$$\mathcal{T}(X^+,X^+) = \{T \in \mathbb{R} \mid T > T_{L_2}(\mu) \text{ and } T \neq 2n\pi \ (n \in \mathbb{Z}_+)\}$$

We do not need to consider the case of $(A,B) = (X^-,X^-)$ by replacing $\mu$ into $1-\mu$, i.e.,

$$\mathcal{T}(X^-,X^-) = \{T \in \mathbb{R} \mid T > T_{L_2}(1-\mu) \text{ and } T \neq 2n\pi \ (n \in \mathbb{Z}_+)\}.$$

In a similar way, the cases of $(A,B) = (X^o,X^+)$ and $(X^+,Y)$ lead to the ones of $(A,B) = (X^o,X^-)$ and $(X^-,Y)$. In addition, the set $\mathcal{T}(A,B)$ satisfies that $\mathcal{T}(A,B) = \mathcal{T}(B,A)$ for any $A, B \in \mathcal{X}$ from its construction. Hence, it is sufficient to only consider the six cases in Table 3.1. To prove that (3.4.1) attains the minimum at some $\boldsymbol{x}_i^*$ under each boundary condition, it is sufficient to show that (3.3.3) is coercive in $\Omega_i$ for each $i \in \{1, ..., 6\}$ from Lemma 3.3.2. Applying Lemma 3.3.3 to Cases 1, 2, and 5 yields the coercivity of $\mathcal{B}|_{\Omega_1}$, $\mathcal{B}|_{\Omega_2}$ and $\mathcal{B}|_{\Omega_5}$. Hence, we obtain the following proposition:

**Proposition 3.4.1.** *For each $i \in \{1, 2, 5\}$, the action functional $\mathcal{B}_T|_{\Omega_i}$ attains the minimum.*

Next, we focus on Case 2. If $T = (n - \frac{1}{2})\pi$, $X^+$ is a subset of $Y$ in the original coordinates and is an unbounded set. Set a constant map sequence $\boldsymbol{a}_n(t) := (n, 0)$. It is easy to check $\mathcal{A}_T > 0$ and $\lim_{n\to\infty} \mathcal{A}_T(\boldsymbol{a}_n; \mu) = 0$, so $\mathcal{A}_T|_{\Omega_2}$ does not attain the minimum. Hence, $\mathcal{A}_T|_{\Omega_2}$ does not possess the minimum if $T = (n - \frac{1}{2})\pi$. By contrast, invoking Lemma 3.3.4 and 3.3.5 yields that $\mathcal{A}_T|_{\Omega_2}$ has coercivity if $T \neq (n - \frac{1}{2})\pi$. Similar considerations apply to Cases 5 and 6 and we get the next proposition.

**Proposition 3.4.2.** *The functionals $\mathcal{B}_T|_{\Omega_3}$, $\mathcal{B}_T|_{\Omega_4}$ and $\mathcal{B}_T|_{\Omega_6}$ are coercive except for $T = 2n\pi$, $T = (2n-1)\pi$ and $T = (n - \frac{1}{2})\pi$ respectively.*

If the obtained minimizers are not singular, we get periodic orbits from the following proposition.

**Proposition 3.4.3.** *If $\boldsymbol{x}^*$ is a collision-free critical point of $\mathcal{B}_T|_{\Omega_i}$ $(i = 1, .., 6)$, it connects with the reversed solution smoothly. In addition, it is a periodic orbit that is orthogonal to each boundary condition.*

*Proof.* The variational standard argument implies that a critical point of $\mathcal{B}_T|_{\Omega_1}$ satisfies $\dot{x}(0) = 0$ and $\dot{y}(T) = 0$. Applying similar arguments to the rest of the boundary conditions, we conclude that each critical point of $\mathcal{B}_T|_{\Omega_i}(i = 1, .., 6)$ is orthogonal to each boundary condition. Combining Lemma 3.3.7 and Proposition 3.3.8 gives a new solution $R\boldsymbol{x}_i^*(-t)$. Moreover, we obtain another solution $-R\boldsymbol{x}_i^*(-t)$ in Cases 5 and 6. Connecting these, we obtain a periodic orbit. ☐

### 3.4.2 Estimate of equilibrium points

The R3BP has three equilibrium points $L_1$, $L_2$, and $L_3$ on the $x$-axis. It is sufficient to consider $L_1$ and $L_2$ by symmetry with respect to $\mu$. It is clear that $L_1 = (l_1, 0) \in \Omega_3$ and $L_2 = (l_2, 0) \in \Omega_5$. In the case of $\mu = 1/2$, $L_1 = (0, 0) \in \Omega_1$. We need to study a condition under which a minimizer is not identical to the equilibrium points. To check this, we calculate the second variation $\mathcal{B}_T''$ at $L_1$ and $L_2$. A simple calculation implies that for $i = 1, 2$,

$$\begin{aligned}\mathcal{B}_T''(L_i;\mu)(\delta_1,\delta_2) &= \int_0^T \dot{\delta}_1^2 + \dot{\delta}_2^2 + \left(1 + \frac{\partial^2 U}{\partial x^2}\right)\delta_1^2 + \left(1 + \frac{\partial^2 U}{\partial y^2}\right)\delta_2^2 + 2(\delta_1\dot{\delta}_2 - \delta_2\dot{\delta}_1)dt \\ &= \int_0^T \dot{\delta}_1^2 + \dot{\delta}_2^2 + \delta_1^2 + \delta_2^2 + \alpha_i(\mu)(2\delta_1^2 - \delta_2^2) + 2(\delta_1\dot{\delta}_2 - \delta_2\dot{\delta}_1)dt,\end{aligned} \tag{3.4.2}$$

where

$$\alpha_i(\mu) = \frac{1}{2}\frac{\partial^2 U(\boldsymbol{x};\mu)}{\partial x^2}\bigg|_{\boldsymbol{x}=L_i} = -\frac{\partial^2 U(\boldsymbol{x};\mu)}{\partial y^2}\bigg|_{\boldsymbol{x}=L_i} \qquad (i = 1, 2).$$

If (3.4.2) at $L_i$ is negative for some $\delta_1$ and $\delta_2$, then $L_i$ is not a minimizer ($i = 1, 2$). In Cases 1 and 3, we take a test path as $\boldsymbol{\delta}(t) = (\delta_1(t), \delta_2(t)) = \left(\nu_1 \cos\left(-\frac{\pi}{T}t\right), \nu_2 \sin\left(-\frac{\pi}{T}t\right)\right)$. Then the second variation can be estimated by

$$\begin{aligned}
&\mathcal{B}_T''(L_1;\mu)(\delta_1,\delta_2)\\
&= \frac{T}{2}\left\{(1+\gamma^2+2\alpha_1(\mu))\nu_1^2 + 4\gamma\nu_1\nu_2 + (1+\gamma^2-\alpha_1(\mu))\nu_2^2\right\}\\
&= \frac{T}{2}\Bigg\{(1+\gamma^2+2\alpha_1(\mu))\left(\nu_1 + \frac{2\gamma}{(1+\gamma+2\alpha_1(\mu))}\nu_2\right)^2\\
&\qquad + \left((1+\gamma^2-\alpha_1(\mu)) - \frac{4\gamma^2}{(1+\gamma^2+2\alpha_1(\mu)}\right)\nu_2^2\Bigg\}
\end{aligned}$$

where $\gamma = -\frac{\pi}{T}$. This calculation shows that if $(1+\gamma^2-\alpha_1(\mu)) - 4\gamma^2/(1+\gamma^2+2\alpha_1(\mu)) < 0$, that is, $\gamma^4 + (\alpha_1(\mu)-2)\gamma^2 + 1 + \alpha_1(\mu) - 2\alpha(\mu)^2 < 0$, then there are constants $\nu_1 > 0$ and $\nu_2 > 0$ such that $\mathcal{B}_T''(L_1;\mu)(\delta_1,\delta_2) < 0$. We conclude that for $i = 1, 2$, the equilibrium point $L_i$ is not a minimizer if

$$T > \pi\sqrt{\frac{2}{-(\alpha_i(\mu)-2)+\sqrt{\alpha_i(\mu)(9\alpha_i(\mu)-8)}}} =: T_{L_i}(\mu). \tag{3.4.3}$$

This is the definition of $T_{L_i}(\mu)$ in Table 3.1.

In Case 5, we take a new test path as $\boldsymbol{\delta}(t) = \left(\nu_1 \cos\left(-\frac{\pi}{2T}t\right), \nu_2 \sin\left(-\frac{\pi}{2T}t\right)\right)$ and set $\gamma = -\frac{\pi}{2T}$ It immediately follows that if $T > T_{L_1}(\mu)/2$, then $L_1$ is not a minimizer.

**Remark 3.4.4.** *One can not precisely calculate the position of $L_1$ except for the case of $\mu = 1/2$. However, if we have two functions $g_i\colon \mathbb{R} \to \mathbb{R}$ ($i = 1, 2$) that satisfy the inequality $g_1(\mu) \le L_1 \le g_2(\mu)$, the second derivative can be estimated by*

$$\begin{aligned}
\frac{\partial^2 U}{\partial x^2} &= 2\frac{1-\mu}{d_1^3} + 2\frac{\mu}{d_2^3} \le 2\frac{1-\mu}{(g_1(\mu)+\mu)^3} + 2\frac{\mu}{((1-\mu)-g_2(\mu))^3} =: \beta_1(\mu)\\
\frac{\partial^2 U}{\partial y^2} &= -\frac{1-\mu}{d_1^3} - \frac{\mu}{d_2^3} \le -\frac{1-\mu}{(g_2(\mu)+\mu)^3} - \frac{\mu}{((1-\mu)-g_1(\mu))^3} =: \beta_2(\mu).
\end{aligned}$$

*Using $\beta_1$ and $\beta_2$, the upper bound of the second variation is given by*

$$\mathcal{B}_T''(L_1;\mu)(\delta_1,\delta_2) \le \int_0^T \dot\delta_1^2 + \dot\delta_2^2 + \delta_1^2 + \delta_2^2 + 2\beta_1(\mu)\delta_1^2 + \beta_2(\mu)\delta_2^2 + 2(\delta_1\dot\delta_2 - \delta_2\dot\delta_1)dt.$$

**Remark 3.4.5.** *For sufficiently small $\mu$, it is known that $d_1 = 1 + 3^{-1/3}\mu^{1/3} + o(\mu^2)$ and $d_2 = 3^{-1/3}\mu^{1/3} + o(\mu^2)$ (See [30]). Applying these yields*

$$\begin{aligned}
\lim_{\mu\to 0}\alpha_i(\mu) &= \lim_{\mu\to 0}\left(1 + \frac{(1-\mu)(d_1^3-1)}{d_1^3 d_2}\right)\\
&= \lim_{\mu\to 0}\left(1 + \frac{(1-\mu)(d_1-1)(d_1^2+d_1+1)}{d_1^3 d_2}\right)\\
&= \lim_{\mu\to 0}\left(1 + \frac{(1-\mu)(d_1^2+d_1+1)}{d_1^3}\right) = 4.
\end{aligned}$$

*Thus for each $i = 1, 2$, $\lim_{\mu\to 0} T_{L_i}(\mu) = \pi/(-1+2\sqrt{7})^{1/2}(=: T_0)$. This period is the same as one in [30]. By contrast, $\lim_{\mu\to 1} T_{L_2}(\mu) = \pi$ and then our theorems imply the existence of $2\pi$-periodic orbits.*

### 3.4.3 Elimination of interior collisions

To guarantee that the obtained minimizers are smooth, it suffices to show that each minimizer has no collision. Marchal's theorem in [33] states that any minimizer has no collision in $(0, T)$ in the $n$-body problem under the fixed-ends constraint ($\boldsymbol{x}(0) = \boldsymbol{a}$, $\boldsymbol{x}(T) = \boldsymbol{b}$). We confirm that it holds for (R3BP$_\mu$).

**Proposition 3.4.6.** *Let $H^1$ denote the Sobolev space. If*

$$\mathcal{B}_T(\boldsymbol{x}^*; \mu) = \inf_{\boldsymbol{x} \in H^1} \mathcal{B}_T(\boldsymbol{x}; \mu),$$

*then for any $\mu \in (0, 1)$, the point $\boldsymbol{x}^*$ has no collision for any $t \in (0, T)$.*

*Proof.* Suppose a collision occurs at $t = a$. By a time transformation, we can assume $a = 0$ without loss of generality. Let

$$\tilde{\mathcal{B}}_T(\boldsymbol{x}; \mu) = \int_{-T'}^{T''} \tilde{L}_{\text{R3BP}}(\boldsymbol{x}, \dot{\boldsymbol{x}}; \mu) dt, \tag{3.4.4}$$

where $T' + T'' = T$ and

$$\begin{aligned} &\tilde{L}_{\text{R3BP}}(\boldsymbol{x}, \dot{\boldsymbol{x}}; \mu) \\ &:= L_{\text{R3BP}}(\boldsymbol{x} + (\mu, 0), \dot{\boldsymbol{x}}; \mu) \\ &= \frac{1}{2}(\dot{x}^2 + \dot{y}^2) + x\dot{y} - y\dot{x} + \frac{1}{2}(x^2 + y^2) + \mu(\dot{y} + x) + \frac{\mu}{\sqrt{x^2 + y^2}} + \frac{1 - \mu}{\sqrt{(x+1)^2 + y^2}}. \end{aligned} \tag{3.4.5}$$

There is no loss of generality in considering $\tilde{\mathcal{B}}_T$ instead of $\mathcal{B}_T$ since we just use a coordinate transformation.

Let $(x_{\text{col}}, y_{\text{col}})$ denote an orbit with a collision at $t = 0$. We take $x_\theta$ and $y_\theta$ as the following:

$$x_\theta = \begin{cases} x_{\text{col}} + R_0(t) \cos\theta & t \in [-T', 0), \\ x_{\text{col}} + R_1(t) \cos\theta & t \in [0, T''] \end{cases}$$

and

$$y_\theta = \begin{cases} y_{\text{col}} + R_0(t) \sin\theta & t \in [-T', 0), \\ y_{\text{col}} + R_1(t) \sin\theta & t \in [0, T'']. \end{cases}$$

where $R_0(t) = \left(1 + \dfrac{t}{T'}\right)\rho$ and $R_1(t) = \left(1 - \dfrac{t}{T''}\right)\rho$.

A simple calculation shows that

$$\int_{S^1} \int_0^T x_\theta \dot{y}_\theta - y_\theta \dot{x}_\theta + \mu(\dot{y}_\theta + x_\theta) dt d\theta = \int_{S^1} \int_0^T x_{\text{col}} \dot{y}_{\text{col}} - y_{\text{col}} \dot{x}_{\text{col}} + \mu(\dot{y}_{\text{col}} + x_{\text{col}}) dt d\theta$$

and

$$\frac{1}{|S^1|}\int_{S^1}\int_0^T \frac{1}{2}(x_\theta^2+y_\theta^2)dtd\theta = \int_0^T \frac{1}{2}(x_{\mathrm{col}}^2+y_{\mathrm{col}}^2)dt + \int_0^T R_1(t)^2dt$$
$$= \int_0^T \frac{1}{2}(x_{\mathrm{col}}^2+y_{\mathrm{col}}^2)dt + \frac{T}{3}\rho^2.$$

The rest of the part is similar to the Kepler problem. As a result in [17], the estimate of interior collisions is given by

$$\frac{1}{|S^1|}\int_{S^1}\tilde{\mathcal{B}}_T(\boldsymbol{x}_\theta;\mu)d\theta - \tilde{\mathcal{B}}_T(\boldsymbol{x}_{\mathrm{col}};\mu)$$
$$\leq \left(\frac{T}{3}+\frac{1}{2T}\right)\gamma^2 t_0^{4/3}(1+O(t_0)) + (\frac{\pi}{2}-3)\frac{t_0^{1/3}}{\gamma}(1+O(t_0)) + ((\frac{\pi}{2}-1)\frac{t_0^{1/3}}{\gamma} + O(t_0^{4/3}\log(1/t_0))$$
$$= (\pi-4)\frac{t_0^{1/3}}{\gamma} + O(t_0^{4/3}\log(1/t_0)) \leq 0,$$

where $t_0$ is sufficiently small and $\rho = \gamma t_0^{2/3} + O(t_0^{2/3})$. □

### 3.4.4 Elimination of boundary collisions

By Proposition 3.4.6, we only need to consider orbits that have a collision at $t = 0$ or $T$. If a collision occurs at $t = 0$, it is shown that the orbit, say $(x_{\mathrm{col}}, y_{\mathrm{col}})$, is represented by

$$x_{\mathrm{col}} = \sum_{j=0}^{\infty} c_{1j}t^{j/3},\ \ y_{\mathrm{col}} = \sum_{j=0}^{\infty} c_{2j}t^{j/3}$$

We say that an orbit has *$\rho$-collision* if it has a collision at $t = 0$ and $\lim_{t\to+0}\dot{y}(t)/\dot{x}(t) = \tan\rho$. In the case of a double collision in the $N$-body problem, Proposition 5.7 of [24] implies that if the collision angle $\rho$ satisfies $-\pi < \rho < \pi$, it is not a minimizer. As seen in Section 3.3, the asymptotic behavior of the R3BP is the same as in the $N$-body problem, so we can adapt the approach in [24] to the R3BP. Hence, in the R3BP, it suffices to consider the case $\rho = \pm\pi$, i.e. the velocity of $y(0)$ is 0.

As seen in Section 3.3, Sundman's estimate is a useful way to study a collision path. Substituting Sundman's estimate into (R3BP$_\mu$) and applying coefficient comparison, we obtain

$$x_{\mathrm{col}}(t) = (1-\mu) + c_1t^{2/3} + o(t^2),\ y_{\mathrm{col}}(t) = c_2t^{5/3} + o(t^2), \quad (t\in[0,\varepsilon]), \tag{3.4.6}$$

where $c_1 = (9/2)^{1/3}\mu^{1/3}$, $c_2 = -(9/2)^{1/3}\mu^{1/3}$, and $\varepsilon$ is sufficiently small. By a polar coordinate, (3.4.1) can be written as

$$\mathcal{B}_T((r,\theta);\mu) = \int_0^T \frac{1}{2}(\dot{r}^2 + r^2\dot{\theta}^2) + r^2\dot{\theta} + \frac{1}{2}r^2 + \frac{1-\mu}{r_1} + \frac{\mu}{r_2}dt$$

where $r_1$ and $r_2$ represent the distance from $(-\mu, 0)$ and from $(1-\mu, 0)$ respectively.

**Proposition 3.4.7** (Local estimate, The case of $\rho = \pm\pi$)**.** *Minimizers under our boundary conditions do not have $\pi$ and $(-\pi)$- collision.*

*Proof.* Applying a polar transformation to (3.4.6), $\pi$-collision orbits are represented by the following:

$$\begin{aligned} r_{\mathrm{col}}(t) &= (1-\mu) + c_1 t^{2/3} + o(t^2) \\ \theta_{\mathrm{col}}(t) &= \frac{c_2}{1-\mu} t^{5/3} + o(t^2). \end{aligned} \tag{3.4.7}$$

For sufficiently small $\varepsilon > 0$, we deform $\theta_{\mathrm{col}}(t)$ to $\theta_{\mathrm{de}}(t) = \dfrac{c_2}{1-\mu}\varepsilon^{2/3} t + o(t^2)$ in $t \in [0, \varepsilon]$ and do not change $r_{\mathrm{col}}(t)$, i.e. $r_{\mathrm{de}} := r_{\mathrm{col}}$. Thus, we obtain

$$\int_0^\varepsilon K(r_{\mathrm{col}}, \theta_{\mathrm{col}}) - K(r_{\mathrm{col}}, \theta_{\mathrm{de}}) dt = \int_0^\varepsilon \frac{1}{2} r_{\mathrm{col}}^2 \{(\dot\theta_{\mathrm{col}}^2 - \dot\theta_{\mathrm{de}}^2) + 2(\dot\theta_{\mathrm{col}} - \dot\theta_{\mathrm{de}})\} dt$$

Because the main terms of $r_{\mathrm{col}}$ are $1-\mu$, it is sufficient to calculate

$$\frac{1}{2}\int_0^\varepsilon (1-\mu)^2 \{(\dot\theta_{\mathrm{col}}^2 - \dot\theta_{\mathrm{de}}^2) + 2(\dot\theta_{\mathrm{col}} - \dot\theta_{\mathrm{de}})\} dt. \tag{3.4.8}$$

Note that $\theta_{\mathrm{col}}$ and $\theta_{\mathrm{de}}$ have the same boundary and this implies

$$\int_0^\varepsilon (\dot\theta_{\mathrm{col}} - \dot\theta_{\mathrm{de}}) dt = 0.$$

By the above remarks, (3.4.8) is calculated as follows:

$$\begin{aligned} &\int_0^\varepsilon \frac{1}{2}(1-\mu)^2 (\dot\theta_{\mathrm{col}}^2 - \dot\theta_{\mathrm{de}}^2) dt + \int_0^\varepsilon (1-\mu)^2 (\dot\theta_{\mathrm{col}} - \dot\theta_{\mathrm{de}}) dt, \\ &= \frac{1}{2}(1-\mu)^2 \int_0^\varepsilon (\dot\theta_{\mathrm{col}} - \dot\theta_{\mathrm{de}})(\dot\theta_{\mathrm{col}} + \dot\theta_{\mathrm{de}}) dt \\ &= \frac{1}{2}(1-\mu)^2 \int_0^\varepsilon \left(\frac{5}{3}\frac{c_2}{1-\mu} t^{2/3} - \frac{c_2}{1-\mu}\varepsilon^{2/3}\right)\left(\frac{5}{3}\frac{c_2}{1-\mu} t^{2/3} + \frac{c_2}{1-\mu}\varepsilon^{2/3} + o(t^2)\right) dt \\ &= \frac{1}{2}(1-\mu)^2 \int_0^\varepsilon \left(\frac{5}{3}\frac{c_2}{1-\mu}\right)^2 t^{4/3} - \left(\frac{c_2}{1-\mu}\right)^2 \varepsilon^{4/3} + o(t^2) dt \\ &= \frac{1}{2}(1-\mu)^2 \cdot \frac{4}{21}\left(\frac{c_2}{1-\mu}\right)^2 \varepsilon^{7/3} + o(\varepsilon^3) = \frac{2}{21}(1-\mu)^2 \left(\frac{c_2}{1-\mu}\right)^2 \varepsilon^{7/3} + o(\varepsilon^3) > 0 \end{aligned}$$

Next, we consider the value of the potential part. The Taylor expansion shows

$$\begin{aligned} r_1^2 &= r_{\mathrm{col}}(s)^2 + 2\,\mu\,(1-\mu)\left(1 + \frac{c_1\, s^2}{1-\mu}\right)\cos\left(\frac{c_2\, s^5}{1-\mu}\right) + \mu^2 \\ r_2^2 &= r_{\mathrm{col}}(s)^2 - (2 - 2\,\mu)\,(1-\mu)\left(1 + \frac{c_1\, s^2}{1-\mu}\right)\cos\left(\frac{c_2\, s^5}{1-\mu}\right) + (1-\mu)^2, \end{aligned} \tag{3.4.9}$$

where $s = t^{1/3}$. Substituting (3.4.9) into the potential $U$, we obtain

$$\begin{aligned} \int_0^\varepsilon U(r_{\mathrm{col}}, \theta_{\mathrm{col}}) - U(r_{\mathrm{col}}, \theta_{\mathrm{de}}) dt &= -\frac{\mu c_2^2}{1-\mu}\varepsilon^{4/3} \int_0^\varepsilon t^2 + o(t^4) dt \\ &= c_4 \varepsilon^{13/3} + o(\varepsilon^5) < 0. \end{aligned}$$

Hence, the orbit $(x_{\mathrm{col}}, y_{\mathrm{col}})$ is not a minimizer. In the same manner, we can see that $(-\pi)$-collision orbits are not minimizers. A similar approach is valid when a collision occurs at $t = T$.

Moreover, collisions with both primaries do not occur since such an orbit can be changed in $t \in [0, \varepsilon]$ similar to the above, and the action value of the deformed orbit is smaller. $\square$

## 3.5 Global behavior of the obtained minimizers and open problems

In this section, we discuss the remaining problems including open problems. Theorems 3.2.1 and 3.2.2 show the existence of periodic solutions; however, we do not know how their minimizers behave in time $t \in (0, T)$. More precisely, we discuss the following:

**Q1.** Do the obtained periodic solutions in Theorems 3.2.1 and 3.2.2 have the same topology as Figures 3.3 and 3.4?

**Q2.** Our main theorems (Theorems 3.2.1 and 3.2.2) show the existence of $2T$- or $4T$-periodic solutions. Are these periods minimal?

**Q3.** Are periodic orbits obtained under different boundary conditions different?

Although we do not answer these questions completely, we can partially solve them.

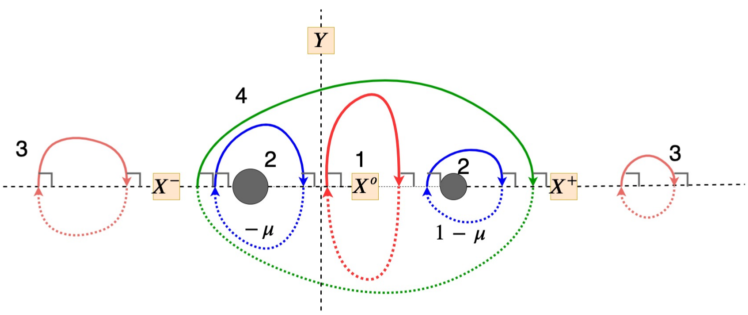


Figure 3.3: Minimizers of Cases 1 - 4

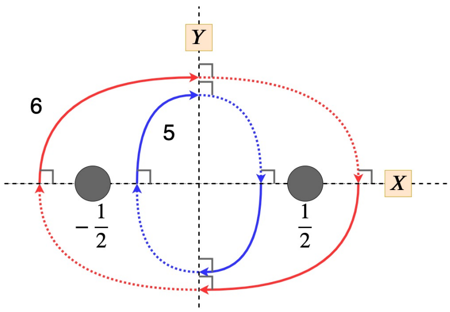


Figure 3.4: Minimizers of Cases 5 and 6

First, we consider Q1. Orbit 5 in Figure 3.4 satisfies the boundary condition of Case 5. In the R3BP, the integral of the second term $x\dot{y} - y\dot{x}$ in (3.3.2) corresponds to the area and gives a negative value for minimizers. If the direction of the orbits is clockwise, the second term is negative. If it is counter-clockwise, it is positive. We focus on minimizers of (3.4.1), so it is sufficient to consider clockwise orbits. By contrast, the integral of the third term $(x^2 + y^2)/2$ in (3.3.2) is a positive value, so it is difficult to see the behavior of minimizers in the R3BP. The same difficulty occurs for Figures 3.3 and 3.4. For example, is orbit 1 in Figure 3.5 a minimizer of Case 1? Hence, all we can show here is that minimizing orbits are clockwise.

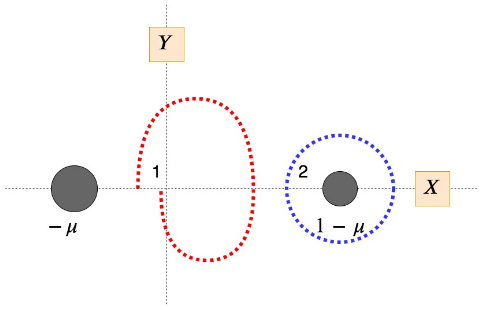


Figure 3.5: Irregular types

We move on to Q2. If we obtain a $T$-periodic solution that follows from one of the main theorems, $T$ may not be the minimal period of the solution. For any $n, m \in \mathbb{N}$, $nT$-periodic and $mT$-periodic solutions may be the same. We can not show that all periodic solutions are distinct, but we can prove the existence of an infinite number of periodic solutions. The proof is based on Rabinowitz's idea in [48].

**Proposition 3.5.1.** *Assume that there is a $T_0$-periodic solution that has a minimal period $T_0 > 0$. Then we get infinitely many $T$-periodic solutions satisfying $T \in (0, T_0)$.*

*Proof.* We choose $T = T_0/4$. Cases $2, 4$, and $6$ in Table 3.1 show the existence of a $T_0/2$-periodic solution. Clearly, its minimal period is not $T_0$, so we obtain a new periodic solution and $T'$ is defined by a minimal period of the new solution. We now apply this argument again with $T$ replaced by $T'$. The rest of the proof is simple. □

We discuss the final question. Q3 asks, for instance, whether periodic orbits of Theorems 3.2.1 and 3.2.2 are different for $\mu = 1/2$. There is another problem. Consider orbit 2 in Figure 3.5. Is this a minimizer of Case 1 or an orbit consisting of minimizers in Case 2? We guess that if $T - T_{L_1}(\mu)$ is sufficiently small, this problem does not occur because a minimizer of this case may be closed to each equilibrium point. However, it remains an open problem whether a periodic solution satisfies another boundary condition for large $T > 0$.

# Chapter 4

# Special cases of the restricted three-body problem

In this chapter, we treat special cases of the restricted three-body problem, *the Hill problem* and *planar two-center problem*.

## 4.1 The Hill problem

### 4.1.1 Main results

The Hill problem models the motion of an asteroid or artificial satellite close to the second primary in the R3BP. Particles around the Earth are the most affected by the gravitational force of the Earth. Thus the motion is modeled by the Kepler problem

$$\begin{aligned}
\ddot{X} &= -\frac{X}{(X^2+Y^2+Z^2)^{3/2}} \\
\ddot{Y} &= -\frac{Y}{(X^2+Y^2+Z^2)^{3/2}} \\
\ddot{Z} &= -\frac{Z}{(X^2+Y^2+Z^2)^{3/2}}.
\end{aligned}$$

Other forces which affect the particles are the gravitational force of the Sun, the Coriolis and the centrifugal force due to the Earth's revolution. The model which involves these force is the spatial Hill problem:

$$\begin{aligned}
\ddot{X} &= 2\dot{Y} + 3X - \frac{X}{(X^2+Y^2+Z^2)^{3/2}} \\
\ddot{Y} &= -2\dot{X} - \frac{Y}{(X^2+Y^2+Z^2)^{3/2}} \\
\ddot{Z} &= -Z - \frac{Z}{(X^2+Y^2+Z^2)^{3/2}}.
\end{aligned} \tag{4.1.1}$$

The Hill problem is more accurate than the Kepler problem for particles around the Earth like artificial satellites (see [30, 56] for more detail). This problem has been studied to design orbits of space probes. See [26] for example.

In Section 4.1, we show the existence of several symmetric periodic orbits in the Hill problem. Let

$$\begin{aligned}
&L_{X+} = \{(X,0,0) \mid X > 0\}, && L_{X-} = \{(X,0,0) \mid X < 0\},\\
&L_{Y+} = \{(0,Y,0) \mid Y > 0\}, && L_{Y-} = \{(0,Y,0) \mid Y < 0\},\\
&P_{XZ} = \{(X,0,Z) \mid (X,Z) \in \mathbb{R}\backslash\{(0,0)\}\}, && P_{YZ} = \{(0,Y,Z) \mid (Y,Z) \in \mathbb{R}\backslash\{(0,0)\}\}.
\end{aligned}$$

Let $T_0 > 0$ be the constant determined by $\cos T_0 = T_0$, which is approximately 0.739.

**Theorem 4.1.1.** *For the spatial Hill problem* (4.1.1), *the followings hold.*

*(i) For each $0 < T < 1$, there is a $2T$-periodic orbit satisfying $\boldsymbol{q}(0) \in L_{X+}, \boldsymbol{q}(T) \in L_{X-}$.*

*(ii) For each $0 < T < 1$, there is a $4T$-periodic orbit satisfying $\boldsymbol{q}(0) \in L_{X+}, \boldsymbol{q}(T) \in L_{Y+}$.*

*(iii) For each $0 < T < T_0$, there is a $4T$-periodic orbit satisfying $\boldsymbol{q}(0) \in L_{X+}, \boldsymbol{q}(T) \in L_{Y-}$.*

*(iv) For each $0 < T < T_0$, there is a $4T$-periodic orbit satisfying $\boldsymbol{q}(0) \in L_{X+}, \boldsymbol{q}(T) \in P_{YZ}$.*

*(v) For each $0 < T < 1$, there is a $2T$-periodic orbit satisfying $\boldsymbol{q}(0) \in L_{Y+}, \boldsymbol{q}(T) \in L_{Y-}$.*

*(vi) For each $0 < T < T_0$, there is a $4T$-periodic orbit satisfying $\boldsymbol{q}(0) \in L_{Y+}, \boldsymbol{q}(T) \in P_{XZ}$.*

See figure 4.1.

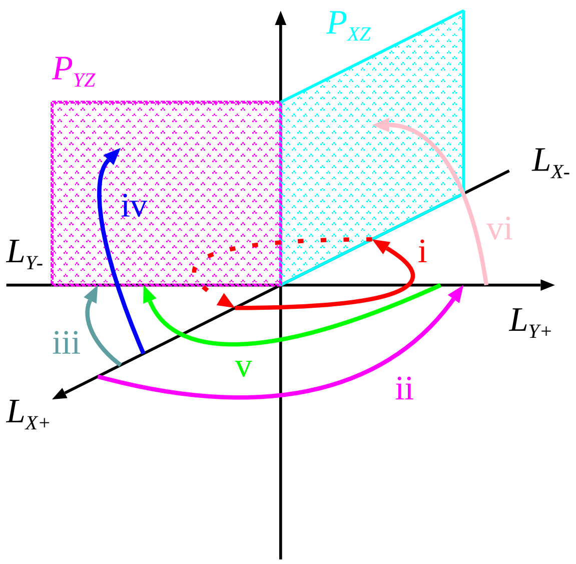


Figure 4.1: Boundary conditions

To prove this theorem, we use a variational method. The Lagrangian for the Hill problem (4.1.1) is

$$\mathcal{L} = \frac{\dot{X}^2}{2} + \frac{\dot{Y}^2}{2} + \frac{\dot{Z}^2}{2} + X\dot{Y} - Y\dot{X} + \frac{3X^2}{2} - \frac{Z^2}{2} + \frac{1}{\sqrt{X^2+Y^2+Z^2}}.$$

The Hill problem is equivalent to the variational problem with respect to the action functional

$$\mathcal{A}_T = \int_0^T \mathcal{L} dt.$$

The result is organized as follows. Next section, we show the coercivity condition for the existence of a minimizer under the boundary conditions corresponding to each orbit in Theorem 4.1.1. We also show that the obtained minimizers have no collision by applying our previous result. In Section 4.1.3, we state the reversibility of the Hill problem and show that the obtained minimizers are periodic orbits. From the viewpoint of an application to the trajectory design for artificial satellites, we need orbits on a prescribed plane. For example, geosynchronous satellites move directly above the Earth's equator. We also prove the existence of several periodic orbits in the constrained problem. Section 4.1.4 is devoted to the study of the existence of periodic orbits of the holonomic constraint system on a prescribed plane. The last section, we show the numerical solutions.

### 4.1.2 Coercivity and the existence of minimizers

For subsets $D_1, D_2 \subset \mathbb{R}^3$, let

$$\Omega(D_1, D_2; T) = \{\gamma \in H^1([0,T], \mathbb{R}^3 \backslash \{\mathbf{0}\}) \mid \gamma(0) \in D_1, \gamma(T) \in D_2\}.$$

Here $H^1$ denotes the Sobolev space. By taking $L_{X+}, \ldots, P_{YZ}$ in Section 1 as $D_1$ and $D_2$, we will show the existence of a minimizer of $\mathcal{A}_T|_{\Omega(D_1,D_2;T)}$. We call the functional $\mathcal{A}_T|_{\Omega(D_1,D_2;T)}$ coercive if $\mathcal{A}_T|_{\Omega(D_1,D_2;T)}(\gamma) \to \infty$ as $\|\gamma\|_{H^1} \to \infty (\gamma \in \Omega(D_1, D_2; T))$. It is well-known that there is a minimizer of $\mathcal{A}_T|_{\Omega(D_1,D_2;T)}$ on $\overline{\Omega(D_1, D_2; T)(\gamma)}$ if the functional is coercive.

By changing variables

$$X = (\cos t)x + (\sin t)y, Y = -(\sin t)x + (\cos t)y, Z = z,$$

the Lagrangian becomes

$$\begin{aligned}\mathcal{L}_{\mathrm{rot}} = &\frac{1}{2}(\dot{x}^2 + \dot{y}^2 + \dot{z}^2) \\ &+ \frac{3(\cos^2 t)x^2}{2} - \frac{3(\cos^2 t)y^2}{2} + 3\cos(t)\sin(t)xy - \frac{x^2}{2} + y^2 \\ &- \frac{z^2}{2} + \frac{1}{\sqrt{x^2+y^2+z^2}}.\end{aligned}$$

We estimate the terms on its second line by using the polar coordinate $(x, y) = r(\cos\theta, \sin\theta)$:

$$\begin{aligned}&\frac{3(\cos^2 t)x^2}{2} - \frac{3(\cos^2 t)y^2}{2} + 3\cos(t)\sin(t)xy - \frac{x^2}{2} + y^2 \\ &= \frac{3r^2\cos(2t-2\theta)}{4} + \frac{1}{4}r^2 \geq -\frac{1}{2}r^2 = -\frac{1}{2}(x^2+y^2).\end{aligned}$$

Therefore, we get

$$\mathcal{L}_{\mathrm{rot}} \geq \frac{1}{2}(\dot{x}^2 + \dot{y}^2 + \dot{z}^2) - \frac{1}{2}x^2 - \frac{1}{2}y^2 - \frac{1}{2}z^2 + \frac{1}{\sqrt{x^2+y^2+z^2}} =: \tilde{\mathcal{L}}.$$

Define

$$\tilde{\mathcal{A}}_T = \int_0^T \tilde{\mathcal{L}} dt.$$

If $\tilde{A}_T|_{\Omega(D_1,D_2;T)}$ is coercive, so is $\mathcal{A}_T|_{\Omega(D_1,D_2;T)}$.

Let

$$(x(0), y(0)) \cdot (x(T), y(T)) = |(x(0), y(0))||(x(T), y(T))| \cos \rho.$$

For example, in the case of $D_1 = L_{X+}, D_2 = L_{X-}$ which corresponds to (i) in Theorem 4.1.1, the boundary condition is represented by

$$\begin{aligned}
&x(0) > 0, y(0) = z(0) = 0 \\
&(\cos T)x(T) + (\sin T)y(T) < 0, -(\sin T)x(T) + (\cos T)y(T) = 0, z(T) = 0 \\
&(x(T), y(T), z(T)) \in \{\xi(\cos(T+\pi), \sin(T+\pi), 0) \mid \xi > 0\}.
\end{aligned}$$

Hence, $\rho = T + \pi$.

Note that

$$\int_0^T |\dot{\boldsymbol{x}}|^2 dt \geq \frac{1}{T} \left( \int_0^T |\dot{\boldsymbol{x}}| dt \right)^2.$$

Let

$$r_{\max} = \max_{t \in [0,T]} |\boldsymbol{x}(t)|.$$

If $|\rho| < \pi/2$,

$$\tilde{\mathcal{A}}_T \geq \frac{1}{2T}(r_{\max}^2 \sin^2 \rho) - \frac{1}{2} T r_{\max}^2 = \frac{r_{\max}^2}{2} (\frac{\sin^2 \rho}{T} - T).$$

If $\pi/2 < |\rho| < \pi$,

$$\tilde{\mathcal{A}}_T \geq \frac{1}{2T}(r_{\max}^2) - \frac{1}{2} T r_{\max}^2 = \frac{r_{\max}^2}{2} (\frac{1}{T} - T).$$

In the case that

$$\|\boldsymbol{x}\|_{H^1} = (\|\dot{\boldsymbol{x}}\|_{L^2}^2 + \|\boldsymbol{x}\|_{L^2}^2)^{1/2} \to \infty$$

and that $\|\boldsymbol{x}\|_{L^2}^2 < \infty$, $\tilde{\mathcal{A}}_T$ diverges to infinity since

$$\tilde{\mathcal{A}}_T \geq \frac{1}{2} \|\dot{\boldsymbol{x}}\|_{L^2}^2 - \frac{1}{2} \|\boldsymbol{x}\|_{L^2}^2.$$

In the case of $\|\boldsymbol{x}\|_{L^2}^2 \to \infty$, $r_{\max} \to \infty$, and hence $\mathcal{A}_T$ diverges if $T < |\sin \rho|(|\rho| < \pi/2)$ or $T < 1(|\rho| > \pi/2)$. Now we adapt these computations to our setting in Theorem 4.1.1.

*(i)* $L_{X+} \to L_{X-}$: since $\rho = \pi + T$, $\mathcal{A}_T$ is coercive if $0 < T < 1$;

*(ii)* $L_{X+} \to L_{Y+}$: since $\rho = \pi/2 + T$, $\mathcal{A}_T$ is coercive if $0 < T < 1$;

*(iii)* $L_{X+} \to L_{Y-}$: since $\rho = \pi/2 - T$, $\mathcal{A}_T$ is coercive if $0 < T < \sin(\pi/2 - T) = \cos T$;

*(iv)* $L_{X+} \to P_{YZ}$: since $\rho = \pi/2 - T$, $\mathcal{A}_T$ is coercive if $0 < T < \sin(\pi/2 - T) = \cos T$;

*(v)* $L_{Y+} \to L_{Y-}$:since $\rho = \pi + T$, $\mathcal{A}_T$ is coercive if $0 < T < 1$;

*(vi)* $L_{Y+} \to P_{XZ}$:since $\rho = \pi/2 - T$, $\mathcal{A}_T$ is coercive if $0 < T < \sin(\pi/2 - T) = \cos T$.

The structure of the collision singularity $(X, Y, Z) = (0, 0, 0)$ is essential same as ones of the restricted three-body problem. We established a method to avoid the collision singularities in the restricted three-body problem. We can apply the method to the Hill problem and show that the obtained minimizers have no collision.

### 4.1.3 Reversibility

Consider ordinary differential equations:

$$\dot{\boldsymbol{x}} = F(\boldsymbol{x}) \qquad (\boldsymbol{x} \in \mathbb{R}^n) \tag{4.1.2}$$

where $F : \mathbb{R}^n \to \mathbb{R}^n$ is a smooth function.

**Definition 4.1.2** (Reversible)**.** *Let $R$ be an linear map from $\mathbb{R}^n$ to $\mathbb{R}^n$. If $F(\boldsymbol{x})$ satisfies*

$$F(R\boldsymbol{x}) + RF(\boldsymbol{x}) = \mathbf{0},$$

*then* (4.1.2) *is said to be reversible with respect to $R$.*

With a simple calculation, we get the following proposition:

**Proposition 4.1.3.** *In a reversible system with respect to $R$, if $\boldsymbol{x}(t)$ is a solution of Eq.* (4.1.2)*, so is $R\boldsymbol{x}(-t)$.*

We define

$$\mathrm{Fix}(R) = \{\boldsymbol{x} \in \mathbb{R}^n \mid R\boldsymbol{x} = \boldsymbol{x}\}.$$

It is easy to see that, for a solution $\boldsymbol{x}(t)$ of (4.1.2) and a real value $s \in \mathbb{R}$, $\boldsymbol{x}(s) \in \mathrm{Fix}(R)$ is satisfied if and only if $\boldsymbol{x}(s + t) = R\boldsymbol{x}(s - t)$.

By letting $(V_X, V_Y, V_Z) = (\dot{X}, \dot{Y}, \dot{Z})$, we rewrite the Hill problem (4.1.1) as the first-order differential equations:

$$\begin{aligned}
\dot{X} &= V_X \\
\dot{Y} &= V_Y \\
\dot{Z} &= V_Z \\
\dot{V}_X &= 2V_Y + 3X - \frac{X}{(X^2 + Y^2 + Z^2)^{3/2}} \\
\dot{V}_Y &= -2V_X - \frac{Y}{(X^2 + Y^2 + Z^2)^{3/2}} \\
\dot{V}_Z &= -Z - \frac{Z}{(X^2 + Y^2 + Z^2)^{3/2}}.
\end{aligned}$$

This system is reversible with respect to the following four linear maps:

$$\begin{aligned}
R_1 &= \mathrm{diag}(1, -1, 1, -1, 1, -1) \\
R_2 &= \mathrm{diag}(1, -1, -1, -1, 1, 1) \\
R_3 &= \mathrm{diag}(-1, 1, 1, 1, -1, -1) \\
R_4 &= \mathrm{diag}(-1, 1, -1, 1, -1, 1).
\end{aligned}$$

For those linear maps,

$$\begin{aligned}
\mathrm{Fix}(R_1) &= \{{}^t(X, Y, Z, V_X, V_Y, V_Z) \mid Y = V_X = V_Z = 0\} \\
\mathrm{Fix}(R_2) &= \{{}^t(X, Y, Z, V_X, V_Y, V_Z) \mid Y = Z = V_X = 0\} \\
\mathrm{Fix}(R_3) &= \{{}^t(X, Y, Z, V_X, V_Y, V_Z) \mid X = V_Y = V_Z = 0\} \\
\mathrm{Fix}(R_4) &= \{{}^t(X, Y, Z, V_X, V_Y, V_Z) \mid X = Z = V_Y = 0\}.
\end{aligned}$$

Consider Case (i). From the first variational formula, $\frac{\partial L}{\partial \dot{\boldsymbol{x}}}(0) \cdot L_{X+} = \frac{\partial L}{\partial \dot{\boldsymbol{x}}}(T) \cdot L_{X-} = 0$ Since

$$\frac{\partial L}{\partial \dot{\boldsymbol{x}}} = (\dot{X} - Y, \dot{Y} + X, \dot{Z}),$$

$$\dot{X}(0) = 0, \dot{X}(T) = 0$$

Therefore, $\begin{pmatrix} \boldsymbol{x}(0) \\ \dot{\boldsymbol{x}}(0) \end{pmatrix}, \begin{pmatrix} \boldsymbol{x}(T) \\ \dot{\boldsymbol{x}}(T) \end{pmatrix} \in \mathrm{Fix}(R_3)$. We have

$$\begin{pmatrix} \boldsymbol{x}(t) \\ \dot{\boldsymbol{x}}(t) \end{pmatrix} = R_3 \begin{pmatrix} \boldsymbol{x}(-t) \\ \dot{\boldsymbol{x}}(-t) \end{pmatrix}, \begin{pmatrix} \boldsymbol{x}(T+t) \\ \dot{\boldsymbol{x}}(T+t) \end{pmatrix} = R_3 \begin{pmatrix} \boldsymbol{x}(T-t) \\ \dot{\boldsymbol{x}}(T-t) \end{pmatrix}.$$

Therefore, we get

$$\begin{aligned}
\begin{pmatrix} \boldsymbol{x}(t+2T) \\ \dot{\boldsymbol{x}}(t+2T) \end{pmatrix} &= \begin{pmatrix} \boldsymbol{x}(T+(t+T)) \\ \dot{\boldsymbol{x}}(T+(t+T)) \end{pmatrix} = R_3 \begin{pmatrix} \boldsymbol{x}(T-(t+T)) \\ \dot{\boldsymbol{x}}(T-(t+T)) \end{pmatrix} \\
&= R_3 \begin{pmatrix} \boldsymbol{x}(-t) \\ \dot{\boldsymbol{x}}(-t) \end{pmatrix} = \begin{pmatrix} \boldsymbol{x}(t) \\ \dot{\boldsymbol{x}}(t) \end{pmatrix}.
\end{aligned}$$

Hence the obtained orbit is $2T$-periodic. The other cases (ii)-(vi) are similar.

### 4.1.4 Holonomic constraint

From the point of view of an application to orbits of artificial satellites, we need orbits on a prescribed plane. A prescribed plane is not invariant under the flow of the Hill problem in general. Hence we constraint the system to a prescribed plane with an external force like a jet by an artificial satellite.

Let $\boldsymbol{c} = (c_1, c_2, c_3)$ be a unit vector and consider the plane perpendicular to $\boldsymbol{c}$ passing the origin(Figure 4.2). The holonomic system is represented by the Lagrangian system with the Lagrangian

$$\bar{\mathcal{L}} = \frac{1}{2}(\dot{x}^2 + \dot{y}^2) + c_3(x\dot{y} - y\dot{x}) + \lambda_1 x^2 + \lambda_2 y^2 + \frac{1}{\sqrt{x^2 + y^2}}$$

where $\lambda_1 \leq 0 \leq \lambda_2$ are the constants determined by

$$\lambda_1 + \lambda_2 = -3c_1^2 + c_3^2 + 2, \quad \lambda_1 \lambda_2 = -\frac{3}{4}c_2^2.$$

The equations are

$$\begin{aligned}
\ddot{x} &= 2c_3\dot{y} + 2\lambda_1 x - \frac{x}{(x^2 + y^2)^{3/2}} \\
\ddot{y} &= -2c_3\dot{x} + 2\lambda_2 y - \frac{y}{(x^2 + y^2)^{3/2}}.
\end{aligned} \tag{4.1.3}$$

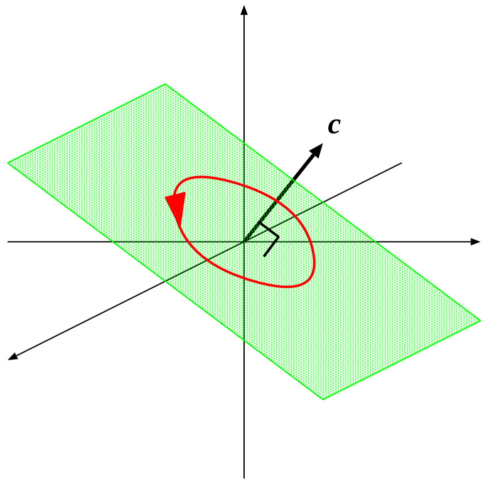


Figure 4.2: Holonomic constraints

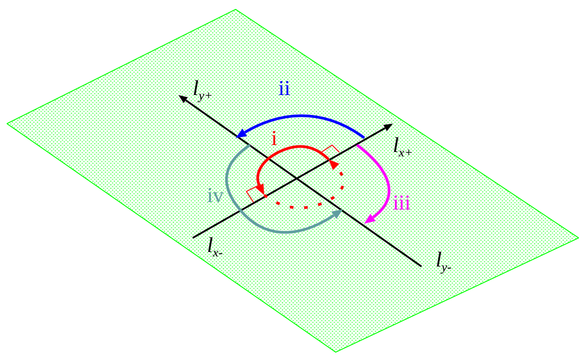


Figure 4.3: Boundary conditions in the constrained problem

Let

$$\begin{aligned} l_{X+} &= \{(X,0) \mid X > 0\} \\ l_{X-} &= \{(X,0) \mid X < 0\} \\ l_{Y+} &= \{(0,Y) \mid Y > 0\} \\ l_{Y-} &= \{(0,Y) \mid Y < 0\}. \end{aligned}$$

See Figure 4.3.

**Theorem 4.1.4.** *For the holonomic system* (4.1.3)*, the followings hold:*

*(i) For each* $0 < T < \min\{\pi/2, 1/(c_3^2 - 2\lambda_1)\}$*, there is a* $2T$*-periodic orbit satisfying* $\boldsymbol{q}(0) \in l_{X+}, \boldsymbol{q}(T) \in l_{X-}$.

*(ii) For each* $0 < T < \min\{\pi/2, 1/(c_3^2 - 2\lambda_1)\}$*, there is a* $4T$*-periodic orbit satisfying* $\boldsymbol{q}(0) \in l_{X+}, \boldsymbol{q}(T) \in l_{Y+}$.

*(iii) For each* $0 < T < \min\{\pi, T_1\}$*, there is a* $4T$*-periodic orbit* $\boldsymbol{q}(0) \in l_{X+}, \boldsymbol{q}(T) \in l_{Y-}$.

*(iv) For each* $0 < T < \min\{\pi/2, 1/(c_3^2 - 2\lambda_1)\}$*, there is a* $2T$*-periodic orbit satisfying* $\boldsymbol{q}(0) \in l_{Y+}, \boldsymbol{q}(T) \in l_{Y-}$.

The proof is similar to one for Theorem 4.1.1. To apply these orbits for artificial satellites, we need to control it for $\boldsymbol{c}$-direction. But this must be less costly than in the case of the Kepler problem.

# 4.2 The two-center problem

## 4.2.1 Introduction and the main theorem

The $n$-center problem is given by the following set of ordinary differential equations (ODEs):

$$\ddot{\boldsymbol{q}} = -\sum_{k=1}^{n} \frac{m_k}{|\boldsymbol{q} - \boldsymbol{a}_k|^3}(\boldsymbol{q} - \boldsymbol{a}_k) \qquad (\boldsymbol{q} \in \mathbb{R}^d), \tag{4.2.1}$$

where $\boldsymbol{a}_k \in \mathbb{R}^d$ is a constant vector. A solution $\boldsymbol{q}(t)$ of (4.2.1) is called a brake orbit if there are real numbers $T_1$ and $T_2$ ($T_2 > T_1$) such that

$$\dot{\boldsymbol{q}}(T_1) = \dot{\boldsymbol{q}}(T_2) = \boldsymbol{0} \tag{4.2.2}$$

and $\boldsymbol{q}(t)$ is not a stationary point, i.e. an equilibrium point. A brake orbit is a periodic orbit with period $2(T_2 - T_1)$, as we will demonstrate in Section 4.2.2.

The two-center problem is a simplified model of the restricted three-body problem [56]. The two-center problem is integrable, but its first integrals are complicated(for further details, see [2]). It is not obvious what types of periodic solutions exist.

Various Lagrange systems have been researched over many years to find periodic solutions with variational methods. In the $n$-center problem, it is shown that there exist periodic orbits that move around one or several primaries ( [58], [64]). The brake orbits that we prove to exist in this chapter do not wind around primaries.

Brake orbits are a special type of periodic orbits. Using collision manifold, Chen [16] proved that brake orbits exist in the planar isosceles three-body problem. Moeckel, Montgomery, and Venturelli [41] showed the existence of brake orbits using variational methods with respect to the Jacobi-Maupertuis functional. However, the Lagrangian functional has not previously been used to find brake orbits.

In this chapter, we will show that a brake orbit exists in the planar two-center problem by using the Lagrangian action functional. We can set $m_1 = 1$ and $\boldsymbol{a}_1 = -\boldsymbol{a}_2 = (1, 0)$ without loss of generality for the planar two-center problem as stated in Section 4.2.4. More precisely, we prove the following theorem:

**Theorem 4.2.1.** *If* $(m, T) \in D$*, then a* $4T$*-periodic brake orbit* $\boldsymbol{q}(t)(= (q_1(t), q_2(t)))$ *exists in the planar two-center problem. The orbit is orthogonal to the* $x$*-axis at* $t = 0$ *and has zero velocity at* $t = T$*. The orbit* $\boldsymbol{q}(t)$ *satisfies* $(q_1(t), q_2(t)) = (q_1(-t), -q_2(-t))$*. Here, the set* $D$ *is defined by*

$$D := \{(m, T) \mid T > \alpha(m)\,, f(m, T, c) \geq 0\,({}^{\exists}c \geq 0)\}$$

*where*

$$\alpha(m) = \frac{\sqrt{2}\pi m^{1/4}}{(1+\sqrt{m})^2}.$$

$$f(m,T,c) = \frac{3}{2}\pi^{2/3}T^{1/3} + \frac{\pi^{2/3}(1+m)^{-1/3}m}{2(1+\pi^{2/3}(1+m)^{-1/3}T^{-2/3})}T^{1/3} \\ - \left(\frac{2}{3}c^2T^{1/3} + \int_0^T \frac{1}{\sqrt{(1-b)^2+c^2t^{4/3}}} + \frac{m}{\sqrt{(1+b)^2+c^2t^{4/3}}}dt\right),$$

*and*

$$b = \frac{\sqrt{m}-1}{\sqrt{m}+1}.$$

Figure 4.4 shows the domain $D$ drawn with MATLAB.

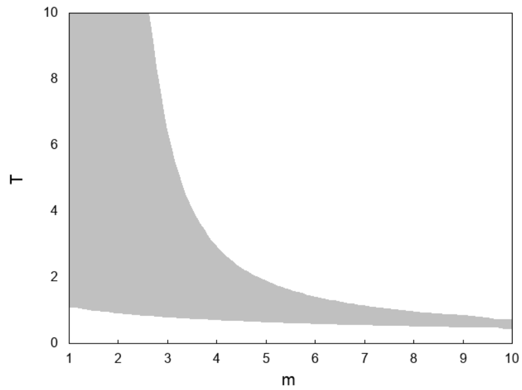


Figure 4.4: Domain $D$

**Remark 4.2.2.** *We can expand the theorem to a larger domain than $D$. See appendix.*

Section 4.2 is organized as follows. Section 4.2.2 and 4.2.3 provide background information on brake orbits and variational methods. In Section 4.2.4, we introduce the variational settings in the planar two-center problem and set the boundary condition. In Section 4.2.5, we complete the proof of Theorem 4.2.1 by eliminating the possibility that the minimizer is an equilibrium solution or a collision path. In Section 4.2.6, we extend the theorem to a larger domain than $D$.

### 4.2.2 Brake orbits

Consider ODEs:

$$\dot{\boldsymbol{q}} = F(\boldsymbol{q}) \quad (\boldsymbol{q} \in \mathbb{R}^n). \tag{4.2.3}$$

**Definition 4.2.3** (Reversible)**.** *Let $R$ be an involuntary liniear map from $\mathbb{R}^n$ to $\mathbb{R}^n$, i.e., $R^2 = E_n$. If* (4.2.3) *satisfies*

$$FR + RF = 0,$$

*then* (4.2.3) *is said to be reversible with respect to $R$ .*

With a simple calculation, we get the following proposition:

**Proposition 4.2.4.** *In reversible systems, if $\boldsymbol{q}(t)$ is a solution of* (4.2.3)*, then so is $R\boldsymbol{q}(-t)$.*

We define

$$\mathrm{Fix}(R) = \{\boldsymbol{q}(s) \in \mathbb{R}^n \mid R\boldsymbol{q}(s) = \boldsymbol{q}(s)\}$$

For a solution $\boldsymbol{q}(t)$ and a real value $s \in \mathbb{R}$, it holds that $\boldsymbol{q}(s) \in \mathrm{Fix}(R)$ is satisfied if and only if $\boldsymbol{q}(s+t) = R\boldsymbol{q}(s-t)$. See [51] for a more detailed explanation of reversible systems.

Consider the following Lagrangian:

$$L(\boldsymbol{q}, \dot{\boldsymbol{q}}) = \frac{1}{2}|\dot{\boldsymbol{q}}|^2 + V(\boldsymbol{q}) \qquad (\boldsymbol{q}, \dot{\boldsymbol{q}} \in \mathbb{R}^n). \tag{4.2.4}$$

The differential equations of the Lagrangian system

$$\begin{pmatrix} \dot{\boldsymbol{q}} \\ \dot{\boldsymbol{p}} \end{pmatrix} = \begin{pmatrix} \boldsymbol{p} \\ -V(\boldsymbol{q}) \end{pmatrix} \tag{4.2.5}$$

are reversible with respect to

$$R = \begin{pmatrix} E_n & \mathbf{0} \\ \mathbf{0} & -E_n \end{pmatrix}.$$

In this case, the fixed space is $\mathrm{Fix}(R) = \{(\boldsymbol{q}, \mathbf{0}) \mid \boldsymbol{q} \in \mathbb{R}^n\}$.

**Proposition 4.2.5.** *Brake orbits of Lagrangian system* (4.2.4) *with $\dot{\boldsymbol{q}}(T_1) = \dot{\boldsymbol{q}}(T_2) = 0$ are $2(T_2 - T_1)$-periodic orbits.*

*Proof.* This system has fix points at $\boldsymbol{p}(T_1) = \dot{\boldsymbol{q}}(T_1) = \boldsymbol{p}(T_2) = \dot{\boldsymbol{q}}(T_2) = 0$. Since $\boldsymbol{q}$ is invariant under $R$, we see that $\boldsymbol{q}(T_1 + t) = \boldsymbol{q}(T_1 - t)$ and $\boldsymbol{q}(T_2 + t) = \boldsymbol{q}(T_2 - t)$, i.e.,

$$\boldsymbol{q}(t) = \boldsymbol{q}(t + 2(T_2 - T_1)).$$

This concludes the proof. □

Since the $n$-center problem is a Lagrangian system with form (4.2.4), we get

**Corollary 4.2.6.** *In the $n$-center problem, if a solution $\boldsymbol{q}$ satisfies* (4.2.2)*, then it is a $2(T_2 - T_1)$-periodic orbit.*

### 4.2.3 Existence of the minimizer

Let $\mathcal{C}_{A,B,T}$ be the set of $C^2$ curves in an open set $\mathcal{D} \subset \mathbb{R}^n$ connecting from $A$ to $B$ :

$$\{\boldsymbol{q} \in C^2([0, T], \mathcal{D}) \mid \boldsymbol{q}(0) \in A,\ \boldsymbol{q}(T) \in B\}$$

where $A, B \subset \mathcal{D}$ are affine spaces. The action functional for (4.2.4) is defined by:

$$\mathcal{A}(\boldsymbol{q}) = \int_0^T L(\boldsymbol{q}, \dot{\boldsymbol{q}}) dt.$$

The following is well-known.

**Proposition 4.2.7.** *Let $L$ be a Lagrangian of the form (4.2.4) and $\mathcal{A}$ be the action functional. If $\boldsymbol{q} \in \mathcal{C}_{A,B,T}$ is a critical value of $\mathcal{A}$, then $\boldsymbol{q}(t)$ satisfies the Euler-Lagrange equation in $(0,T)$. Moreover, in the case (4.2.4), $\dot{\boldsymbol{q}}(0)$ is orthogonal to $A$ and $\dot{\boldsymbol{q}}(T)$ is orthogonal to $B$. If $A = \mathcal{D}$ ($B = \mathcal{D}$ resp.), then $\dot{\boldsymbol{q}}(0) = 0$ ($\dot{\boldsymbol{q}}(T) = 0$ resp.)*

We take

$$H^1(I, \mathcal{D}) = \left\{ \boldsymbol{q} \colon I \to \mathcal{D} \mid \boldsymbol{q} \in L^2(I, \mathcal{D}), \frac{d\boldsymbol{q}}{dt} \in L^2(I, \mathcal{D}) \right\}$$

where $I = [0,T]$. The norm is defined by

$$\|\boldsymbol{q}\|_{H^1} := \sqrt{\int_0^T |\boldsymbol{q}(t)|^2 + |\dot{\boldsymbol{q}}(t)|^2 dt}.$$

**Definition 4.2.8** (coercive)**.** *Let $\Omega \subset H^1(I, \mathcal{D})$. We call the functional $\mathcal{A}|_\Omega$ coercive if $\mathcal{A}(\boldsymbol{q}) \to \infty$ as $\|\boldsymbol{q}\|_{H^1} \to \infty$ ($\boldsymbol{q} \in \Omega$).*

In general, action functionals for potential systems are weakly semi-continuous [27].

**Lemma 4.2.9** ( [60])**.** *Assume that $\mathcal{A}$ is weakly lower semi-continuous. If $\mathcal{A}|_\Omega$ is coercive, then there exists a minimizer $\boldsymbol{q}^*$ of $\mathcal{A}$ in the weak closure $\bar{\Omega}$ of $\Omega$.*

**Lemma 4.2.10.** *Define $\Omega$ by*

$$\Omega = \{\boldsymbol{q} \in H^1(I, \mathcal{D}) \mid \boldsymbol{q}(0) \in A, \boldsymbol{q}(T) \in B\}.$$

*If $A$ is a bounded set and non-empty, then $\mathcal{A}|_\Omega$ is coercive.*

*Proof.* Although we now prove this lemma, note that similar proofs have been applied in other settings (see for example [12]).

For any $\boldsymbol{q} \in \Omega$, we take

$$\delta(\boldsymbol{q}) = \max_{s_1, s_2 \in [0,T]} |\boldsymbol{q}(s_1) - \boldsymbol{q}(s_2)|.$$

By the Cauchy-Schwarz inequality, we have

$$\delta(\boldsymbol{q})^2 \le \left( \int_0^T |\dot{\boldsymbol{q}}| dt \right)^2 \le T \int_0^T |\dot{\boldsymbol{q}}|^2 dt.$$

Setting $\xi = \sup_{\boldsymbol{q} \in A} |\boldsymbol{q}|$, we see that

$$|\boldsymbol{q}(t)| \le |\boldsymbol{q}(0)| + |\boldsymbol{q}(t) - \boldsymbol{q}(0)| \le \xi + \delta(\boldsymbol{q}).$$

Since

$$\|\boldsymbol{q}\|_{L^2}^2 = \int_0^T |\boldsymbol{q}(t)|^2 dt \le (\xi + \delta(\boldsymbol{q}))^2 T \le (\xi + \sqrt{T} \|\dot{\boldsymbol{q}}\|_{L^2})^2 T,$$

we obtain

$$\|\boldsymbol{q}\|_{H^1}^2 = \|\boldsymbol{q}\|_{L^2}^2 + \|\dot{\boldsymbol{q}}\|_{L^2}^2 \le (\xi + \sqrt{T} \|\dot{\boldsymbol{q}}\|_{L^2})^2 T + \|\dot{\boldsymbol{q}}\|_{L^2}^2.$$

Hence we get

$$\mathcal{A}(\boldsymbol{q}) \to \infty \ (\|\boldsymbol{q}\|_{H^1} \to \infty).$$

□

### 4.2.4 Variational settings for the two-center problem

We consider the planar two-center problem i.e. take $n = 2$ and $d = 2$ in (4.2.1). We fix masses and positions of the primaries as follows:

- $m_1 = 1,\ \ m_2 = m \geq 1.$
- Fix the position of the primaries at $\boldsymbol{a}_1$ and $\boldsymbol{a}_2$.
- $\boldsymbol{a}_1 = \boldsymbol{a} = (1, 0),\ \ \boldsymbol{a}_2 = -\boldsymbol{a}.$

We can assume the above setting without loss of generality for the two-center problem, because for any $\boldsymbol{a}_1,\ \boldsymbol{a}_2 \in \mathbb{R}^2$, $m_1 > 0$ and $m_2 > 0$, the problem can be reduced to the above case with appropriate transformations and scaling.

We define its action functional by

$$\mathcal{A}(\boldsymbol{q}) = \int_0^T L(\boldsymbol{q}, \dot{\boldsymbol{q}})dt, \tag{4.2.6}$$

where $L(\boldsymbol{q}, \dot{\boldsymbol{q}}) = \dfrac{1}{2}|\dot{\boldsymbol{q}}|^2 + \dfrac{1}{|\boldsymbol{q} - \boldsymbol{a}|} + \dfrac{m}{|\boldsymbol{q} + \boldsymbol{a}|}$ and $\boldsymbol{q} \in H^1(I, \mathbb{R}^2)$. The planar two-center problem is equivalent to the following variational problem:

$$\mathcal{A}'(\boldsymbol{q}) = 0. \tag{4.2.7}$$

We fix a positive number $T$ and search for a brake orbit $\boldsymbol{q}(t) = (q_1(t), q_2(t))$ satisfying

- $q_1(0) \in (-1, 1)$ and $q_2(0) = 0$.
- $\dot{\boldsymbol{q}}(T) = \boldsymbol{0}$.
- $q_1(t) = q_1(-t), q_2(t) = -q_2(-t)$.

To obtain such brake orbits, we take a class of curves as follows:

$$\Omega = \{\boldsymbol{q}(t) = (q_1(t), q_2(t)) \in H^1([0, T], \mathbb{R}^2) \mid -1 < q_1(0) < 1, q_2(0) = 0\}.$$

From Lemma 4.2.9 and 4.2.10, (4.2.6)has a minimizer in the weak closure $\bar{\Omega}$ of $\Omega$. Let $\boldsymbol{q}^*(t) = (q_1^*(t), q_2^*(t))$ be a minimizer. If $\boldsymbol{q}^*$ is neither a trivial solution nor a collision solution, then from Proposition 4.2.5 and 4.2.7, it is a quarter part of a brake orbit (See Figure 4.5).

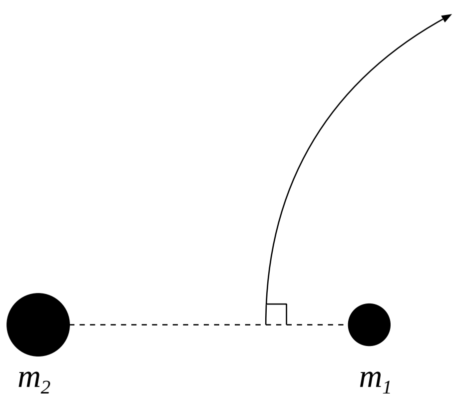


Figure 4.5: $\boldsymbol{q}^*(t)$ $(t \in [0, T])$

The system is reversible with respect to:

$$R\begin{pmatrix} x \\ y \\ p_x \\ p_y \end{pmatrix} = \begin{pmatrix} x \\ -y \\ -p_x \\ p_y \end{pmatrix} \quad \left( R = \begin{pmatrix} 1 & 0 & 0 & 0 \\ 0 & -1 & 0 & 0 \\ 0 & 0 & -1 & 0 \\ 0 & 0 & 0 & 1 \end{pmatrix} \right).$$

By corollary 4.2.4 if $\boldsymbol{q}(t) = (q_1(t), q_2(t))$ is a solution, then so is $\boldsymbol{q}(t) = (q_1(-t), -q_2(-t))$. Thus, we get the entire trajectory of a $4T$-periodic brake orbit as shown in Figure 4.6.

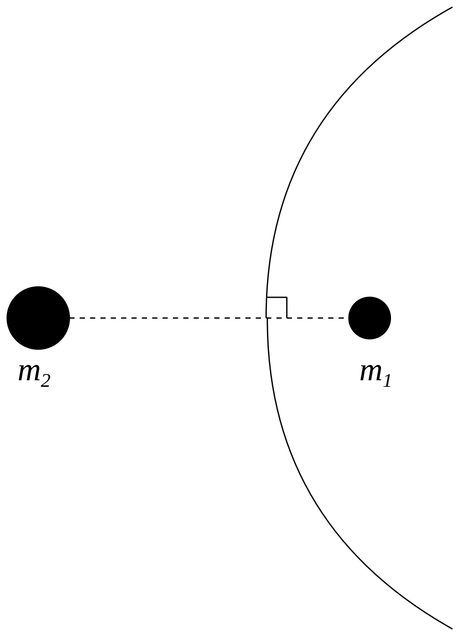


Figure 4.6: A whole brake orbit

### 4.2.5 Proof of the main theorem

Let $\boldsymbol{q}_{eq}$ denote an equilibrium point of (4.2.6), i.e.

$$\frac{1}{|\boldsymbol{q}_{\mathrm{eq}} - \boldsymbol{a}|^3}(\boldsymbol{q}_{\mathrm{eq}} - \boldsymbol{a}) + \frac{m}{|\boldsymbol{q}_{\mathrm{eq}} + \boldsymbol{a}|^3}(\boldsymbol{q}_{\mathrm{eq}} + \boldsymbol{a}) = \boldsymbol{0}.$$

From a simple calculation, $\boldsymbol{q}_{\mathrm{eq}}$ is determined by:

$$\boldsymbol{q}_{\mathrm{eq}} = (b, 0) \quad \left( b = \frac{\sqrt{m} - 1}{\sqrt{m} + 1} \right).$$

and the value of the action functional at $\boldsymbol{q}_{\mathrm{eq}}$ is

$$\mathcal{A}(\boldsymbol{q}_{\mathrm{eq}}) = \int_0^T \frac{1}{|\boldsymbol{q}_{\mathrm{eq}} - \boldsymbol{a}|} + \frac{m}{|\boldsymbol{q}_{\mathrm{eq}} + \boldsymbol{a}|} dt = \frac{1}{2}(1 + \sqrt{m})^2 T.$$

We will obtain a condition under the equilibrium point is not the minimizer by estimating the second variation, which is $\mathcal{A}''(\boldsymbol{q})(\boldsymbol{\delta})$ is given by

$$\mathcal{A}''(\boldsymbol{q})(\boldsymbol{\delta}) = \int_0^T (\boldsymbol{\delta}(t), \dot{\boldsymbol{\delta}}(t)) \nabla^2 L(\boldsymbol{q})(\boldsymbol{\delta}(t), \dot{\boldsymbol{\delta}}(t))^{\mathrm{T}} dt,$$

where $\boldsymbol{q} \in H^1([0,T], \mathbb{R}^2)$ and $\boldsymbol{\delta} \in H^1([0,T], \mathbb{R}^2)$. (For details, see [62].) If there exists $\boldsymbol{\delta}$ such that $\mathcal{A}''(\boldsymbol{q})(\boldsymbol{\delta})$ is negative, then $\boldsymbol{q}$ is not the minimizer of (4.2.6). Since

$$\nabla^2 L(\boldsymbol{q}_{\mathrm{eq}}) = \begin{pmatrix} 2\gamma & 0 & 0 & 0 \\ 0 & -\gamma & 0 & 0 \\ 0 & 0 & 1 & 0 \\ 0 & 0 & 0 & 1 \end{pmatrix} \quad \left(\gamma = \frac{(1+\sqrt{m})^4}{8\sqrt{m}}\right),$$

we obtain

$$\mathcal{A}''(\boldsymbol{q}_{\mathrm{eq}})(\boldsymbol{\delta}) = \int \dot{\delta}_1^2 + \dot{\delta}_2^2 + \gamma(2\delta_1^2 - \delta_2^2) dt. \tag{4.2.8}$$

We substitute

$$\boldsymbol{\delta} = (\delta_1(t), \delta_2(t)) = (0, \sin \omega t) \quad \left(\omega = \frac{\pi}{2T}\right) \tag{4.2.9}$$

into (4.2.8). Since

$$\begin{aligned} &\int_0^T \dot{\delta}_1^2 + \dot{\delta}_2^2 + \gamma(2\delta_1^2 - \delta_2^2) dt \\ &= \omega^2 \left(\frac{T}{2} + \frac{1}{4\omega}\sin(2\omega T)\right) - \gamma\left(\frac{T}{2} - \frac{1}{4\omega}\sin(2\omega T)\right) \\ &= \frac{T}{2}(\omega^2 - \gamma), \end{aligned}$$

the second variation of $\boldsymbol{q}_{\mathrm{eq}}$ for (4.2.9) is negative if

$$\frac{\pi}{2\sqrt{\gamma}} = \frac{\sqrt{2}\pi m^{1/4}}{(1+\sqrt{m})^2} < T.$$

Thus, the following lemma is proved.

**Lemma 4.2.11.** *If* $T > \dfrac{\sqrt{2}\pi m^{1/4}}{(1+\sqrt{m})^2}$, $\boldsymbol{q}_{\mathrm{eq}}$ *is not a minimizer of* $\mathcal{A}(\boldsymbol{q})$.

Next, we give an estimate of collisions.

**Lemma 4.2.12.** *The set* $\Omega_{\mathrm{col}}$ *is given by*

$$\Omega_{\mathrm{col}} = \{\boldsymbol{q} \in \Omega \mid \boldsymbol{q} \textit{ has collisions.}\},$$

*Then,* $\mathcal{A}|_{\Omega_{\mathrm{col}}}$ *is minimized by an orbit that moves along the x-axis (see Figure* 4.7*).*

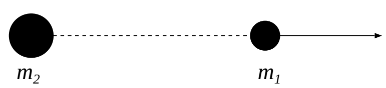


Figure 4.7: Minimizer with collisions

*Proof.* Assume that $\boldsymbol{q}_{\mathrm{col}}$ collides with $m_1$ and

$$\boldsymbol{q}_{\mathrm{col}}(t) = r(t)(\cos\theta(t), \sin\theta(t)) + (1,0).$$

The value of action functional at $\boldsymbol{q}_{\mathrm{col}}$ is

$$\begin{aligned}
\mathcal{A}(\boldsymbol{q}_{\mathrm{col}}) &= \int_0^T \frac{1}{2}|\dot{\boldsymbol{q}}_{\mathrm{col}}|^2 + \frac{1}{|\boldsymbol{q}_{\mathrm{col}} - \boldsymbol{a}|} + \frac{m}{|\boldsymbol{q}_{\mathrm{col}} + \boldsymbol{a}|} dt \\
&= \int_0^T \frac{1}{2}(\dot{r}^2 + (r\dot{\theta})^2) + \frac{1}{|r|} + \frac{m}{\sqrt{r^2 + 4 + 2r\cos\theta}} dt \\
&\geq \int_0^T \frac{1}{2}\dot{r}^2 + \frac{1}{|r|} + \frac{m}{\sqrt{r^2 + 4 + 2r}} dt.
\end{aligned}$$

This inequality becomes an equality if and only if $\theta(t)$ is identically zero. We can obtain a similar estimate in the case where $\boldsymbol{q}_{\mathrm{col}}$ collides with $m_2$, and it is no less than the former one since $m \geq 1$. It follows that the collision path moves on the $x$-axis as in Figure 4.7. □

We call the solution of Lemma 4.2.12 a collision-ejection solution of the two-center problem and represent it by

$$\boldsymbol{q}_{\mathrm{col}}(t) = (q_{\mathrm{col}}(t), 0).$$

By Lemma 4.2.12, we consider only a collision-ejection solution to get a lower bound estimate for the value of the action functional for any collision path.

**Lemma 4.2.13** ( [27]). *Let $\mu > 0$, $\rho > 0$ be constants. For $r \in H^1([0,T],\mathbb{R})$, define*

$$\mathcal{B}(r) = \int_0^T \frac{\mu}{2}\dot{r}^2 + \frac{\rho}{|r|} dt. \tag{4.2.10}$$

*If there exists $t_0 \in [0,T]$ satisfying $r(t_0) = 0$, then the inequality,*

$$\mathcal{B}(r) \geq B(\mu,\rho,T) := \frac{3}{2}\pi^{2/3}\rho^{2/3}\mu^{1/3}T^{1/3},$$

*holds and $\mathcal{B}(r) = B(\mu,\rho,T)$ if and only if $r(t)$ is a collision-ejection solution of the Kepler problem. Moreover, if $r(t)$ is a collision-ejection solution with $r(0) = 0$, then*

$$r(T) = 2\pi^{-2/3}\mu^{-1/3}\rho^{1/3}T^{2/3}.$$

In (4.2.10), we take $\mu = 1$ and $\rho = m + 1$. Let $\tilde{\boldsymbol{q}}(t) = (\tilde{q}(t), 0)$ where $\tilde{q}(t) - 1$ is a minimizer of (4.2.10). From Lemma 4.2.13, we have

$$\tilde{q}(T) = 2\pi^{-2/3}T^{2/3}(m+1)^{1/3} + 1. \tag{4.2.11}$$

**Lemma 4.2.14.**

$$q_{\mathrm{col}}(T) < \tilde{q}(T).$$

*Proof.* Suppose

$$q_{\mathrm{col}}(T) \geq \tilde{q}(T) \tag{4.2.12}$$

and

$$F_{\mathrm{col}}(q) = -\frac{1}{q-1} - \frac{m}{q+1},\ \tilde{F}(q) = -\frac{m+1}{q-1}.$$

Note that we now have

$$q_{\mathrm{col}}(0) = \tilde{q}(0) = 1 \tag{4.2.13}$$
$$\dot{q}_{\mathrm{col}}(T) = \dot{\tilde{q}}(T) = 0 \tag{4.2.14}$$
$$0 > F_{\mathrm{col}}(q) > \tilde{F}(q). \tag{4.2.15}$$

We take

$$t_0 := \sup\{t \geq 0 \mid q_{\mathrm{col}}(t) = \tilde{q}(t)\}.$$

By (4.2.12) and (4.2.13), there exists $t_0 (< T)$ such that $q_{\mathrm{col}}(t_0) = \tilde{q}(t_0)$. By (4.2.12) and (4.2.15), $0 > F_{\mathrm{col}}(q_{\mathrm{col}}(t)) > \tilde{F}(\tilde{q}(t))$ holds. By $\ddot{q}_{\mathrm{col}} = F_{\mathrm{col}}, \ddot{\tilde{q}} = \tilde{F}$ and (4.2.14), for any $t \in [t_0, T)$, the following inequality holds:

$$0 > \dot{q}_{\mathrm{col}}(t) = \int_T^t \ddot{q}_{\mathrm{col}} dt = \int_T^t F_{\mathrm{col}}(q_{\mathrm{col}}(t)) dt > \int_T^t \tilde{F}(\tilde{q}(t)) dt = \int_T^t \ddot{\tilde{q}} dt = \dot{\tilde{q}}(t).$$

Since $q_{\mathrm{col}}(t_0) = \tilde{q}(t_0)$, we obtain

$$0 > \int_T^{t_0} \dot{\tilde{q}}(t) - \dot{q}_{\mathrm{col}}(t) dt = q_{\mathrm{col}}(T) - \tilde{q}(T).$$

This contradicts (4.2.12). □

**Lemma 4.2.15.** *For any $\boldsymbol{q}_{\mathrm{col}}$ in collision solutions,*

$$\mathcal{A}(\boldsymbol{q}_{\mathrm{col}}) > g(m,T) := \frac{3}{2}\pi^{2/3} T^{1/3} + \frac{\pi^{2/3}(1+m)^{-1/3} m}{2(1+\pi^{2/3}(1+m)^{-1/3} T^{-2/3})} T^{1/3}$$

*Proof.* From Lemma 4.2.12, we have

$$\begin{aligned}\int_0^T \frac{1}{|\boldsymbol{q}_{\mathrm{col}} + \boldsymbol{a}|} dt = \int_0^T \frac{1}{q_{\mathrm{col}} + 1} dt \geq \frac{m}{q_{\mathrm{col}}(T) + 1} \int_0^T dt = \frac{m}{q_{\mathrm{col}}(T)+1} T \\ > \frac{\pi^{2/3}(1+m)^{-1/3} m}{2(1+\pi^{2/3}(1+m)^{-1/3} T^{-2/3})} T^{1/3}.\end{aligned}$$

By (4.2.11), we obtain

$$\begin{aligned}\mathcal{A}(\boldsymbol{q}_{\mathrm{col}}) &= \int_0^T \frac{1}{2} |\dot{\boldsymbol{q}}_{\mathrm{col}}|^2 + \frac{1}{|\boldsymbol{q}_{\mathrm{col}} - \boldsymbol{a}|} dt + \int_0^T \frac{m}{|\boldsymbol{q}_{\mathrm{col}} + \boldsymbol{a}|} dt \\ &> \frac{3}{2}\pi^{2/3} T^{1/3} + \frac{\pi^{2/3}(1+m)^{-1/3} m}{2(1+\pi^{2/3}(1+m)^{-1/3} T^{-2/3})} T^{1/3}.\end{aligned}$$

□

At the end of our proof, we show that the value of the test path is smaller than one of the collision path.

**Lemma 4.2.16.** *If $f(m,T,c) \geq 0$, the collision path $\boldsymbol{q}_{\mathrm{col}}$ is not a minimizer.*

*Proof.* We take a test path:

$$\boldsymbol{q}_c(t) = (b, ct^{\frac{2}{3}}) \quad (c \geq 0).$$

If $\mathcal{A}(\boldsymbol{q}_{\mathrm{col}}) > \mathcal{A}(\boldsymbol{q}_c)$, then $\boldsymbol{q}_{\mathrm{col}}$ is not a minimizer. The value of the functional with respect to the test path is

$$\mathcal{A}(\boldsymbol{q}_c) = \frac{2}{3}c^2T^{1/3} + \int_0^T \frac{1}{\sqrt{(1-b)^2 + c^2t^{4/3}}} + \frac{m}{\sqrt{(1+b)^2 + c^2t^{4/3}}}dt.$$

By Lemma 4.2.15, it is sufficient to show that if $g(m,T) \geq \mathcal{A}(\boldsymbol{q}_c)$. This inequality is equivalent to $f(m,T,c) \geq 0$. □

Now, we show that domain $D$ is nonempty without numerical calculation. Let

$$\tilde{g}(T) := \frac{3}{2}\pi^{2/3}T^{1/3}.$$

Clearly $g(m,T) > \tilde{g}(T)$ holds, therefore we obtain $\tilde{g}(T) \geq \mathcal{A}(\boldsymbol{q}_{\mathrm{eq}})$, i.e. if

$$T < \frac{3\sqrt{3}\pi}{(1+\sqrt{m})^3} (= \beta(m)),$$

then $\boldsymbol{q}_{\mathrm{col}}$ is not a minimizer and if $T > \alpha(m)$, then $\boldsymbol{q}_{\mathrm{eq}}$ is not a minimizer. If there exists $T$ such that $\alpha(m) < T < \beta(m)$, then

$$\emptyset \neq \{(m,T) \mid \alpha(m) < T < \beta(m)\,, f(m,T,0) \geq 0\} \subset D,$$

so $D$ is nonempty. The inequality $\alpha(m) < \beta(m)$ is equivalent to

$$\sqrt{m}(\sqrt{m}+1)^2 - \frac{27}{2} < 0. \tag{4.2.16}$$

For $1 \leq m < 3.1164778$, (4.2.16) holds.

### 4.2.6 Extension of $D$

In this section, we will reconsider the estimate of (4.2.6) of collisions. For all $\lambda \in (0,1)$, let

$$\mathcal{A}(q) = \mathcal{A}_1(\lambda, q-1) + \mathcal{A}_2(\lambda, q+1),$$

where

$$\mathcal{A}_1(\lambda, q) = \int_0^T \frac{1-\lambda}{2}\dot{q}^2 + \frac{1}{|q|}dt \tag{4.2.17}$$

and

$$\mathcal{A}_2(\lambda, q) = \int_0^T \frac{\lambda}{2}\dot{q}^2 + \frac{m}{|q|}dt. \tag{4.2.18}$$

By [27], we get the following estimate of (4.2.17):

$$\mathcal{A}_1(\lambda, q-1) > \frac{3}{2}\pi^{2/3}(1-\lambda)^{1/3}T^{1/3}.$$

To estimate (4.2.18), we will use a comparison of (4.2.18) and a part of the linear Kepler orbit.

We fix $H$ and assume $-m/2 < H < 0$. Let $Q(t)$ denote a collision-ejection solution with respect to (4.2.18) satisfying $Q(t_0) = 2$, $\dot{Q}(T + t_0) = 0$ and

$$H = \frac{\lambda}{2}\dot{Q}^2 - \frac{m}{|Q|}.$$

Thus, we obtain

$$\begin{aligned}
\mathcal{A}_2(\lambda, q+1) &> \int_{t_0}^{T+t_0} \frac{\lambda}{2}\dot{Q}^2 + \frac{m}{|Q|}dt \\
&= \int_0^{T+t_0} \frac{\lambda}{2}\dot{Q}^2 + \frac{m}{|Q|}dt - Ht_0 - 2\int_0^{t_0} \frac{m}{|Q|}dt.
\end{aligned}$$

Gordon [27] gives

$$\int_0^{T+t_0} \frac{\lambda}{2}\dot{Q}^2 + \frac{m}{|Q|}dt = \frac{3}{2}\pi^{2/3}\lambda^{1/3}m^{2/3}(T+t_0)^{1/3}.$$

**Lemma 4.2.17.** *If $-H < 0$, let $T(x, H)$ denote the time from 0 to $x$ with energy $H$. Then, it holds the following equation holds:*

$$T(x, H) = m\sqrt{\frac{\lambda}{2(-H)^3}}\left\{\sin^{-1}\left(\sqrt{\frac{-xH}{m}}\right) - \sqrt{\frac{-xH}{m}\left(1 + \frac{xH}{m}\right)}\right\}$$

*Proof.* By the definition of $T(x, H)$, we get

$$\begin{aligned}
T(x, H) &= \sqrt{\frac{\lambda}{2}}\int_0^x \frac{1}{\dot{Q}}dQ = \sqrt{\frac{\lambda}{2}}\int_0^x \sqrt{\frac{Q}{HQ+m}}dQ \\
&= m\sqrt{\frac{\lambda}{2(-H)^3}}\int_0^{-\frac{H}{m}x} \sqrt{\frac{q}{1-q}}dq \\
&= m\sqrt{\frac{\lambda}{2(-H)^3}}\int_0^{\theta_0} (1 - \cos 2\theta)d\theta \quad (\theta_0 = \sin^{-1}\left(\sqrt{\frac{-xH}{m}}\right)) \\
&= m\sqrt{\frac{\lambda}{2(-H)^3}}\left\{\sin^{-1}\left(\sqrt{\frac{-xH}{m}}\right) - \sqrt{\frac{-xH}{m}\left(1 + \frac{xH}{m}\right)}\right\}.
\end{aligned}$$

This completes the proof. □

The relation of $T$ and $t_0$ is indicated by the above lemma:

$$\begin{aligned} T &= (T+t_0) - t_0 = T(x_{\max}, H) - T(2, H) \\ &= m\sqrt{\frac{\lambda}{2(-H)^3}}\left\{\cos^{-1}\left(\sqrt{\frac{-2H}{m}}\right) + \sqrt{\frac{-2H}{m}\left(1+\frac{2H}{m}\right)}\right\} \end{aligned}$$

Substituting $H = -\dfrac{m}{2}y$ for any $y \in (0,1)$, we obtain

$$T := \bar{T}(m.\lambda, y) = 2\sqrt{\frac{\lambda}{m}} \cdot \frac{1}{y}\left\{\frac{\cos^{-1}\left(\sqrt{y}\right)}{\sqrt{y}} + \sqrt{1-y}\right\}$$

and

$$t_0 = 2\sqrt{\frac{\lambda}{m}} \cdot \frac{1}{y}\left\{\frac{\sin^{-1}\left(\sqrt{y}\right)}{\sqrt{y}} - \sqrt{1-y}\right\}.$$

It follows that

$$T + t_0 = \frac{\pi m}{2}\sqrt{\frac{\lambda}{2(-H)^3}} = \frac{\pi}{y}\sqrt{\frac{\lambda}{my}} \tag{4.2.19}$$

and

$$-Ht_0 = \sqrt{m\lambda}\left\{\frac{\sin^{-1}\left(\sqrt{y}\right)}{\sqrt{y}} - \sqrt{1-y}\right\}.$$

Moreover, we have

$$\begin{aligned} 2\int_0^{t_0} \frac{m}{|Q|}dt &= 2m\sqrt{\frac{\lambda}{2(-H)}}\int_0^{t_0}\frac{1}{Q}\sqrt{\frac{Q}{-Q-(m/H)}}dQ \\ &= 2m\sqrt{\frac{\lambda}{2(-H)}}\int_0^{2}\sqrt{\frac{1}{q(1-q)}}dq \\ &= 2m\sqrt{\frac{\lambda}{2(-H)}}\int_0^{\theta_0} 2d\theta \quad (\theta_0 = \sin^{-1}\left(\sqrt{\frac{-2H}{m}}\right)) \\ &= 2m\sqrt{\frac{2\lambda}{-H}}\sin^{-1}\left(\sqrt{\frac{-2H}{m}}\right) = 4\sqrt{\frac{m\lambda}{y}}\sin^{-1}\left(\sqrt{y}\right). \end{aligned}$$

Hence, since for all $\lambda \in (0,1)$ and $y \in (0,1)$,

$$\mathcal{A}_2(\lambda, q) > \sqrt{m\lambda}\left\{\frac{3}{\sqrt{y}}\cos^{-1}\left(\sqrt{y}\right) - \sqrt{1-y}\right\},$$

we get

$$\mathcal{A}(q_{\mathrm{col}}) > \bar{g}(m, \lambda, y), \tag{4.2.20}$$

where

$$\bar{g}(m,\lambda,y)=\frac{3}{2}\pi^{2/3}(1-\lambda)^{1/3}\bar{T}(m,\lambda,y)^{1/3}+\sqrt{m\lambda}\left\{\frac{3}{\sqrt{y}}\cos^{-1}\left(\sqrt{y}\right)-\sqrt{1-y}\right\}.$$

In the same way as the proof of Lemma 4.2.16, if $\bar{g}(m,\lambda,y)-\mathcal{A}(\boldsymbol{q}_c)\geq 0$, then $q_{\mathrm{col}}$ is not a minimizer.

From the above discussion, we show the following theorem extending the domain beyond $D$.

**Theorem 4.2.18.** *If $(m,T)\in D'$, then $4T$-periodic brake orbits $\boldsymbol{q}(t)(=(q_1(t),q_2(t)))$ satisfying the same condition of Theorem 4.2.1 exists in the planar two-center problem. Here, the set $D'$ is defined by*

$$D':=\left\{(m,T)\in\mathbb{R}^2\,\middle|\,\begin{array}{l}T>\alpha(m)\ \textit{and}\ {}^{\exists}\lambda,y\in(0,1)\ \textit{such that}\\ \bar{f}(m,\lambda,y,c)\geq 0\ \textit{and}\ T=\bar{T}(m,\lambda,y).\end{array}\right\}$$

*where*

$$\bar{f}(m,\lambda,y,c)=\bar{g}(m,\lambda,y)-\mathcal{A}(\boldsymbol{q}_c)$$

*and*

$$\bar{T}(m,\lambda,y)=2\sqrt{\frac{\lambda}{m}}\cdot\frac{1}{y}\left\{\frac{\cos^{-1}\left(\sqrt{y}\right)}{\sqrt{y}}+\sqrt{1-y}\right\}.$$

Figure 4.8 illustrates domain $D'$.

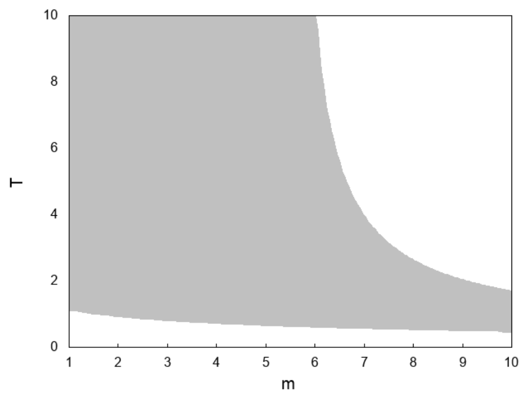


Figure 4.8: the domain $D'$

# Chapter 5

# Braid types of periodic solutions in the planar $n$-body problem

## 5.1 Introduction

Consider the motion of $m$ points in the plane $\mathbb{R}^2$

$$\boldsymbol{x}(t) = (x_1(t), \dots, x_m(t)),$$

where $x_i(t) \in \mathbb{R}^2$ is the position of the $i$th point at $t \in \mathbb{R}$. Let $Q_m(t) = \{x_1(t), \dots, x_m(t)\}$. We assume the following.

- $\boldsymbol{x}(t)$ is collision-free, i.e., for any $t \in \mathbb{R}$, $x_i(t) \neq x_j(t)$ if $i \neq j$.
- There exists $t_0 > 0$ such that

$$Q_m(t + t_0) = Q_m(t).$$

Then we have a (geometric) braid

$$b(\boldsymbol{x}(t), [0, t_0]) = \bigcup_{t \in [0, t_0]} \big\{(x_1(t), t), \dots, (x_m(t), t)\big\} \subset \mathbb{R}^2 \times [0, t_0]$$

with base points $Q_m(0) (= Q_m(t_0))$. The actual location of base points is irrelevant for the study of braids. To remove the data of the location, we consider its braid type $\big\langle b(\boldsymbol{x}(t), [0, t_0])\big\rangle$ instead of the braid (See Section 5.3.1 for the definition of braid types).

We investigate periodic solutions of the planar $N$-body problem given by the following ODEs.

$$m_i \ddot{x}_i = -\sum_{j \neq i} m_i m_j \frac{x_i - x_j}{|x_i - x_j|^3}, \quad x_i \in \mathbb{R}^2,\ m_i > 0\ (i = 1, \dots, N). \tag{5.1.1}$$

Suppose that $\boldsymbol{x}(t) = (x_1(t), \dots, x_N(t))$ is a periodic solution with period $T$ of (5.1.1). The solution $\boldsymbol{x}(t)$ determines a (pure) braid $b(\boldsymbol{x}(t), [0, T])$ and its braid type $\big\langle b(\boldsymbol{x}(t), [0, T]\big\rangle$. Braid types can be used to classify periodic solutions of the planar $N$-body problem.

**Question 5.1.1** (Montgomery [44], (cf. Moore [45])). *For any pure braid $b$ with $N$ strands, is there a periodic solution of the planar $N$-body problem whose braid type is equal to $\langle b \rangle$?*

Question 5.1.1 is wide open for every $N > 3$. In the case of $N = 3$ Question 5.1.1 is true by work of Moeckel-Montgomery [40]. For other studies on braids obtained from periodic solutions, see a pioneer work by Moore [45]. See also [23, 42, 43].

**Remark 5.1.2.** *We consider the following Newton equations*

$$m_i \ddot{x}_i = -\sum_{j \neq i} m_i m_j \frac{x_i - x_j}{|x_i - x_j|^{\alpha+1}}, \quad x_i \in \mathbb{R}^2,\ m_i > 0\ (i = 1, \ldots, N), \tag{5.1.2}$$

*where $\alpha \geq 1$. The case $\alpha = 2$ corresponds to (5.1.1) describing the motion of $n$ bodies under the influence of the gravitation. One can ask the same question as Question 5.1.1 for the planar $N$-body problem given by (5.1.2). It is known by Montgomery [43] that Question 5.1.1 is true for any "tied" braid type when $\alpha \geq 3$ (i.e., under the assumption that the force is strong).*

According to the Nielsen-Thurston classification of surface automorphisms [20], braids fall into three types: periodic, reducible and pseudo-Anosov. (See Section 5.3.3.) To a braid $b$ of pseudo-Anosov type, there is an associated stretch factor $\lambda(b) > 1$, and this is a conjugacy invariant of pseudo-Anosov braids. Since the Nielsen-Thurston type is also a conjugacy invariant, one can define the stretch factor $\lambda(\langle b \rangle) := \lambda(b)$ for the pseudo-Anosov braid type $\langle b \rangle$ of $b$. See (5.3.1) in Section 5.3.3.

The stretch factor tells us a dynamical complexity of pseudo-Anosov braids. In this chapter we ask the following question related to Question 5.1.1.

**Question 5.1.3.** *Let $b$ be a pure braid with $N$ strands. Suppose that $b$ is of pseudo-Anosov type. Is there a periodic solution of the planar $N$-body problem whose braid type is equal to $\langle b \rangle$?*

The stretch factor of each pseudo-Anosov braid with 3 strands is a quadratic irrational (Section 5.3.4). This is not necessarily true for pseudo-Anosov braids with more than 3 strands. Moore [45] and Chenciner-Montgomery [18] found a simple choreographic solution to the 3-body problem such that the three bodies chase one another along a figure-8 curve. The braid type of the solution is pseudo-Anosov and its stretch factor is the 6th power of the 1st metallic ratio $\mathfrak{s}_1$ (Example 5.3.6), i.e., golden ratio, where the $k$th metallic ratio $\mathfrak{s}_k$ ($k \in \mathbb{N}$) is given by

$$\mathfrak{s}_k = \frac{1}{2}(k + \sqrt{k^2 + 4}) = k + \cfrac{1}{k + \cfrac{1}{k + \cfrac{1}{k + \ddots}}}$$

The study of braid types of the periodic solutions has been relatively less investigated. We hope that the following result sheds some light on Question 5.1.3. Let $\lfloor \cdot \rfloor$ be the floor function.

**Theorem 5.1.4.** *For $n \geq 2$ and $p \in \{1, \ldots, \lfloor \frac{n}{2} \rfloor\}$, there exists a periodic solution $\boldsymbol{x}_{n,p}(t)$ of the planar $2n$-body problem with equal masses whose braid type $X_{n,p}$ is pseudo-Anosov with the stretch factor $(\mathfrak{s}_{2p})^{\frac{2n}{d}}$, where $d = \gcd(n,p)$.*

A representative of the braid type $X_{n,p}$ in Theorem 5.1.4 is the $(\frac{n}{d})$th power $(\beta_{n,p})^{\frac{n}{d}}$ of the $2n$-braid $\beta_{n,p}$ introduced in Section 5.4. In 2006, the third author proved the existence of a family of multiple choreographic solutions $\boldsymbol{x}_{n,p}(t)$ of the planer $2n$-body problem with equal masses [52]. Some of the solutions in the family had already found by Chen [11,12] and Ferraio-Terracini [21]. The orbit of the periodic solution $\boldsymbol{x}_{n,p}(t)$ consists of $2d$ closed curves, each of which is the trajectory of $\frac{n}{d}$ bodies. The braid types $X_{n,p}(t)$ in Theorem 5.1.4 are realized by $\boldsymbol{x}_{n,p}(t)$ given in [52]. More precisely, for $n \geq 2$ and $p \in \{1, \ldots, \lfloor \frac{n}{2} \rfloor\}$, there exists a periodic solution

$$\boldsymbol{x}_{n,p}(t) = (x_1(t), \ldots, x_{2n}(t))$$

with period $T > 0$ of the planar $2n$-body problem such that

$$x_i(t + (\tfrac{d}{n})T) = x_{\sigma_{n,p}(i)}(t) \text{ for } i = 1, \ldots, 2n,$$

where $\sigma_{n,p} = (1, 3, \ldots, 2n-1)^p (2, 4, \ldots, 2n)^{-p} \in \mathfrak{S}_{2n}$ is a permutation of $2n$ elements. Thus, the braid $y_{n,p} := b(\boldsymbol{x}_{n,p}(t), [0, (\frac{d}{n})T])$ and the braid type $Y_{n,p} := \langle y_{n,p} \rangle$ are obtained from the solution $\boldsymbol{x}_{n,p}(t)$, and the $(\frac{n}{d})$th power $(y_{n,p})^{\frac{n}{d}}$ represents the braid type $X_{n,p}$. See Figure 5.1 for periodic solutions $\boldsymbol{x}_{n,p}(t)$ for $0 \leq t \leq (\frac{d}{n})T$. Theorem 5.1.4 follows from the following (see Remark 5.3.4).

**Theorem 5.1.5.** *For $n \geq 2$ and $p \in \{1, \ldots, \lfloor \frac{n}{2} \rfloor\}$, the braid type $Y_{n,p}$ is pseudo-Anosov with the stretch factor $(\mathfrak{s}_{2p})^2$. In particular, the braid type $X_{n,p}$ of the solution $\boldsymbol{x}_{n,p}(t)$ is pseudo-Anosov with the stretch factor $(\mathfrak{s}_{2p})^{\frac{2n}{d}}$.*

Since $\mathfrak{s}_k < \mathfrak{s}_{k'}$ if $k < k'$, we immediately have the following result.

**Corollary 5.1.6.** *Let $X_{n,p}$ be the braid type as in Theorem 5.1.5. For $n \geq 2$ and $p, p' \in \{1, \ldots, \lfloor \frac{n}{2} \rfloor\}$ with $p < p'$, we have the following.*

*(1) $\lambda(X_{n,p}) < \lambda(X_{n,p'})$ if $\gcd(n,p) = \gcd(n,p')$. In particular $X_{n,p} \neq X_{n,p'}$.*

*(2) $\lambda(X_{n,p}) < \lambda(X_{n,p'})$ if $n$ is prime. In particular $X_{n,p} \neq X_{n,p'}$.*

The $2n$ bodies for the solution $\boldsymbol{x}_{n,p}(t)$ form a regular $2n$-gon at the initial time $t = 0$, and the next first time is $t = (\frac{d}{2n})T$ when the $2n$ bodies form a regular $2n$-gon again. See Figure 5.1 for $\boldsymbol{x}_{n,p}(t)$ at $t = (\frac{d}{2n})T$. From the viewpoint of the configuration of the "next" regular $2n$-gon, it is proved in [52] that $\boldsymbol{x}_{n,p}(t)$ and $\boldsymbol{x}_{n,p'}(t)$ are distinct solutions for distinct $p, p' \in \{1, \ldots, \lfloor \frac{n}{2} \rfloor\}$ (Remark 5.2.1). On the other hand, from the viewpoint of braid types, Corollary 5.1.6 tells us that $X_{n,p}$ is different from $X_{n,p'}$ if $\gcd(n,p) = \gcd(n,p')$.

Table 5.1 shows the stretch factor $\lambda_{n,p} = \lambda(X_{n,p})$ and the entropy $\log(\lambda_{n,p})$ for several pairs $(n,p)$. One can see from this table that $\lambda(X_{n,p}) \neq \lambda(X_{n,p'})$ if $p \neq p'$ up to $n = 11$. Therefore the braid types $X_{n,p}$ and $X_{n,p'}$ of the solutions for $p \neq p' \in \{1, \ldots, \lfloor \frac{n}{2} \rfloor\}$ are distinct up to $n = 11$.

Because of an intriguing formula of metallic ratios, $\mathfrak{s}_k^3 = \mathfrak{s}_{k^3+3k}$ for example, stretch factors $\lambda(X_{n,p})$ happen to coincide with the ones for different pairs $(n,p')$ occasionally (see

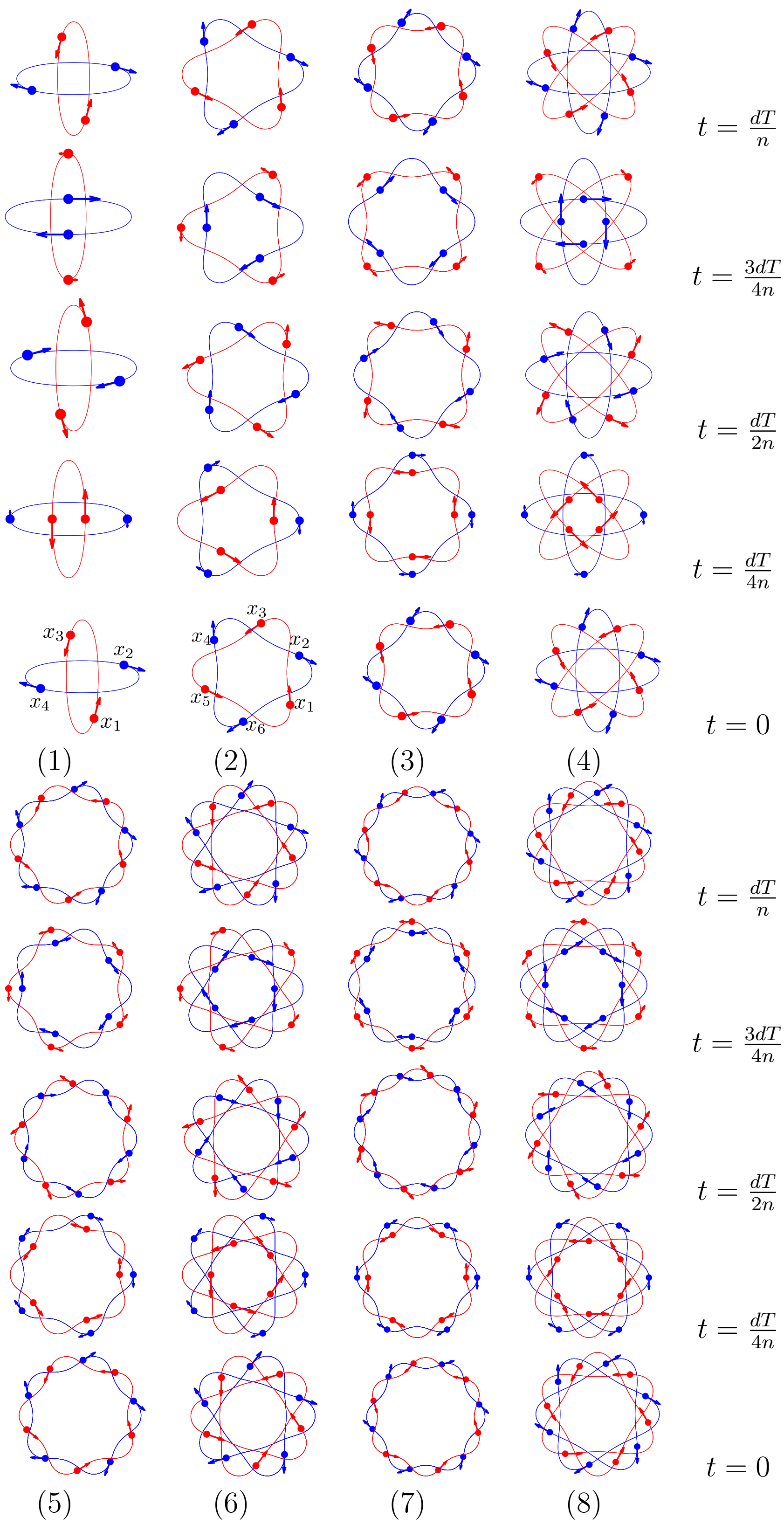


Figure 5.1: $\boldsymbol{x}_{n,p}(t)$ for $0 \le t \le (\frac{d}{n})T$: (1) $\boldsymbol{x}_{2,1}(t)$. (2) $\boldsymbol{x}_{3,1}(t)$. (3) $\boldsymbol{x}_{4,1}(t)$. (4) $\boldsymbol{x}_{4,2}(t)$. (5) $\boldsymbol{x}_{5,1}(t)$. (6) $\boldsymbol{x}_{5,2}(t)$. (7) $\boldsymbol{x}_{6,1}(t)$. (8) $\boldsymbol{x}_{6,2}(t)$.

Table 5.1: Some examples obtained from Theorem 5.1.4.

| $(n,p)$ | $d$ | $X_{n,p} = \langle(\beta_{n,p})^{\frac{n}{d}}\rangle$ | $\lambda_{n,p} = (\mathfrak{s}_{2p})^{\frac{2n}{d}}$ | $\log(\lambda_{n,p}) = (\frac{2n}{d})\log(\mathfrak{s}_{2,p})$ |
|---|---|---|---|---|
| $(2,1)$ | 1 | $(\beta_{2,1})^2$ | $(\mathfrak{s}_2)^4$ | 3.525494348078172 |
| $(3,1)$ | 1 | $(\beta_{3,1})^3$ | $(\mathfrak{s}_2)^6$ | 5.288241522117257 |
| $(4,1)$ | 1 | $(\beta_{4,1})^4$ | $(\mathfrak{s}_2)^8$ | 7.050988696156343 |
| $(4,2)$ | 2 | $(\beta_{4,2})^2$ | $(\mathfrak{s}_4)^4$ | 5.774541900715241 |
| $(5,1)$ | 1 | $(\beta_{5,1})^5$ | $(\mathfrak{s}_2)^{10}$ | 8.813735870195430 |
| $(5,2)$ | 1 | $(\beta_{5,2})^5$ | $(\mathfrak{s}_4)^{10}$ | 14.436354751788103 |
| $(6,1)$ | 1 | $(\beta_{6,1})^6$ | $(\mathfrak{s}_2)^{12}$ | 10.576483044234514 |
| $(6,2)$ | 2 | $(\beta_{6,2})^3$ | $(\mathfrak{s}_4)^6$ | 8.661812851072861 |
| $(6,3)$ | 3 | $(\beta_{6,3})^2$ | $(\mathfrak{s}_6)^4$ | 7.273785836928267 |
| $(7,1)$ | 1 | $(\beta_{7,1})^7$ | $(\mathfrak{s}_2)^{14}$ | 12.339230218273601 |
| $(7,2)$ | 1 | $(\beta_{7,2})^7$ | $(\mathfrak{s}_4)^{14}$ | 20.210896652503344 |
| $(7,3)$ | 1 | $(\beta_{7,3})^7$ | $(\mathfrak{s}_6)^{14}$ | 25.458250429248935 |
| $(8,1)$ | 1 | $(\beta_{8,1})^8$ | $(\mathfrak{s}_2)^{16}$ | 14.101977392312687 |
| $(8,2)$ | 2 | $(\beta_{8,2})^4$ | $(\mathfrak{s}_4)^8$ | 11.549083801430482 |
| $(8,3)$ | 1 | $(\beta_{8,3})^8$ | $(\mathfrak{s}_6)^{16}$ | 29.095143347713069 |
| $(8,4)$ | 4 | $(\beta_{8,4})^2$ | $(\mathfrak{s}_8)^4$ | 8.378850189044405 |
| $(9,1)$ | 1 | $(\beta_{9,1})^9$ | $(\mathfrak{s}_2)^{18}$ | 15.864724566351773 |
| $(9,2)$ | 1 | $(\beta_{9,2})^9$ | $(\mathfrak{s}_4)^{18}$ | 25.985438553218586 |
| $(9,3)$ | 3 | $(\beta_{9,3})^3$ | $(\mathfrak{s}_6)^6$ | 10.910678755392400 |
| $(9,4)$ | 1 | $(\beta_{9,4})^9$ | $(\mathfrak{s}_8)^{18}$ | 37.704825850699820 |
| $(10,1)$ | 1 | $(\beta_{10,1})^{10}$ | $(\mathfrak{s}_2)^{20}$ | 17.627471740390860 |
| $(10,2)$ | 2 | $(\beta_{10,2})^5$ | $(\mathfrak{s}_4)^{10}$ | 14.436354751788103 |
| $(10,3)$ | 1 | $(\beta_{10,3})^{10}$ | $(\mathfrak{s}_6)^{20}$ | 36.368929184641338 |
| $(10,4)$ | 2 | $(\beta_{10,4})^5$ | $(\mathfrak{s}_8)^{10}$ | 20.947125472611013 |
| $(10,5)$ | 5 | $(\beta_{10,5})^2$ | $(\mathfrak{s}_{10})^4$ | 9.249753365091010 |
| $(11,1)$ | 1 | $(\beta_{11,1})^{11}$ | $(\mathfrak{s}_2)^{22}$ | 19.390218914429944 |
| $(11,2)$ | 1 | $(\beta_{11,2})^{11}$ | $(\mathfrak{s}_4)^{22}$ | 31.759980453933828 |
| $(11,3)$ | 1 | $(\beta_{11,3})^{11}$ | $(\mathfrak{s}_6)^{22}$ | 40.005822103105473 |
| $(11,4)$ | 1 | $(\beta_{11,4})^{11}$ | $(\mathfrak{s}_8)^{22}$ | 46.083676039744226 |
| $(11,5)$ | 1 | $(\beta_{11,5})^{11}$ | $(\mathfrak{s}_{10})^{22}$ | 50.873643508000555 |

Example 5.4.1). Nevertheless, we conjecture that $X_{n,p} \neq X_{n,p'}$ for all $p, p' \in \{1, \dots, \lfloor \frac{n}{2} \rfloor\}$ with $p \neq p'$.

The organization of Chapter 5 is as follows. In Section 5.2 we introduce a family of periodic solutions $\boldsymbol{x}_{n,p}(t)$ in [52] of the planar $2n$-body problem. In Section 5.3 we briefly review the necessarily background on braid groups. We prove Theorem 5.1.5 in Section 5.4. In Section 5.5, we give new numerical periodic solutions $\boldsymbol{x}_{n,p}(t)$ of the planar $2n$-body problem when $p > \lfloor \frac{n}{2} \rfloor$.

## 5.2 Periodic solutions of the planar $2n$-body problem

This section is devoted to explain the periodic solutions $\boldsymbol{x}_{n,p}(t)$. The existence was proven with the variational method. They have high symmetries because they can be represented as elements of a functional space limited by several group actions. The minimizers of the action functional under the symmetry correspond to those solutions. They are also regarded as orbits on the *shape sphere*. They are constructed through minimizing methods, and we omit analytic techniques for the proof and describe geometric properties of $\boldsymbol{x}_{n,p}(t)$ including the group actions and shape sphere.

### 5.2.1 Symmetry

Let $G$ be a finite group. We consider a 2-dimensional orthogonal representation $\rho : G \to O(2)$, a homomorphism $\sigma : G \to \mathfrak{S}_{2n}$ to the symmetric group on $2n$ elements, and another 2-dimensional orthogonal representation $\tau : G \to O(2)$. We will denote by $\Lambda$, the set of $T$-periodic orbits. The action of $G$ to $\Lambda$ is defined by

$$g \cdot ((x_1, \dots, x_{2n})(t)) = (\rho(g) x_{\sigma(g^{-1})(1)}, \dots, \rho(g) x_{\sigma(g^{-1})(2n)})(\tau(g^{-1})(t))$$

for $g \in G$ and $\boldsymbol{x}(t) = (x_1, \dots, x_{2n})(t) \in \Lambda$, where the above $\rho$, $\sigma$, $\tau$ represent respectively actions of $G$ on $\mathbb{R}^2$ by orthogonal transformations, on indices $\{1, 2, \dots, 2n\}$ by permutations, and on the circle $\mathbb{R}/T\mathbb{Z}$. Specifically, we take $G$ as the group $G_{n,p} := \langle g_n, h_{n,p} \rangle$ generated by the two elements $g_n$ and $h_{n,p}$, where

$$\begin{aligned}
\rho(g_n) &= \begin{pmatrix} \cos(\frac{\pi}{n}) & -\sin(\frac{\pi}{n}) \\ \sin(\frac{\pi}{n}) & \cos(\frac{\pi}{n}) \end{pmatrix}, \\
\sigma(g_n) &= (1, 2, \dots, 2n), \\
\tau(g_n) &= \begin{pmatrix} 1 & 0 \\ 0 & -1 \end{pmatrix} \text{ and} \\
\rho(h_{n,p}) &= 1, \\
\sigma(h_{n,p}) &= (1, 3, \dots, 2n-1)^{-p} (2, 4, \dots, 2n)^p, \\
\tau(h_{n,p}) &= \begin{pmatrix} \cos(\frac{2\pi d}{n}) & -\sin(\frac{2\pi d}{n}) \\ \sin(\frac{2\pi d}{n}) & \cos(\frac{2\pi d}{n}) \end{pmatrix} \quad (d := \gcd(n, p)).
\end{aligned}$$

Let us denote by $\Lambda^G_{n,p}$, the invariant set under the action of $G_{n,p}$ in $\Lambda$, i.e.,

$$\Lambda^G_{n,p} = \{\boldsymbol{x}(t) \in \Lambda \mid x_i(t) = \rho(g) x_{\sigma(g^{-1})(i)}(\tau(g^{-1})(t)) \\ (i = 1, 2, \dots, 2n,\ g \in G_{n,p},\ t \in \mathbb{R})\}.$$

We now check the properties of $\Lambda^G_{n,p}$. First, from the invariance under $g_n$, we have

$$g_n \cdot ((x_1, x_2, \dots, x_{2n})(t)) = (e^{\frac{\pi i}{n}} x_{2n}, e^{\frac{\pi i}{n}} x_1, \dots, e^{\frac{\pi i}{n}} x_{2n-1})(-t).$$

Here we identify $\mathbb{R}^2$ with $\mathbb{C}$. In particular, $x_1(t), x_2(-t), \dots, x_{2n-1}(t), x_{2n}(-t)$ forms a regular $2n$-gon, and $n$ bodies with odd indices and $n$ bodies with even indices rotate in mutually opposite directions.

Second, since

$$\begin{aligned} \rho(g_n^2) &= \begin{pmatrix} \cos(\frac{2\pi}{n}) & -\sin(\frac{2\pi}{n}) \\ \sin(\frac{2\pi}{n}) & \cos(\frac{2\pi}{n}) \end{pmatrix}, \\ \sigma(g_n^2) &= (1, 3, \dots, 2n-1)(2, 4, \dots, 2n) \text{ and} \\ \tau(g_n^2) &= 1, \end{aligned}$$

the configuration always consists of two regular $n$-gons, which are formed by $n$ bodies $x_1(t), x_3(t), \dots, x_{2n-1}(t)$ of odd indices and $n$ bodies $x_2(t), x_4(t), \dots, x_{2n}(t)$ of even indices. Thus, to determine the positions of $2n$ bodies $x_1, \dots, x_{2n}$, it is sufficient to know the positions of two bodies $x_1$ and $x_2$. In fact for each $k \in \{1, \dots, n\}$ and $t \in \mathbb{R}$,

$$x_{2k-1}(t) = \omega^{(k-1)} x_1(t), \;\; x_{2k}(t) = \omega^{(k-1)} x_2(t),$$

where $\omega = e^{2\pi i/n}$. This enables us to use the shape sphere (introduced in Section 5.2.2) which represents configurations of $2n$ bodies in the periodic solutions.

Lastly, the invariance under $h_{n,p}$ tells us that

$$h_{n,p} \cdot ((x_1, x_2, \dots, x_{2n})(t)) = (x_{\sigma(h_{n,p}^{-1})(1)}, x_{\sigma(h_{n,p}^{-1})(2)}, \dots, x_{\sigma(h_{n,p}^{-1})(2n)})(t - \tfrac{dT}{n}),$$

and hence

$$x_i\left(t + \tfrac{dT}{n}\right) = x_{\sigma(h_{n,p}^{-1})(i)}(t) \;\; (i = 1, 2, \dots, 2n),$$

where

$$\sigma(h_{n,p}^{-1}) = (1, 3, \dots, 2n-1)^p (2, 4, \dots, 2n)^{-p} \in \mathfrak{S}_{2n}. \tag{5.2.1}$$

This implies that $\boldsymbol{x}_{n,p}(t)$ consists of $2d$ closed curves and $\frac{n}{d}$ bodies chase one another along each closed curve. See Figure 5.1.

### 5.2.2 The shape sphere

We consider the group action on the circle $S^1$ to $\mathbb{C}^2$ by

$$z \cdot (x_1, x_2) = (z x_1, z x_2), \;\; z \in S^1, (x_1, x_2) \in \mathbb{C}^2.$$

The quotient space $(\mathbb{C}^2 - \{0\})/S^1$ under the above action is realized by the following projection:

$$\begin{aligned} \pi\colon \mathbb{C}^2 - \{0\} &\longrightarrow \mathbb{R}^3 - \{0\} \; (\cong (\mathbb{C}^2 - \{0\})/S^1) \\ (x_1, x_2) &\longmapsto \boldsymbol{u}(t) = (u_1, u_2, u_3) \end{aligned}$$

where

$$\begin{aligned}(u_1, u_2, u_3) &= (|x_1|^2 - |x_2|^2, 2\mathrm{Re}(x_1\bar{x_2}), 2\mathrm{Im}(x_1\bar{x_2}))\\ &= (r_1^2 - r_2^2, 2r_1r_2\cos(\theta_1-\theta_2), 2r_1r_2\sin(\theta_1-\theta_2)).\end{aligned}$$

Here $x_1 = r_1e^{i\theta_1}$ and $x_2 = r_2e^{i\theta_2}$. Set the rays

$$\begin{aligned}\mathrm{A}_\pm &= \{(\pm s, 0, 0) \mid s \in \mathbb{R}_{>0}\},\\ \mathrm{B}_{2k} &= \left\{\left(0, s\cos(\frac{2\pi k}{n}), s\sin(\frac{2\pi k}{n}) \mid s \in \mathbb{R}_{>0}\right)\right\} \ (k \in \mathbb{Z}) \text{ and}\\ \mathrm{B}_{2k-1} &= \left\{\left(0, s\cos(\frac{(2k-1)\pi}{n}), s\sin(\frac{(2k-1)\pi}{n}) \mid s \in \mathbb{R}_{>0}\right)\right\} \ (k \in \mathbb{Z}).\end{aligned}$$

In the quotient space $(\mathbb{C}^2 - \{0\})/S^1$, the sets $\mathrm{A}_\pm$ and $\mathrm{B}_{2k}$ correspond to collisions of the original $2n$ bodies. If $\boldsymbol{u}(t) \in \mathrm{A}_+$ (resp. $\mathrm{A}_-$), then all bodies with odd (resp. even) indeces collide at $t \in \mathbb{R}$ and if $\boldsymbol{u}(t) \in \mathrm{B}_{2k}$, then two regular $n$-gons fit. See Figure 5.4 for the configurations of 8 bodies corresponding to $\mathrm{B}_0$, $\mathrm{B}_2$, $\mathrm{B}_4$ and $\mathrm{B}_6$.

Let $\boldsymbol{u}(t)(= \boldsymbol{u}_{n,p}(t))$ be a curve corresponding to the solution $\boldsymbol{x}_{n,p}(t)$. As a result, $\boldsymbol{u}(t)$ passes through neither $\mathrm{A}_\pm$ nor $\mathrm{B}_{2k}$, because $\boldsymbol{x}_{n,p}(t)$ has no collision ( [52, Proposition 3]). On the other hand, each $\mathrm{B}_{2k-1}$ represents a configuration where $2n$ bodies form a regular $2n$-gon. See Figure 5.4 for the configurations of 8 bodies corresponding to $\mathrm{B}_{-1}$, $\mathrm{B}_1$, $\mathrm{B}_3$ and $\mathrm{B}_5$.

Set

$$M(k) = \begin{pmatrix} -1 & 0 & 0\\ 0 & \cos(\frac{2\pi k}{n}) & \sin(\frac{2\pi k}{n})\\ 0 & \sin(\frac{2\pi k}{n}) & -\cos(\frac{2\pi k}{n})\end{pmatrix}.$$

It is easy to see that $M(k)$ is an orthogonal matrix with eigenvalues $\lambda = 1, -1$. The eigenvector for $\lambda = 1$ is $\mathrm{B}_k$, and hence $M(k)$ represents $\pi$-rotation with respect to $\mathrm{B}_k$. The invariance under $g_n$ is associated with

$$\begin{pmatrix} u_1(-t)\\ u_2(-t)\\ u_3(-t)\end{pmatrix} = M(-1)\begin{pmatrix} u_1(t)\\ u_2(t)\\ u_3(t)\end{pmatrix}$$

and it implies that $\boldsymbol{u}(t)$ and $\boldsymbol{u}(-t)$ are symmetric with respect to $\mathrm{B}_{-1}$. In other words, rotating this curve $\pi$ with respect to $\mathrm{B}_{-1}$, $\boldsymbol{u}(t)$ coincides with $\boldsymbol{u}(-t)$. In particular $\boldsymbol{u}(0) \in \mathrm{B}_{-1}$. Similarly, the invariance under $h_{n,p}$ is associated with

$$\begin{pmatrix} u_1(t+2\bar{T})\\ u_2(t+2\bar{T})\\ u_3(t+2\bar{T})\end{pmatrix} = \begin{pmatrix} 1 & 0 & 0\\ 0 & \cos(\frac{4\pi p}{n}) & -\sin(\frac{4\pi p}{n})\\ 0 & \sin(\frac{4\pi p}{n}) & \cos(\frac{4\pi p}{n})\end{pmatrix}\begin{pmatrix} u_1(t)\\ u_2(t)\\ u_3(t)\end{pmatrix},$$

where $\bar{T} = \frac{dT}{2n}$. Substituting $-(t+\bar{T})$ into $t$ and applying the invariance under $g_n$, we obtain

$$\begin{pmatrix} u_1(-t+\bar{T})\\ u_2(-t+\bar{T})\\ u_3(-t+\bar{T})\end{pmatrix} = M(2p-1)\begin{pmatrix} u_1(t+\bar{T})\\ u_2(t+\bar{T})\\ u_3(t+\bar{T})\end{pmatrix}.$$

Taking $t = 0$ gives

$$\begin{pmatrix} u_1(\bar{T}) \\ u_2(\bar{T}) \\ u_3(\bar{T}) \end{pmatrix} = M(2p-1) \begin{pmatrix} u_1(\bar{T}) \\ u_2(\bar{T}) \\ u_3(\bar{T}) \end{pmatrix},$$

and hence $\boldsymbol{u}(t+\bar{T})$ and $\boldsymbol{u}(-t+\bar{T})$ are symmetric with respect to $\mathrm{B}_{2p-1}$ and $\boldsymbol{u}(\bar{T}) \in \mathrm{B}_{2p-1}$. It means that the original configuration of $2n$ bodies forms a regular $2n$-gon again at $t = \bar{T}$. Other symmetries with respect to $\mathrm{B}_{2jp-1}$ for $j = 2, 3, \dots$ can be seen in the same manner.

**Remark 5.2.1.** *It is proved in [52, Proposition 5] that $\boldsymbol{u}(t) \notin \mathrm{B}_{2k-1}$ for all $t \in (0, \bar{T})$ and $k \in \mathbb{Z}$ . It implies that $\boldsymbol{x}_{n,p}(t)$ and $\boldsymbol{x}_{n,p'}(t)$ are distinct smooth solution for $p \neq p'$ in the sense that $\boldsymbol{u}(\bar{T})$ belongs to $\mathrm{B}_{2p-1}$, that is in the sense that the configuration of the first regular $2n$-gon lives in the distinct $\mathrm{B}_{2p-1}$ for each $p$.*

Consider the projection from $\mathbb{R}^3 - \{0\}$ to the 2-sphere $\mathbb{S}^2$. The projective space is called the *shape sphere*. The image of $\boldsymbol{u}(t) \in \mathbb{R}^3 - \{0\}$ under the projection is also denoted by the same notation $\boldsymbol{u}(t)$, and we call a family $\{\boldsymbol{u}(t)\}_t$ (on the shape sphare) the *shape curve*. Determining the shape curve $\boldsymbol{u}(t)$ for $t \in (0, \bar{T})$, we obtain the shape curve $\boldsymbol{u}(t)$ for all $t \in \mathbb{R}$ from the above symmetries. For example, we show the shape curves $\boldsymbol{u}(t)$ for $t \in \mathbb{R}$ when $(n, p) = (3, 1)$ and $(n, p) = (4, 2)$ in Figure 5.2. Each point $\mathrm{B}_i$ in Figure 5.2 indicates the projection of the ray $\mathrm{B}_i$ onto the shape sphere. The solid arrows (resp. the dotted arrows) illustrate the shape curve $\boldsymbol{u}(t)$ in the front side on the shape sphere, i.e., $u_1(t)(= |x_1(t)|^2 - |x_2(t)|^2) > 0$, (resp. the back side, i.e., $u_1(t) < 0$). The dotted arrow of label 2 follows from symmetry of the solid arrow of label 1 with respect to $\mathrm{B}_1$. The remaining cases are treated in the same fashion.

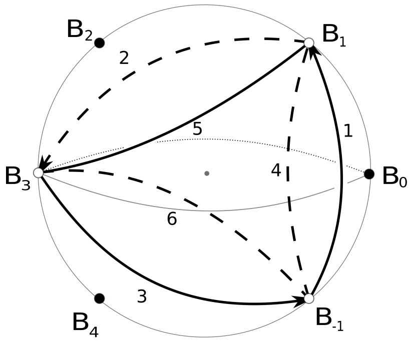


(a) $(n, p) = (3, 1)$

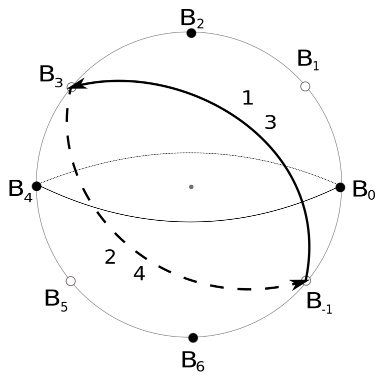


(b) $(n, p) = (4, 2)$

Figure 5.2: The shape curve $\boldsymbol{u}(t)$ for $t \in \mathbb{R}$ when (1) $(n, p) = (3, 1)$ and (2) $(n, p) = (4, 2)$.

The point $\mathrm{B}_i$ in the figure is the projection of the ray $\mathrm{B}_i$ onto the shape sphere.

**Remark 5.2.2.** *Though the set $\Lambda^G_{n,p}$ does not determine how the shape curve $\boldsymbol{u}(t)$ moves on the shape sphere for $t \in (0, \bar{T})$, we can prove through variational arguments that it does not happen like Figure 5.3(1) or (2). See [52, Propositions 5 and 6] for the proof.*

Figure 5.4 illustrates the projection of the shape curve $\boldsymbol{u}(t)$ onto the $u_2u_3$-plane together with the configuration of 8 bodies corresponding to each $\mathrm{B}_i$ when $(n, p) = (4, 1)$ and $(4, 2)$.

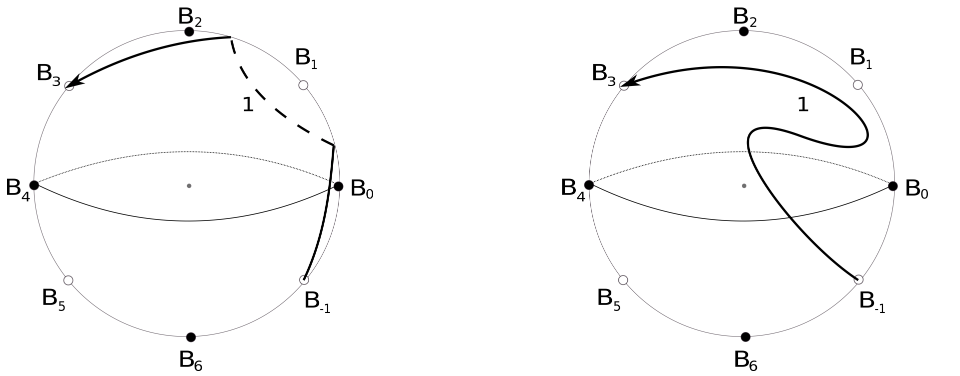


(a) Error type 1: Across the $u_2u_3$-plane (b) Error type 2: Non-monotonicity

Figure 5.3: Error types of the shape curve $\boldsymbol{u}(t)$ $(0 \leq t \leq \bar{T})$ when $(n, p) = (4, 2)$. (1) Error type 1: $\boldsymbol{u}(t)$ $(0 \leq t \leq \bar{T})$ is across the $u_2u_3$-plane. (2) Error type 2: $\boldsymbol{u}(t)$ is not monotone. For the shape curve $\boldsymbol{u}(t)$ $(0 \leq t \leq \bar{T})$, see the solid arrow with label 1 in Figure 5.2(2).

# 5.3 Braid groups and mapping class groups

## 5.3.1 Geometric braids

In this section, we recall definitions of (geometric) braids and the braid types. For the basics on braid groups, see Birman [8]. Let $D$ be a closed disk in the plane $\mathbb{R}^2$ and $Q_m = \{q_1, \ldots, q_m\}$ be a set of $m$ points in the interior of $D$. Let $\gamma_1, \ldots, \gamma_m$ be mutually disjoint $m$ arcs in $D \times [0, 1]$ with the following properties.

- $\partial(\gamma_1 \cup \cdots \cup \gamma_m) = \{(q_1, t), \ldots, (q_m, t) \mid t \in \{0, 1\}\} \subset D \times \{0, 1\}$,
- $\gamma_i$ $(i = 1, \ldots, m)$ starts at $(q_i, 0) = \gamma_i \cap (D \times \{0\})$ and it goes up monotonically with respect to the $[0, 1]$-factor. In particular $\gamma_i \cap (D \times \{t\})$ consists of a single point for $0 \leq t \leq 1$.

We call $b = \gamma_1 \cup \cdots \cup \gamma_m \subset D \times [0, 1]$ a *(geometric) braid with base points* $Q_m$ and call each $\gamma_i$ a *strand* of the braid $b$. We say that braids $b$ and $b'$ with base points $Q_m$ are *equivalent* if there is a 1-parameter family of braids with base points $Q_m$ deforming $b$ to $b'$. By abuse of notations, the equivalence class $[b]$ is also denote by $b$.

For braids $b$ and $b'$ with base points $Q_m$, the product $bb'$ is defined as follows. We first stuck $b$ on $b'$ and concatenate them to get disjoint arcs properly embedded in $D \times [0, 2]$. By normalizing its height, we obtain a braid (in $D \times [0, 1]$) with the same base points $Q_m$ and this is the braid $bb'$. The set of all braids with base points $Q_m$ with this product gives a group structure. The group is called the *(geometric) braid group with base points* $Q_m$ and it is denoted by $B(Q_m)$. Note that the identity element $1_{Q_m} \in B(Q_m)$ is given by a braid consisting of straight arcs.

Let $A_m = \{a_1, \ldots, a_m\}$ be a set of $m$ points in the interior of $D$ such that $a_1, \ldots, a_m$ lie on a segment in this order. We write $B_m = B(A_m)$ and call $B_m$ the *m-braid group*. The isomorphism class of the above braid group $B(Q_m)$ with base points $Q_m$ does not depend on the location of base points, and $B(Q_m)$ is isomorphic to $B_m$. To define braid types

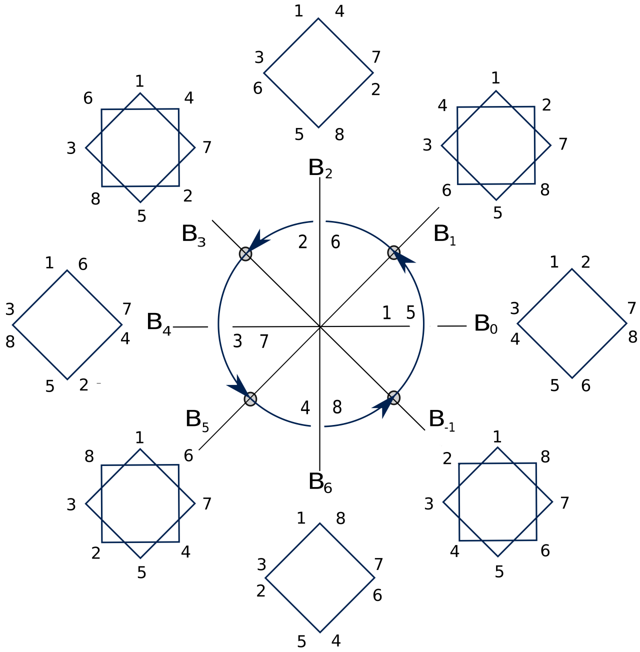


(a) $(n, p) = (4, 1)$

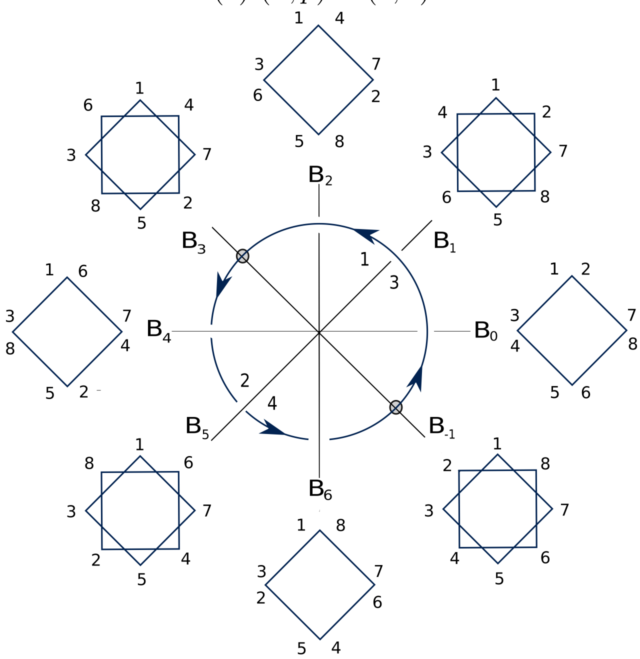


(b) $(n, p) = (4, 2)$

Figure 5.4: The projection of the shape curve $\boldsymbol{u}(t)$ for $t \in \mathbb{R}$ onto the $u_2u_3$-plane when (1) $(n, p) = (4, 1)$ and (2) $(n, p) = (4, 2)$. The configuration of 8 bodies corresponding to $\mathrm{B}_i$ is illustrated.

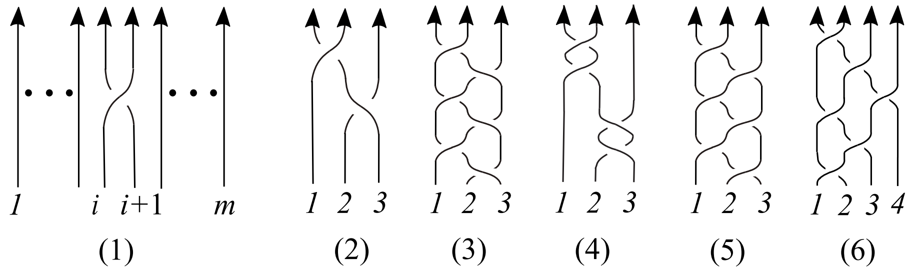


Figure 5.5: (1) $\sigma_i \in B_m$. (2) $\sigma_1\sigma_2^{-1} \in B_3$. (3) $(\sigma_1\sigma_2^{-1})^3 \in P_3 < B_3$. (4) $\sigma_1^2\sigma_2^{-2} \in P_3 < B_3$. (5) A full twist $\Delta^2 \in P_3 < B_3$. (6) A half twist $\Delta \in B_4$.

of geometric braids with arbitrary base points $Q_m$, we now take an isomorphism between $B(Q_m)$ and $B_m$. We first choose an orientation preserving homeomorphism $f : D \to D$ such that $f(A_m) = Q_m$. Then take an isotopy $\{f_t\}_{0\le t\le 1}$ on $D$ between the identity map $\mathrm{id}_D$ and $f$, i.e., $f_0 = \mathrm{id}_D$ and $f_1 = f$. We consider two kinds of mutually disjoint $m$ arcs $\gamma^+$ and $\gamma^-$ properly embedded in $D \times [0,1]$ as follows.

$$\begin{aligned}\gamma^+ &= \bigcup_{t\in[0,1]} \{(f_t(a_1),t),\dots,(f_t(a_m),t)\},\\ \gamma^- &= \bigcup_{t\in[0,1]} \{(f_{1-t}(a_1),t),\dots,(f_{1-t}(a_m),t)\}.\end{aligned}$$

Note that $Q_m = f_1(A_m) = \{f(a_1),\dots,f(a_m)\}$ and $A_m = f_0(A_m) = \{a_1,\dots,a_m\}$. Because of this, it makes sense to stack a braid $b \in B(Q_m)$ on $\gamma^+$, and we obtain the resulting disjoint $m$ arcs $b\cdot\gamma^+ \subset D\times[0,2]$. Then we stack $\gamma^-$ on $b\cdot\gamma^+$. As a result we have disjoint $m$ arcs

$$\gamma^- \cdot b \cdot \gamma^+ \subset D \times [0,3].$$

By normalizing the height of the arcs, we obtain a braid (in $D\times[0,1]$) with base points $A_m$, and we still denote it by the same notation $\gamma^-\cdot b\cdot\gamma^+$. In particular if $b = 1_{Q_m} \in B(Q_m)$, then $\gamma^- 1_{Q_m}\gamma^+ = 1_{A_m} \in B_m$. The correspondence $b \mapsto \gamma^-\cdot b\cdot\gamma^+$ gives us an isomorphism between $B(Q_m)$ and $B_m$.

For an element $b \in B_m$, we put indices $1,\dots,m$ at the bottoms of strands so that the index $i$ indicates $(a_i,0) \in D\times\{0\}$. Let $\sigma_i$ be an element of $B_m$ as in Figure 5.5(1). The braid group $B_m$ is generated by $\sigma_1,\sigma_2,\dots,\sigma_{m-1}$, and it has the following braid relations.

(B1) $\sigma_i\sigma_j = \sigma_j\sigma_i$ ($|i-j|\ge 2$).

(B2) $\sigma_i\sigma_{i+1}\sigma_i = \sigma_{i+1}\sigma_i\sigma_{i+1}$ ($1 \le i \le m-2$).

See Figure 5.5(2)–(6) for some braids. There is a surjective homomorphism

$$\hat\sigma : B_m \to \mathfrak{S}_m$$

from $B_m$ to the symmetry group $\mathfrak{S}_m$ of $m$ elements sending each $\sigma_j$ to the transposition $(j,j+1)$. The kernel of $\hat\sigma$ is called the *pure braid group* (or *colored braid group*) $P_m < B_m$. An element of $P_m$ is called a *pure braid*. See Figure 5.5(3)(4)(5) for some pure braids.

Let $Z(B_m)$ be the center of $B_m$ which is an infinite cyclic group generated by a *full twist* $\Delta^2$, where a *half twist* $\Delta = \Delta_m \in B_m$ is given by

$$\Delta_m = (\sigma_1\sigma_2\dots\sigma_{m-1})(\sigma_1\sigma_2\dots\sigma_{m-2})\dots(\sigma_1\sigma_2)\sigma_1.$$

See Figure 5.5(6) for a half twist $\Delta \in B_4$.

Given a braid $b \in B_m$, consider the projection $\bar{b}$ in the quotient group

$$\mathcal{B}_{2n} = B_{2n}/Z(B_{2n}).$$

The *braid type* $\langle b \rangle$ of $b$ is a conjugacy class of $\bar{b}$ in $\mathcal{B}_{2n}$.

In the case of the braid group $B(Q_m)$ with base points $Q_m$, the *braid type* $\langle b \rangle$ of $b \in B(Q_m)$ is defined by the braid type $\langle \gamma^- \cdot b \cdot \gamma^+ \rangle$ of the braid $\gamma^- \cdot b \cdot \gamma^+ \in B_m$ (with base points $A_m$), where $\gamma^+$ and $\gamma^-$ are arcs as above. The braid type $\langle b \rangle$ is well-defined, i.e., it does not depend on the above orientation preserving homeomorphism $f : D \to D$ and the isotopy $\{f_t\}_{0 \le t \le 1}$.

**Example 5.3.1.**

*(1) For the* 3*-braid* $\sigma_1\sigma_2^{-1}$*, it follows that*

$$\hat{\sigma}(\sigma_1\sigma_2^{-1}) = \hat{\sigma}(\sigma_1)\hat{\sigma}(\sigma_2^{-1}) = (12)(23) = (123) \in \mathfrak{S}_3,$$

*see Figure 5.5(2). Hence* $\hat{\sigma}((\sigma_1\sigma_2^{-1})^3) = 1 \in \mathfrak{S}_3$ *which means that* $(\sigma_1\sigma_2^{-1})^3 \in P_3$.

*(2) For the* 3*-braid* $\sigma_1^2\sigma_2^{-2}$*, it follows that*

$$\hat{\sigma}(\sigma_1^2\sigma_2^{-2}) = \hat{\sigma}(\sigma_1^2)\hat{\sigma}(\sigma_2^{-2}) = 1 \cdot 1 = 1 \in \mathfrak{S}_3,$$

*see Figure 5.5(4). Hence* $\sigma_1^2\sigma_2^{-2} \in P_3$.

**Example 5.3.2.** *For the Euler's periodic solution of the planar* 3*-body problem, three bodies are collinear at every instant. A full twist* $\Delta^2 = (\sigma_1\sigma_2\sigma_1)^2 = (\sigma_1\sigma_2)^3 \in B_3$ *(Figure 5.5(5)) represents the braid type of the solution. Since* $Z(B_3)$ *is generated by* $\Delta^2$*, the braid type of the Euler's periodic solution is trivial. Similarly, it is the trivial braid type for the Lagrange's periodic solution of the planar* 3*-body problem, since the triangle formed by the three bodies is equilateral for all time.*

### 5.3.2 Mapping class groups

Let $X_1, \dots, X_n$ be possibly empty subspaces of an orientable manifold $M$. For instance $M$ is a connected orientable surface $\Sigma_{g,m}$ of genus $g \ge 0$ with $m$ punctures (possibly $m = 0$) and $X_i$ $(i = 1, \dots, n)$ is a finite set in $\Sigma_{g,m}$. Let $\mathrm{Homeo}_+(M, X_1, \dots, X_n)$ be the group of orientation-preserving self-homeomorphisms of $M$ that map $X_i$ onto $X_i$ for each $i = 1, \dots, n$. We do not require that homeomorphisms fix the boundary $\partial M$ pointwise. The mapping class group $\mathrm{MCG}(M, X_1, \dots, X_n)$ is defined by

$$\mathrm{MCG}(M, X_1, \dots, X_n) = \pi_0(\mathrm{Homeo}_+(M, X_1, \dots, X_n)),$$

that is the group of isotopy classes of elements of $\mathrm{Homeo}_+(M, X_1, \dots, X_n)$. When $X$ is an empty subspace of $M$, then we write $\mathrm{MCG}(M) = \mathrm{MCG}(M, X)$. We apply elements of mapping class groups from right to left, i.e., we apply $g$ first for the product $fg$.

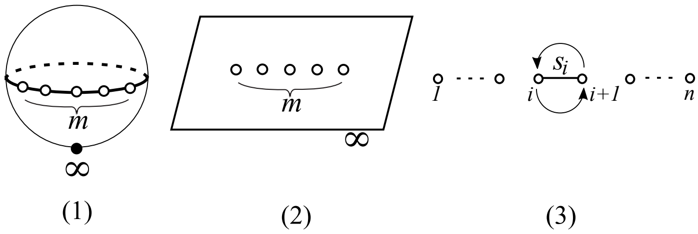


Figure 5.6: (1) A pair $(\Sigma_{0,m}, \{\infty\})$. (2) An $m$-punctured plane. (3) A half twist $h_i$.

Let $D_m = D \setminus A_m$ be an $m$-punctured disk, where $A_m = \{a_1, \dots, a_m\}$ is the set of $m$ points in the interior of $D$ as in Section 5.3.1. By definition, $\mathrm{MCG}(D_m)$ is the group of isotopy classes of elements of $\mathrm{Homeo}_+(D_m)$ which fix $\partial D$ setwise. In this chapter, we mainly consider an $m$-punctured disk $D_m$ or an $m$-punctured sphere $\Sigma_{0,m}$ as an orientable manifold $M$ for the mapping class groups. We take a point in $\Sigma_{0,m}$ and call it $\infty$. An element $f \in \mathrm{Homeo}_+(\Sigma_{0,m}, \{\infty\})$ means that $f$ fixes the point $\infty$. Puncturing the point $\infty$, we think of $\mathrm{MCG}(\Sigma_{0,m}, \{\infty\})$ as a subgroup of $\mathrm{MCG}(\Sigma_{0,m+1})$. Also we may regard $\mathrm{MCG}(\Sigma_{0,m}, \{\infty\})$ as the mapping class group of an $m$-punctured plane. See Figure 5.6(1)(2).

The mapping class group $\mathrm{MCG}(D_m)$ is generated by $h_1, \dots, h_{m-1}$, where $h_i$ is the right-handed *half twist* about a segment $s_i$ connecting the $i$th and $(i+1)$th punctures, see Figure 5.6(3). More precisely, let $\mathbb{D}_i \subset \mathrm{int}(D)$ be a closed disk such that $\mathbb{D}_i$ contains the two points $a_i$ and $a_{i+1}$ together with a segment $s_i$ between the punctures $a_i$ and $a_{i+1}$. Moreover $\mathbb{D}_i$ contains no other points of $A_m$. Then the right-handed half-twist $h_i \in \mathrm{MCG}(D_m)$ is a mapping class that fixes the exterior of $\mathbb{D}_i$ and rotates $s_i$ in $\mathbb{D}_i$ by $\pi$ in the counter-clockwise direction. Hence $h_i$ interchanges the $i$th puncture with the $(i+1)$th puncture.

We now recall a relation between $B_m$ and $\mathrm{MCG}(D_m)$. There is a surjective homomorphism

$$\Gamma : B_m \to \mathrm{MCG}(D_m)$$

which sends $\sigma_i$ to $h_i$ for $i = 1, \dots, m-1$. The kernel of $\Gamma$ is the center $Z(B_m)$, and hence $\mathcal{B}_m = B_m / Z(B_m)$ is isomorphic to $\mathrm{MCG}(D_m)$. Collapsing $\partial D$ to the point $\infty$ in the sphere, we have a homomorphism

$$\mathfrak{c} : \mathrm{MCG}(D_n) \to \mathrm{MCG}(\Sigma_{0,m}, \{\infty\}).$$

By abuse of notations, we simply denote by $b$, the mapping class $\mathfrak{c}(\Gamma(b)) \in \mathrm{MCG}(\Sigma_{0,m}, \{\infty\})$. Also we denote by $\langle b \rangle$, the conjugacy class $\big\langle \mathfrak{c}(\Gamma(b)) \big\rangle$ of $\mathfrak{c}(\Gamma(b)) \in \mathrm{MCG}(\Sigma_{0,m}, \{\infty\})$. Note that this notation $\langle b \rangle$ is the same as the braid type of $b \in B_m$.

### 5.3.3 Nielsen-Thurston classification

According to the Nielsen-Thurston classification [59], mapping classes fall into three types: periodic, reducible and pseudo-Anosov. Assume that $3g - 3 + m \geq 1$. A mapping class $\phi \in \mathrm{MCG}(\Sigma_{g,m})$ is *periodic* if $\phi$ is of finite order. A mapping class $\phi \in \mathrm{MCG}(\Sigma_{g,m})$ is *reducible* if there is a collection of mutually disjoint and non-homotopic essential simple closed curves $C_1, \dots, C_j$ in $\Sigma_{g,m}$ for $j \geq 1$ such that $C_1 \cup \dots \cup C_j$ is preserved by $\phi$. Here a simple closed curve $C$ in $\Sigma_{g,m}$ is *essential* if each component of $\Sigma_{g,m} \setminus C$ has negative Euler characteristic. (There is a mapping class that is periodic and reducible.) A mapping class $\phi \in \mathrm{MCG}(\Sigma_{g,m})$ is *pseudo-Anosov* if $\phi$ is neither periodic nor reducible. Note that the Nielsen-Thurston type is a conjugacy invariant, i.e., two mapping classes are conjugate to each other in $\mathrm{MCG}(\Sigma_{g,m})$, then their Nielsen-Thurston types are the same.

Pseudo-Anosov mapping classes have many important properties for the study of dynamical systems. For more details which we describe below, see [19, 20]. A homeomorphism $\Phi : \Sigma_{g,m} \to \Sigma_{g,m}$ is *pseudo-Anosov* if there exist a constant $\lambda = \lambda(\Phi) > 1$ and a pair of transverse measured foliations $(\mathcal{F}^+, \mu^+)$ and $(\mathcal{F}^-, \mu^-)$ such that

$$\Phi((\mathcal{F}^+, \mu^+)) = (\mathcal{F}^+, \lambda\mu^+) \quad \textit{and} \;\; \Phi((\mathcal{F}^-, \mu^-)) = (\mathcal{F}^-, \tfrac{1}{\lambda}\mu^-).$$

This means that $\Phi$ preserves both foliations $\mathcal{F}^+$ and $\mathcal{F}^-$, and it contracts the leaves of $\mathcal{F}^-$ by $\frac{1}{\lambda}$ and it expands the leaves of $\mathcal{F}^+$ by $\lambda$. The invariant foliations $\mathcal{F}^+$ and $\mathcal{F}^-$ are called the *unstable and stable foliations* for $\Phi$, and $\lambda > 1$ is called the *stretch factor* for $\Phi$.

**Remark 5.3.3.** *The invariant foliations $\mathcal{F}^+$ and $\mathcal{F}^-$ for the pseudo-Anosov homeomorphism $\Phi$ are singular foliations which mean that they have common singularities in the interior of $\Sigma_{g,m}$ or at punctures of $\Sigma_{g,m}$. The number of singularities is finite. A 1-pronged singularity may occur at a puncture of $\Sigma_{g,m}$, yet there are no 1-pronged singularities in the interior of $\Sigma_{g,m}$.*

Each pseudo-Anosov mapping class $\phi \in \mathrm{MCG}(\Sigma_{g,m})$ contains a pseudo-Anosov homeomorphism $\Phi$ as a representative of $\phi$. We set $\lambda(\phi) = \lambda(\Phi)$ and call it the *stretch factor* of the mapping class $\phi = [\Phi]$. The stretch factor $\lambda(\phi)$ is a conjugacy invariant of pseudo-Anosov mapping classes. Moreover $\lambda(\phi)$ is the largest eigenvalue of a Perron-Frobenius integral matrix. Thus $\lambda(\phi)$ is an algebraic integer which is a real number grater than 1 and $|\lambda'| < \lambda(\phi)$ holds for each conjugate element $\lambda' \neq \lambda(\phi)$. The logarithm $\log(\lambda(\phi))$ of the stretch factor $\lambda(\phi)$ is called the *entropy* of $\phi$.

**Remark 5.3.4.** *If $\phi \in \mathrm{MCG}(\Sigma_{g,m})$ is pseudo-Anosov, then $\phi^k$ is pseudo-Anosov for all $k \geq 1$ and the equality $\lambda(\phi^k) = (\lambda(\phi))^k$ holds.*

Recall the two homomorphisms

$$\begin{aligned} &\Gamma\colon B_m \to \mathrm{MCG}(D_m), \textit{and} \\ &\mathfrak{c}\colon \mathrm{MCG}(D_m) \to \mathrm{MCG}(\Sigma_{0,m}, \{\infty\}) < \mathrm{MCG}(\Sigma_{0,m+1}). \end{aligned}$$

We say that a braid $b \in B_m$ is *periodic* (resp. *reducible*, *pseudo-Anosov*) if the mapping class $\mathfrak{c}(\Gamma(b))$ is of the corresponding type. When $b$ is a pseudo-Anosov braid, the *stretch factor* $\lambda(b)$ of $b$ is defined by the stretch factor $\lambda(\mathfrak{c}(\Gamma(b)))$ of the mapping class $\mathfrak{c}(\Gamma(b))$. In this case, it makes sense to say that the braid type $\langle b \rangle$ is *pseudo-Anosov*, and we can define the *stretch factor* $\lambda(\langle b \rangle)$ of the braid type $\langle b \rangle$ by

$$\lambda(\langle b \rangle) = \lambda(b) = \lambda(\mathfrak{c}(\Gamma(b))), \tag{5.3.1}$$

since both Nielsen-Thurston type and the stretch factor are conjugacy invariants.

### 5.3.4 Pseudo-Anosov 3-braids

It is well-known that for positive integers $k_j$'s, $\ell_j$'s and $r$, the 3-braid

$$\sigma_1^{k_1}\sigma_2^{-\ell_1}\dots\sigma_1^{k_r}\sigma_2^{-\ell_r}$$

is pseudo-Anosov. Moreover any pseudo-Anosov 3-braid $\alpha$ is conjugate to a braid

$$\sigma_1^{k_1}\sigma_2^{-\ell_1}\dots\sigma_1^{k_r}\sigma_2^{-\ell_r}$$

in $B_3$ which is unique up to a cyclic permutation. See Murasugi [46] for example. Then the stretch factor $\lambda(\alpha)$ is the eigenvalue greater than 1 of

$$M_{(k_1,\ell_1,\dots,k_r,\ell_r)} = \begin{pmatrix}1 & 1\\ 0 & 1\end{pmatrix}^{k_1}\begin{pmatrix}1 & 0\\ 1 & 1\end{pmatrix}^{\ell_1}\cdots\begin{pmatrix}1 & 1\\ 0 & 1\end{pmatrix}^{k_r}\begin{pmatrix}1 & 0\\ 1 & 1\end{pmatrix}^{\ell_r}. \tag{5.3.2}$$

See Handel [28] for example.

**Example 5.3.5** (Metallic 3-braids (Appendix A in [22]))**.** *For $p \geq 1$, the 3-braid $\sigma_1^{2p}\sigma_2^{-2p}$ is pseudo-Anosov, and the stretch factor $\lambda(\sigma_1^{2p}\sigma_2^{-2p})$ is the eigenvalue greater than 1 of $M_{(2p,2p)} = \begin{pmatrix}1+4p^2 & 2p\\ 2p & 1\end{pmatrix}$. Thus*

$$\lambda(\sigma_1^{2p}\sigma_2^{-2p}) = (p+\sqrt{p^2+1})^2 = \left(\frac{1}{2}(2p+\sqrt{4p^2+4})\right)^2 = (\mathfrak{s}_{2p})^2.$$

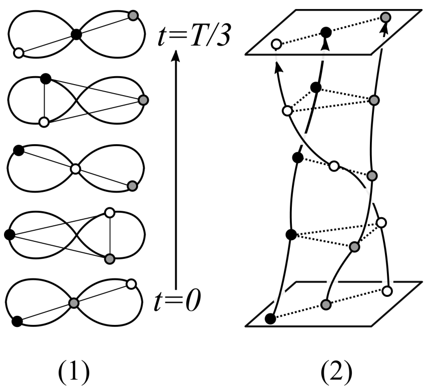


Figure 5.7: (1) The figure-8 solution $\boldsymbol{x}(t)$ with period $T$. (2) A representative braid $\sigma_1^{-1}\sigma_2 \in \langle b(\boldsymbol{x}(t),[0,\frac{T}{3}])\rangle$.

**Example 5.3.6.** *Let us consider the figure-8 solution $\boldsymbol{x}(t) = (x_1(t), x_2(t), x_3(t))$ by Moore [45] and Chenciner-Montgomery [18], see Figure 5.7. The periodic solution $\boldsymbol{x}(t)$ has a property such that*

$$x_1(t+\tfrac{T}{3}) = x_2(t),\ \ x_2(t+\tfrac{T}{3}) = x_3(t),\ \ x_3(t+\tfrac{T}{3}) = x_1(t),$$

*where $T > 0$ is the period of $\boldsymbol{x}(t)$. This property tells us that $\boldsymbol{x}(t)$ determines a braid $b(\boldsymbol{x}(t),[0,\frac{T}{3}])$. One sees that $\sigma_1^{-1}\sigma_2 \in B_3$ is a representative of $\langle b(\boldsymbol{x}(t),[0,\frac{T}{3}])\rangle$ and $(\sigma_1^{-1}\sigma_2)^3$ represents the braid type $\langle b(\boldsymbol{x}(t),[0,T])\rangle$ of the solution $\boldsymbol{x}(t)$. It is easy to see that $\sigma_1^{-1}\sigma_2$ is conjugate with $\sigma_1\sigma_2^{-1}$ in $B_3$. By (5.3.2), $\sigma_1\sigma_2^{-1}$ is a pseudo-Anosov braid with the stretch factor $(\mathfrak{s}_1)^2$. Thus the braid type of the figure-8 solution is pseudo-Anosov with the stretch factor $(\mathfrak{s}_1)^6$ (Remark 5.3.4), and hence it is a non-trivial braid type in contrast with the Euler's solution and Lagrange's solution (Example 5.3.2).*

## 5.4 Proof of Theorem 5.1.5

For $n \geq 2$ and $p \geq 1$, we define braids $u_n, v_n, \beta_{n,p} \in B_{2n}$ as follows.

$$\begin{aligned} u_n &= (\sigma_1\sigma_2\ldots\sigma_{2n-1})(\sigma_1\sigma_3\ldots\sigma_{2n-1})^{-1}, \\ v_n &= (\sigma_1\sigma_2\ldots\sigma_{2n-1})^{-1}(\sigma_1\sigma_3\ldots\sigma_{2n-1}) \text{ and} \\ \beta_{n,p} &= u_n^p v_n^p. \end{aligned}$$

See also Figure 5.8 together with the braid relation (B1) in Section 5.3.1. It is easy to check that $\hat{\sigma}(u_n) = (1, 3, \ldots, 2n-1)$ and $\hat{\sigma}(v_n) = (2, 4, \ldots, 2n)^{-1}$. Hence by (5.2.1), we have

$$\hat{\sigma}(\beta_{n,p}) = \hat{\sigma}(u_n^p v_n^p) = (1, 3, \ldots, 2n-1)^p(2, 4, \ldots, 2n)^{-p} = \sigma(h_{n,p}^{-1}). \tag{5.4.1}$$

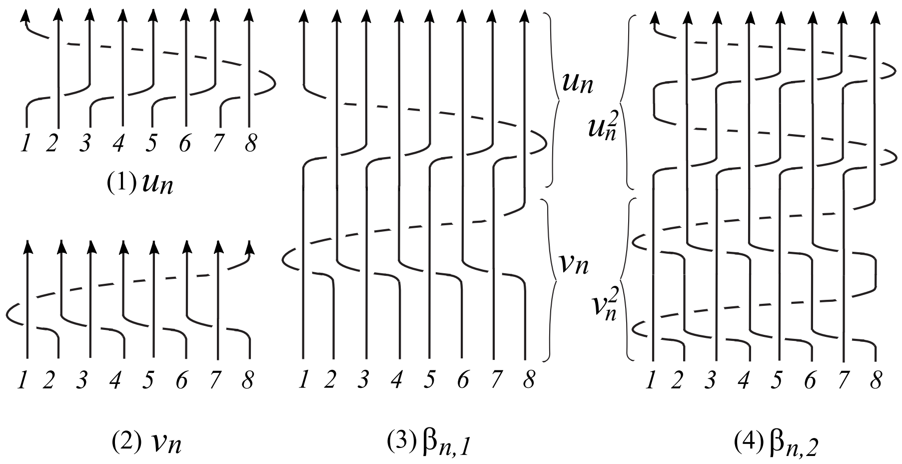


Figure 5.8: Case $n = 4$. (1) $u_n$. (2) $v_n$. (3) $\beta_{n,1} = u_n v_n$. (4) $\beta_{n,2} = u_n^2 v_n^2$.

*Proof of Theorem 5.1.5.* The proof consists of the following two steps. In Step 1, we prove that for $n \geq 2$ and *any* $p \geq 1$, the braid $\beta_{n,p}$ is pseudo-Anosov with $\lambda(\beta_{n,p}) = (\mathfrak{s}_{2p})^2$. (We have no restriction on $p$ in Step 1.) In Step 2, we prove that for any $n \geq 2$ and $p \in \{1, \ldots, \lfloor \frac{n}{2} \rfloor\}$, the braid types of $\beta_{n,p}$ and $y_{n,p} = b(\boldsymbol{x}_{n,p}(t), [0, \frac{d}{n}])$ are the same. In other words, $\beta_{n,p} \in \langle y_{n,p} \rangle$. Since $X_{n,p} = \left\langle (y_{n,p})^{\frac{n}{d}} \right\rangle$, it follows that $X_{n,p} = \left\langle (\beta_{n,p})^{\frac{n}{d}} \right\rangle$. Hence by Step 1 together with Remark 5.3.4, $X_{n,p}$ is a pseudo-Anosov braid type with the stretch factor

$$\lambda(X_{n,p}) = \lambda\big((\beta_{n,p})^{\frac{n}{d}}\big) = (\lambda(\beta_{n,p}))^{\frac{n}{d}} = (\mathfrak{s}_{2p})^{\frac{2n}{d}}.$$

**Step 1.** For $n \geq 2$ and $p \geq 1$, the braid $\beta_{n,p}$ is pseudo-Anosov with $\lambda(\beta_{n,p}) = (\mathfrak{s}_{2p})^2$. In particular $\lambda(\beta_{n,p}) < \lambda(\beta_{n,p'})$ if $p < p'$.

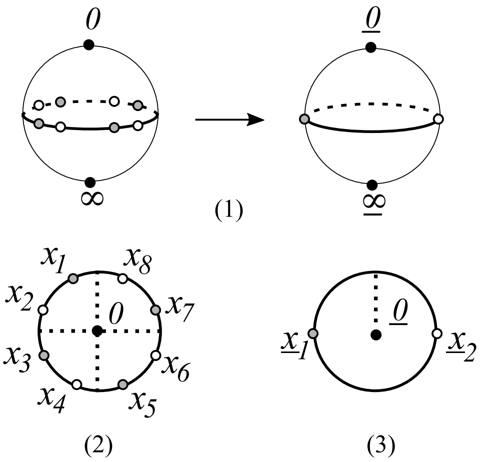


Figure 5.9: Case $n = 4$. (1) An $n$-fold branched cover $\mathfrak{p} : \Sigma_{0,2n} \to \Sigma_{0,2}$ with branched points $\underline{0}$ and $\underline{\infty}$, where punctures lie on the equators. (2) The upper hemisphere for $\Sigma_{0,2n}$. (3) The upper hemisphere for $\Sigma_{0,2}$.

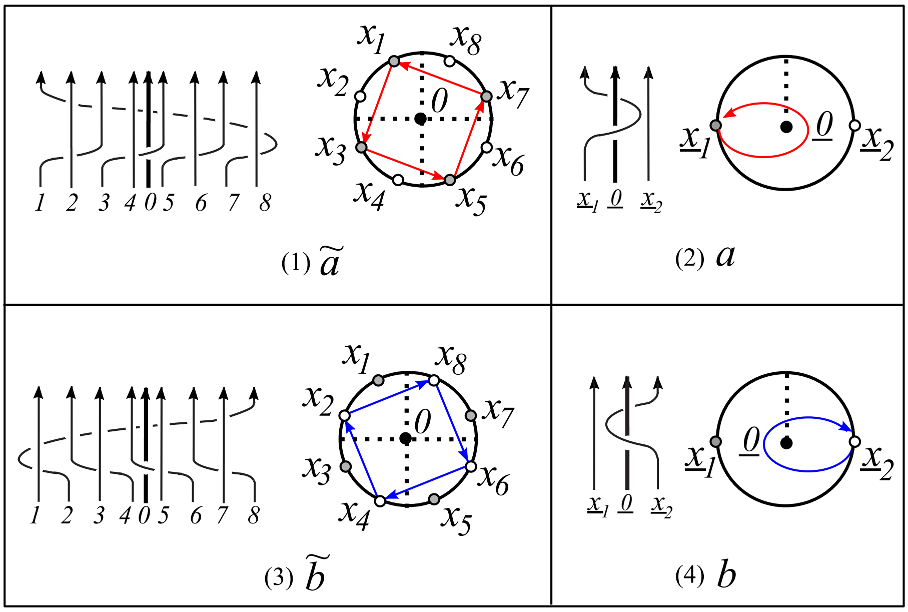


Figure 5.10: Case $n = 4$. (1) A lift $\widetilde{a} = \widetilde{a_n} \in \mathrm{MCG}(\Sigma_{0,2n}, \{0\}, \{\infty\})$ of (2) $a = \sigma_1^2 \in \mathrm{MCG}(\Sigma_{0,2}, \{\underline{0}\}, \{\underline{\infty}\})$. (3) A lift $\widetilde{b} = \widetilde{b_n} \in \mathrm{MCG}(\Sigma_{0,2n}, \{0\}, \{\infty\})$ of (4) $b = \sigma_2^{-2} \in \mathrm{MCG}(\Sigma_{0,2}, \{\underline{0}\}, \{\underline{\infty}\})$. For (2) and (4), $a$ and $b$ (as elements of $B_3$) have base points $\underline{x}_1$, $\underline{0}$, and $\underline{x}_2$.

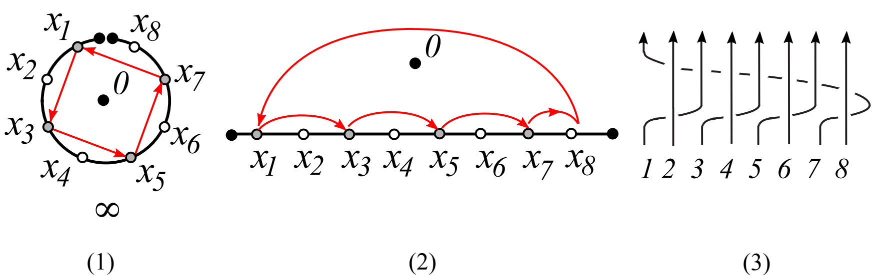


Figure 5.11: Case $n = 4$. (1) An arc in the equator. (2) A segment in the plane. (3) The braid $u_n$ corresponding to $\widetilde{a}^\bullet \in \mathrm{MCG}(\Sigma_{0,2n}, \{\infty\})$. (The arc in (1) is identified with the segment in (2).) For (1) and (2), arrows indicate the image of the punctures under $\widetilde{a}$.

Proof of Step 1. We consider a 2-punctured sphere $\Sigma_{0,2}$ and denote the two punctures of $\Sigma_{0,2}$ by $\underline{x}_1$ and $\underline{x}_2$. We pick two points in $\Sigma_{0,2}$ and call them $\underline{0}$ (the north pole) and $\underline{\infty}$ (the south pole). Given $n \geq 2$, we take an $n$-fold branched cover

$$\mathfrak{p} : \Sigma_{0,2n} \to \Sigma_{0,2}$$

with branched points $\underline{0}$ and $\underline{\infty}$. (We cut a longitude of $\Sigma_{0,2}$ between $\underline{0}$ and $\underline{\infty}$, take $n$ copies of the resulting surface, and past them to make an $2n$-punctured sphere.) We denote lifts of $\underline{0}, \underline{\infty} \in \Sigma_{0,2}$ by $0, \infty \in \Sigma_{0,2n}$ respectively. Let $x_1, x_2, \dots, x_{2n}$ be punctures of $\Sigma_{0,2n}$ such that $\mathfrak{p}$ sends $x_{2k}$ (resp. $x_{2k-1}$) to $\underline{x}_2$ (resp. $\underline{x}_1$). In the view from $0 \in \Sigma_{0,2n}$ in the upper hemisphere, we may assume that $x_1, \dots, x_{2n}$ lie on the equator counterclockwise and these $2n$ punctures form the regular $2n$-gon. See Figure 5.9.

Let $a = \sigma_1^2$, $b = \sigma_2^{-2} \in B_3$. Since $a$ and $b$ are pure 3-braids, we can regard $a$ and $b$ as elements of $\mathrm{MCG}(\Sigma_{0,2}, \{\underline{0}\}, \{\underline{\infty}\})$, see Figure 5.10(2)(4). We lift $a$ and $b$ to $\Sigma_{0,2n}$, and call them

$$\widetilde{a}, \widetilde{b} \in \mathrm{MCG}(\Sigma_{0,2n}, \{0\}, \{\infty\}) < \mathrm{MCG}(\Sigma_{0,2n+1}, \{\infty\}).$$

(Clearly both $\widetilde{a}$ and $\widetilde{b}$ fix the two points 0 and $\infty$.) We have

$$\begin{aligned} \widetilde{a}(x_{2k-1}) &= x_{2k+1} \text{ and } \widetilde{a}(x_{2k}) = x_{2k} \text{ for } k = 1, \dots, n, \\ \widetilde{b}(x_{2k-1}) &= x_{2k-1} \text{ and } \widetilde{b}(x_{2k}) = x_{2k-2} \text{ for } k = 1, \dots, n, \end{aligned}$$

where we interpret indices modulo $2n$. Notice that $\widetilde{a}$ rotates the regular $n$-gon $x_1x_3 \dots x_{2n-1}$ by $\frac{\pi}{n}$ counterclockwise about the north pole 0; $\widetilde{b}$ rotates the regular $n$-gon $x_2x_4 \dots x_{2n}$ by $\frac{\pi}{n}$ clockwise about the same point 0, see Figure 5.10(1)(3). In other words, under the action of $\widetilde{a}$, each puncture $x_{2i-1}$ ($i = 1, \dots, 2n$) with odd index is passing through in front of the puncture $x_{2i}$ with even index from the view of the north pole $0 \in \Sigma_{0,2n}$. Similarly, under the action of $\widetilde{b}$, each puncture $x_{2i}$ ($i = 1, \dots, 2n$) with even index is passing through in front of the puncture $x_{2i-1}$ with odd index.

Forgetting the point $0 \in \Sigma_{0,2n}$, we think of $\widetilde{a}$ and $\widetilde{b}$ as elements, say $\widetilde{a}^\bullet$ and $\widetilde{b}^\bullet$ of $\mathrm{MCG}(\Sigma_{0,2n}, \{\infty\})$ respectively. To find the planar $2n$-braids for $\widetilde{a}^\bullet$ and $\widetilde{b}^\bullet$, we cut the equator of $\Sigma_{0,2n}$ at a point between the consecutive punctures $x_{2n}$ and $x_1$ (in the cyclic order) into an arc, and we regard the arc as a segment in the plane containing the punctures $x_1, \dots, x_{2n}$ in this order, see Figure 5.11(1)(2). Then from the actions of $\widetilde{a}^\bullet$ and $\widetilde{b}^\bullet$ on $2n$ punctures in the plane, one sees that $2n$-braids corresponding to $\widetilde{a}^\bullet$, $\widetilde{b}^\bullet$ are given by

$u_n$, $v_n \in B_{2n}$ respectively. See Figure 5.11(3). (Although we do not need braid representatives corresponding to $\widetilde{a}$ and $\widetilde{b}$ in the proof of Step 1, Figure 5.10(1) and (3) illustrate these representatives for $\widetilde{a}$ and $\widetilde{b}$ respectively in case $n = 4$.)

We define

$$\phi_p = (\widetilde{a})^p(\widetilde{b})^p \in \mathrm{MCG}(\Sigma_{0,2n}, \{0\}, \{\infty\}) < \mathrm{MCG}(\Sigma_{0,2n+1}, \{\infty\}).$$

It follows that $\phi_p$ is a lift of $a^pb^p = \sigma_1^{2p}\sigma_2^{-2p} \in \mathrm{MCG}(\Sigma_{0,2}, \{\underline{0}\}, \{\underline{\infty}\})$. Recall that $a^pb^p$ is a pseudo-Anosov mapping class with the stretch factor $(\mathfrak{s}_{2p})^2$, see Example 5.3.5. Since $\phi_p$ is a lift of $a^pb^p$, $\phi_p$ is also pseudo-Anosov with the same stretch factor as $a^pb^p$. Hence $\lambda(\phi_p) = (\mathfrak{s}_p)^2$.

Forgetting the point $0 \in \Sigma_{0,2n}$, we obtain $\phi_p^\bullet \in \mathrm{MCG}(\Sigma_{0,2n}, \{\infty\})$ from $\phi_p = (\widetilde{a})^p(\widetilde{b})^p$. Note that $\phi_p^\bullet = (\widetilde{a}^\bullet)^p(\widetilde{b}^\bullet)^p$ is a mapping class corresponding to the braid $\beta_{n,p} = u_n^p v_n^p$.

**Claim.** The stable/unstable foliation $\mathcal{F}^{+/-}$ of $\phi_p$ is not 1-pronged at $0 \in \Sigma_{0,2n}$.

For the proof of Step 1, it is enough to prove Claim. The reason is that if $\mathcal{F}^{+/-}$ is not 1-pronged at the point $0 \in \Sigma_{0,2n}$, then the same singular foliations $\mathcal{F}^+$ and $\mathcal{F}^-$ are still invariant foliations for $\phi_p^\bullet$, see Remark 5.3.3. This implies that $\phi_p^\bullet$ (and hence the braid $\beta_{n,p}$) is pseudo-Anosov with the same stretch factor $(\mathfrak{s}_p)^2$ as $\phi_p$, i.e.,

$$\lambda(\beta_{n,p})\Big(= \lambda(\phi_p^\bullet)\Big) = \lambda(\phi_p) = (\mathfrak{s}_{2p})^2.$$

*Proof of Claim.* Let us consider the stable/unstable foliation $\underline{\mathcal{F}}^+$ and $\underline{\mathcal{F}}^-$ for the pseudo-Anosov element $a^pb^p$. Then $\underline{\mathcal{F}}^{+/-}$ has 1-pronged singularities at each of the two punctures of $\Sigma_{0,2}$ and at each of the two points $\underline{0}$ and $\underline{\infty}$. Let $\mathcal{F}^+$ and $\mathcal{F}^-$ denote lifts of $\underline{\mathcal{F}}^+$ and $\underline{\mathcal{F}}^-$ respectively. It follows that $\mathcal{F}^{+/-}$ is the stable/unstable foliation for $\phi_p$, and $\mathcal{F}^{+/-}$ has a 1-pronged singularity at each of the $2n$ punctures and $\mathcal{F}^{+/-}$ has $n$-pronged singularities ($n \geq 2$) at the points 0 and $\infty$ in $\Sigma_{0,2n}$. In particular $\mathcal{F}^{+/-}$ is not 1-pronged at $0 \in \Sigma_{0,2n}$. This completes the proof of Claim.

By Claim, we finished the proof of Step 1.

Recall that $y_{n,p} = b(\boldsymbol{x}_{n,p}(t), [0, 2\bar{T}])$ and $\bar{T} = \frac{dT}{2n}$.

**Step 2.** $\beta_{n,p} \in \langle y_{n,p}\rangle$. In particular $(\beta_{n,p})^{\frac{n}{d}} \in X_{n,p} = \big\langle (y_{n,p})^{\frac{n}{d}} \big\rangle$.

Proof of Step 2. Let us consider the shape curve $\boldsymbol{u}(t)$ ($t \in [0, 2\bar{T}]$) for the solution $\boldsymbol{x}_{n,p}(t)$. By the arguments in Section 5.2.2, the shape curve $\boldsymbol{u}(t)$ ($t \in [0, 2\bar{T}]$) satisfies the following properties.

(s1) $\boldsymbol{u}(0) \in \mathrm{B}_{-1}$, $\boldsymbol{u}(\bar{T}) \in \mathrm{B}_{2p-1}$ and $\boldsymbol{u}(2\bar{T}) \in \mathrm{B}_{4p-1}$.

(s2) $u_1(t) > 0$ for $0 < t < \bar{T}$.

(s3) $u_1(t) < 0$ for $\bar{T} < t < 2\bar{T}$.

(s4) $x_i(2\bar{T}) = x_{\sigma(h_{n,p}^{-1})(i)}(0)$ for $i = 1, \ldots, 2n$.

Recall that $n$ bodies with odd indices and $n$ bodies with even indices rotate in mutually opposite directions. The above (s1) ($\boldsymbol{u}(0) \in \mathrm{B}_{-1}$, $\boldsymbol{u}(\bar{T}) \in \mathrm{B}_{2p-1}$) and (s2) tell us that each of bodies $x_{2i}(t)$'s ($i = 1, \ldots, n$) with even indices is passing through in front of bodies with odd indices (in the time interval $(0, \bar{T})$) from the view of the origin $0 \in \mathbb{R}^2$. Similarly (s1)

($\boldsymbol{u}(\bar{T}) \in \mathrm{B}_{2p-1}$, $\boldsymbol{u}(2\bar{T}) \in \mathrm{B}_{4p-1}$) and (s3) imply that each of bodies $x_{2i-1}(t)$'s ($i = 1, \dots, n$) with odd indices is passing through in front of the bodies with even indices (in the time interval $(\bar{T}, 2\bar{T})$). These properties connect up $(\widetilde{b})^p \in \mathrm{MCG}(\Sigma_{0,2n}, \{0\}, \{\infty\})$ with $\boldsymbol{u}(t)$ for $t \in [0, \bar{T}]$ (resp. $(\widetilde{a})^p \in \mathrm{MCG}(\Sigma_{0,2n}, \{0\}, \{\infty\})$ with $\boldsymbol{u}(t)$ for $t \in [\bar{T}, 2\bar{T}]$), see Figure 5.10(3)(4). Recall that the permutation $\hat{\sigma}(\beta_{n,p})$ of the braid $\beta_{n,p} = u_n^p v_n^p$ coincides with $\sigma(h_{n,p}^{-1})$, see (5.4.1). Putting these properties together with (s4), we conclude that the $2n$-braid $u_n^p v_n^p (= \beta_{n,p})$ is a representative of the braid type $\langle y_{n,p} \rangle$ of $y_{n,p} = b(\boldsymbol{x}_{n,p}(t), [0, 2\bar{T}])$. This completes the proof of Step 2.

By Steps 1 and 2, we have finished the proof of Theorem 5.1.5. □

We end this section with an example.

**Example 5.4.1.** *Corollary 5.1.6 and Table 5.1 may suggest that $\lambda(X_{n,p})$ does not coincide with $\lambda(X_{n,p'})$ for different pairs $(n, p) \neq (n, p')$. However, the stretch factors happen to coincide for different pairs occasionally: The $k$th metallic ratio $\mathfrak{s}_k$ has a formula $(\mathfrak{s}_k)^3 = \mathfrak{s}_{k^3+3k}$ for each $k \in \mathbb{N}$. In particular $(\mathfrak{s}_6)^3 = \mathfrak{s}_{234}$ when $k = 6$. We now claim that $\lambda(X_{n,3}) = \lambda(X_{n,117})$ for all $n = 3^2 2^k$ with $k \geq 5$. Then $117 \leq \lfloor \frac{n}{2} \rfloor$. By Theorem 5.1.4, we have $\lambda(X_{n,3}) = (\mathfrak{s}_6)^{\frac{2n}{3}} = (\mathfrak{s}_6)^{3 \cdot 2^{k+1}}$ and $\lambda(X_{n,117}) = (\mathfrak{s}_{234})^{\frac{2n}{9}} = (\mathfrak{s}_{234})^{2^{k+1}}$. By the equality $(\mathfrak{s}_6)^3 = \mathfrak{s}_{234}$, we have*

$$\lambda(X_{n,3}) = ((\mathfrak{s}_6)^3)^{2^{k+1}} = (\mathfrak{s}_{234})^{2^{k+1}} = \lambda(X_{n,117}).$$

## 5.5 New numerical periodic solutions of the $2n$-body problem

We numerically found the periodic solutions $\boldsymbol{x}_{n,p}(t)$ for $p = 1, \dots, \lfloor \frac{n}{2} \rfloor$ in Figure 5.1. In order to obtain those, we consider the Fourier series of the solutions and compute the Fourier coefficient by using the steepest descent method. Though the existence of the periodic orbits theoretically guarantees for $p = 1, \dots, \lfloor \frac{n}{2} \rfloor$, new numerical solutions are obtained for several pairs with $(n, p)$ with $\lfloor \frac{n}{2} \rfloor < p < n$. See Figure 5.12.

Then it is natural to ask the following question.

**Question 5.5.1.** *For $n \geq 2$ and $\lfloor \frac{n}{2} \rfloor < p < n$, does there exist a periodic solution $\boldsymbol{x}_{n,p}(t)$ of the planar $2n$-body problem whose braid type $X_{n,p}$ is given by the braid $(\beta_{n,p})^{\frac{n}{d}}$ with $d = \gcd(n, p)$?*

If the answer of Question 5.5.1 is positive, then Theorem 5.1.4 is extended to some pairs $(n, p)$ with $\lfloor \frac{n}{2} \rfloor < p < n$, i.e. if the answer of Question 5.5.1 is positive, then the braid type $X_{n,p}$ of the periodic solution $\boldsymbol{x}_{n,p}(t)$ of the planar $2n$-body problem is pseudo-Anosov with the stretch factor $(\mathfrak{s}_{2p})^{\frac{2n}{d}}$. See also Step 1 of the proof of Theorem 5.1.5.

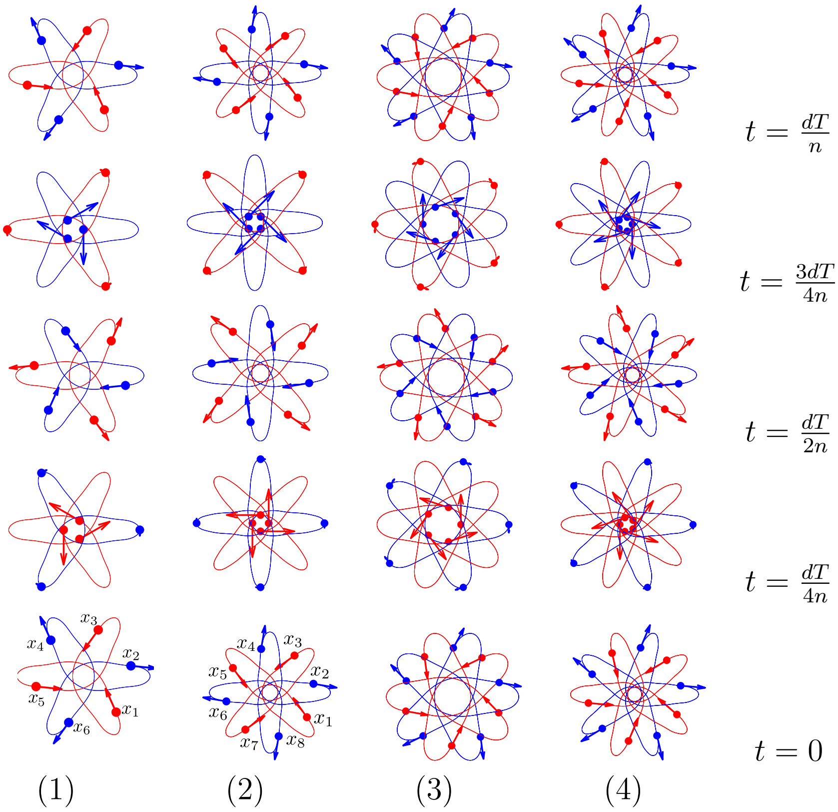


Figure 5.12: (1) $\boldsymbol{x}_{3,2}(t)$. (2) $\boldsymbol{x}_{4,3}(t)$. (3) $\boldsymbol{x}_{5,3}(t)$. (4) $\boldsymbol{x}_{5,4}(t)$.

# Chapter 6

# Conclusions

In this thesis, using minimizing methods, we proved infinitely many transition orbits in twist maps as well as multiple periodic solutions of the restricted three-body problem and related problems. Moreover, as a related issue to periodic solutions of the $n$-body problem, we examined braid types determined from a family of periodic solutions in the planar $2n$-body problem. We summarize our key results as follows.

*(i)* In Chapter 2, we established the variational structure for infinite transition orbits between two periodic orbits. We first introduced several results for finite transition orbits and the corresponding variational structures [49, 66]. The functionals or functions such as (1.1.7) and (1.2.4) always take infinite values for infinite transition orbits. We therefore solved this problem by considering a renormalized function defined on a set $X_{k,\rho}$, which is determined by two bi-infinite sequences, $k$ and $\rho$. Moreover, we showed that, for some $k$ and $\rho$, the renormalized function has a minimizer on $X_{k,\rho}$ and the minimizer implies infinite transition orbits.

*(ii)* In Chapters 3 and 4, we examined the restricted three-body problem and two related problems. Chapter 3 provided the proof for multiple periodic solutions that rotate clockwise around one or two primaries. Chapter 4 dealt with the Hill problem and the two-center problem. In the first half, we considered a holonomic constraint and showed the existence of periodic orbits, such as orbits restricted to a specific plane, in a similar way to the local estimate used in Chapter 3. In the latter half, using the global estimate, we demonstrated the existence of brake orbits in the planar two-center problem, which can be regarded as a simpler model of the restricted three-body problem.

*(iii)* In Chapter 5, we studied braid types of planar periodic solutions. More precisely, we studied braid types determined from periodic solutions with high symmetries of the planar $2n$-body problem in [52]. We first showed that each $2n$-braid type can be regarded as a 3-braid by using a covering space and that all of their braid types are pseudo-Anosov. In addition, we found that their stretch factors are always powers of metallic ratios.

We conclude this thesis by stating potential future works.

*(i)* In Chapter 2, we assumed that two periodic configurations, $u^0$ and $u^1$, have the same rotation number. Future work could consider the case where the rotation numbers

are different. As a related paper to this problem, we refer to [63], which discusses minimal configurations in such a case.

*(ii)* In Chapter 3, all of the obtained orbits rotate clockwise around one or two primaries. Therefore, the following question arises: how do we show the existence of periodic orbits that rotate counterclockwise or that involve both clockwise and counterclockwise rotations (as in Figure 6.1)?

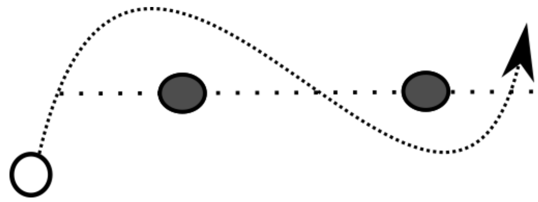

Figure 6.1: One of the remaining cases we have not proved

*(iii)* Chapter 5 established the braid types determined from a family of periodic solutions of the $2n$-body problem. However, Montgomery's question (Question 5.1.1), which motivated our study, focused on showing the existence of periodic solutions determined from braids, so our result does not answer his question. Given an $n$-braid or $n$-braid type, there remains the question of how to show the existence of a periodic solution that realizes the $n$-braid or $n$-braid type in the case of $n \geq 4$.

# Acknowledgements

The author would like to express her sincere gratitude to her supervisor, Associate Professor Mitsuru Shibayama, for his continued encouragement. Without his guidance and persistent help, this thesis would not have been possible. She likewise thank the past and present members of Dynamical Systems Group, especially Professor Kazuyuki Yagasaki and Assistant Professor Yoshiyuki Yamaguchi for their helpful comments on my research. She would also like to thank her friends for their emotional support. Part of this research was supported by Grant-in-Aid for JSPS Fellows (20J21214) from the Japan Society for the Promotion of Science.

# Bibliography


[1] G. Arioli, F. Gazzola, and S. Terracini, *Minimization properties of Hill's orbits and applications to some $N$-body problems*, Ann. Inst. H. Poincaré C Anal. Non Linéaire **17** (2000), no. 5, 617–650.

[2] V. I. Arnold, *Mathematical Methods of Classical Mechanics*, Graduate Texts in Mathematics, vol. 60, Springer-Verlag, New York, 1989.

[3] S. Aubry, *The twist map, the extended Frenkel-Kontorova model and the devil's staircase*, vol. 7, 1983, Order in chaos (Los Alamos, N.M., 1982), pp. 240–258.

[4] S. Aubry and G. Abramovici, *Chaotic trajectories in the standard map. The concept of anti-integrability*, Phys. D **43** (1990), no. 2-3, 199–219.

[5] S. Aubry and P. Y. Le Daeron, *The discrete Frenkel-Kontorova model and its extensions. I. Exact results for the ground-states*, Phys. D **8** (1983), no. 3, 381–422.

[6] V. Bangert, *Mather sets for twist maps and geodesics on tori*, Dynam. Report. Ser. Dynam. Systems Appl. **1** (1988), 1–56.

[7] V. Barutello, D. L. Ferrario, and S. Terracini, *On the singularities of generalized solutions to n-body-type problems*, Int. Math. Res. Not. IMRN (2008), Art. ID rnn 069, 78.

[8] J. S. Birman, *Braids, Links, and Mapping Class Groups*, Annals of Mathematics Studies, No. 82, Princeton University Press, Princeton, N.J.; University of Tokyo Press, Tokyo, 1974.

[9] A. Blumenthal, J. Xue, and L.-S. Young, *Lyapunov exponents for random perturbations of some area-preserving maps including the standard map*, Ann. of Math. (2) **185** (2017), no. 1, 285–310.

[10] A. J. Casson and S. A. Bleiler, *Automorphisms of Surfaces after Nielsen and Thurston*, London Mathematical Society Student Texts, vol. 9, Cambridge University Press, Cambridge, 1988.

[11] K.-C. Chen, *Action-minimizing orbits in the parallelogram four-body problem with equal masses*, Arch. Ration. Mech. Anal. **158** (2001), no. 4, 293–318.

[12] ———, *Binary decompositions for planar n-body problems and symmetric periodic solutions*, Arch. Ration. Mech. Anal. **170** (2003), no. 3, 247–276.

[13] ———, *Variational methods on periodic and quasi-periodic solutions for the $N$-body problem*, Ergodic Theory Dynam. Systems **23** (2003), no. 6, 1691–1715.

[14] ———, *Variational constructions for some satellite orbits in periodic gravitational force fields*, Amer. J. Math. **132** (2010), no. 3, 681–709.

[15] K.-C. Chen and G. Yu, *Syzygy sequences of the $N$-center problem*, Ergodic Theory Dynam. Systems **38** (2018), no. 2, 566–582.

[16] N.-C. Chen, *Periodic brake orbits in the planar isosceles three-body problem*, Nonlinearity **26** (2013), no. 10, 2875–2898.

[17] A. Chenciner, *Action minimizing solutions of the Newtonian $n$-body problem: from homology to symmetry*, Proceedings of the International Congress of Mathematicians, Vol. III (Beijing, 2002), Higher Ed. Press, Beijing, 2002, pp. 279–294.

[18] A. Chenciner and R. Montgomery, *A remarkable periodic solution of the three-body problem in the case of equal masses*, Ann. of Math. (2) **152** (2000), no. 3, 881–901.

[19] B. Farb and D. Margalit, *A Primer on Mapping Class Groups*, Princeton Mathematical Series, vol. 49, Princeton University Press, Princeton, NJ, 2012.

[20] A. Fathi, F. Laudenbach, and V. Poénaru (eds.), *Travaux de Thurston Sur les Surfaces*, Astérisque, vol. 66, Société Mathématique de France, Paris, 1979, Séminaire Orsay, With an English summary.

[21] D. L. Ferrario and S. Terracini, *On the existence of collisionless equivariant minimizers for the classical $n$-body problem*, Invent. Math. **155** (2004), no. 2, 305–362.

[22] M. D. Finn and J.-L. Thiffeault, *Topological optimization of rod-stirring devices*, SIAM Rev. **53** (2011), no. 4, 723–743.

[23] M. Fontaine and C. García-Azpeitia, *Braids of the $N$-body problem I: cabling a body in a central configuration*, Nonlinearity **34** (2021), no. 2, 822–851.

[24] G. Fusco, G. F. Gronchi, and P. Negrini, *Platonic polyhedra, topological constraints and periodic solutions of the classical $N$-body problem*, Invent. Math. **185** (2011), no. 2, 283–332.

[25] I. M. Gelfand and S. V. Fomin, *Calculus of Variations*, Prentice-Hall, Inc., Englewood Cliffs, N.J., 1963.

[26] M. Giancotti, S. Campagnola, Y. Tsuda, and J. Kawaguchi, *Families of periodic orbits in Hill's problem with solar radiation pressure: application to Hayabusa 2*, Celestial Mech. Dynam. Astronom. **120** (2014), no. 3, 269–286.

[27] W. B. Gordon, *A minimizing property of Keplerian orbits*, Amer. J. Math. **99** (1977), no. 5, 961–971.

[28] M. Handel, *The forcing partial order on the three times punctured disk*, Ergodic Theory Dynam. Systems **17** (1997), no. 3, 593–610.

[29] A. Katok, *Some remarks of Birkhoff and Mather twist map theorems*, Ergodic Theory Dynam. Systems **2** (1982), no. 2, 185–194.

[30] J. Llibre, R. Martínez, and C. Simó, *Tranversality of the invariant manifolds associated to the Lyapunov family of periodic orbits near $L_2$ in the restricted three-body problem*, J. Differential Equations **58** (1985), no. 1, 104–156.

[31] A. J. Maciejewski and M. Przybylska, *Non-integrability of the three-body problem*, Celestial Mech. Dynam. Astronom. **110** (2011), no. 1, 17–30.

[32] R. S. MacKay, J. D. Meiss, and J. Stark, *Converse KAM theory for symplectic twist maps*, Nonlinearity **2** (1989), no. 4, 555–570.

[33] C. Marchal, *How the method of minimization of action avoids singularities*, vol. 83, 2002, Modern celestial mechanics: from theory to applications (Rome, 2001), pp. 325–353.

[34] H. Masur and S. Tabachnikov, *Rational billiards and flat structures*, Handbook of dynamical systems, Vol. 1A, North-Holland, Amsterdam, 2002, pp. 1015–1089.

[35] J. N. Mather, *Existence of quasiperiodic orbits for twist homeomorphisms of the annulus*, Topology **21** (1982), no. 4, 457–467.

[36] ______, *A criterion for the nonexistence of invariant circles*, Inst. Hautes Études Sci. Publ. Math. (1986), no. 63, 153–204.

[37] ______, *Modulus of continuity for Peierls's barrier*, Periodic solutions of Hamiltonian systems and related topics (Il Ciocco, 1986), NATO Adv. Sci. Inst. Ser. C: Math. Phys. Sci., vol. 209, Reidel, Dordrecht, 1987, pp. 177–202.

[38] ______, *Variational construction of connecting orbits*, Ann. Inst. Fourier (Grenoble) **43** (1993), no. 5, 1349–1386.

[39] R. Moeckel, *A variational proof of existence of transit orbits in the restricted three-body problem*, Dyn. Syst. **20** (2005), no. 1, 45–58.

[40] R. Moeckel and R. Montgomery, *Realizing all reduced syzygy sequences in the planar three-body problem*, Nonlinearity **28** (2015), no. 6, 1919–1935.

[41] R. Moeckel, R. Montgomery, and A. Venturelli, *From brake to syzygy*, Arch. Ration. Mech. Anal. **204** (2012), no. 3, 1009–1060.

[42] J. Montaldi and K. Steckles, *Classification of symmetry groups for planar $n$-body choreographies*, Forum Math. Sigma **1** (2013), Paper No. e5, 55.

[43] R. Montgomery, *The $N$-body problem, the braid group, and action-minimizing periodic solutions*, Nonlinearity **11** (1998), no. 2, 363–376.

[44] ______, *Some open questions in the $n$-body problem (zoom talk)*, Sydney Dynamical Group Seminars, 2021.

[45] C. Moore, *Braids in classical dynamics*, Phys. Rev. Lett. **70** (1993), no. 24, 3675–3679.

[46] K. Murasugi, *On Closed* 3*-Braids*, Memoirs of the American Mathematical Society, No. 151, American Mathematical Society, Providence, R.I., 1974.

[47] H. Poincaré, *New Methods of Celestial Mechanics. Vol. 1*, History of Modern Physics and Astronomy, vol. 13, American Institute of Physics, New York, 1993.

[48] P. H. Rabinowitz, *Minimax Methods in Critical Point Theory with Applications to Differential Equations*, CBMS Regional Conference Series in Mathematics, vol. 65, Published for the Conference Board of the Mathematical Sciences, Washington, DC; by the American Mathematical Society, Providence, RI, 1986.

[49] ______, *The calculus of variations and the forced pendulum*, Hamiltonian dynamical systems and applications, NATO Sci. Peace Secur. Ser. B Phys. Biophys., Springer, Dordrecht, 2008, pp. 367–390.

[50] P. H. Rabinowitz and E. W. Stredulinsky, *Extensions of Moser-Bangert Theory*, Progress in Nonlinear Differential Equations and their Applications, vol. 81, Progress in Nonlinear Differential Equations and their Applications, 2011.

[51] M. B. Sevryuk, *Reversible Systems*, Lecture Notes in Mathematics, vol. 1211, Springer-Verlag, Berlin, 1986.

[52] M. Shibayama, *Multiple symmetric periodic solutions to the* $2n$*-body problem with equal masses*, Nonlinearity **19** (2006), no. 10, 2441–2453.

[53] ______, *Variational proof of the existence of the super-eight orbit in the four-body problem*, Arch. Ration. Mech. Anal. **214** (2014), no. 1, 77–98.

[54] ______, *Variational construction of orbits realizing symbolic sequences in the planar Sitnikov problem*, Regul. Chaotic Dyn. **24** (2019), no. 2, 202–211.

[55] C. Simó, *New families of solutions in* $N$*-body problems*, European Congress of Mathematics, Vol. I (Barcelona, 2000), Progr. Math., vol. 201, Birkhäuser, Basel, 2001, pp. 101–115.

[56] V. Szebehely, *Theory of Orbit*, Academic Press, New York, 1967.

[57] S. Tabachnikov, *Geometry and Billiards*, Student Mathematical Library, vol. 30, American Mathematical Society, Providence, RI; Mathematics Advanced Study Semesters, University Park, PA, 2005.

[58] K. Tanaka, *A prescribed-energy problem for a conservative singular Hamiltonian system*, Arch. Rational Mech. Anal. **128** (1994), no. 2, 127–164.

[59] W. P. Thurston, *On the geometry and dynamics of diffeomorphisms of surfaces*, Bull. Amer. Math. Soc. (N.S.) **19** (1988), no. 2, 417–431.

[60] L. Tonelli, *The calculus of variations*, Bull. Amer. Math. Soc. **31** (1925), no. 3-4, 163–172.

[61] A. Tsygvintsev, *The meromorphic non-integrability of the three-body problem*, J. Reine Angew. Math. **537** (2001), 127–149.

[62] H. Urakawa, *Calculus of Variations and Harmonic Maps*, Translations of Mathematical Monographs, vol. 132, American Mathematical Society, Providence, RI, 1993.

[63] Z. Xia, *Arnold diffusion: a variational construction*, Proceedings of the International Congress of Mathematicians, Vol. II (Berlin, 1998), no. Extra Vol. II, 1998, pp. 867–877.

[64] G. Yu, *Periodic solutions of the planar* $N$*-center problem with topological constraints*, Discrete Contin. Dyn. Syst. **36** (2016), no. 9, 5131–5162.

[65] ______, *Simple choreographies of the planar Newtonian* $N$*-body problem*, Arch. Ration. Mech. Anal. **225** (2017), no. 2, 901–935.

[66] ______, *Chaotic dynamics of monotone twist maps*, Acta Math. Sin. (Engl. Ser.) **38** (2022), 179–204.

# List of the author's papers related to this thesis

Chapter 2 consists of

- Y. Kajihara, *Variational structures for infinite transition orbits of twist maps*, submitted.

Chapter 3 consists of

- Y. Kajihara and M. Shibayama, *Variational existence proof for multiple periodic orbits in the planar circular restricted three-body problem*, Nonlinearity **35** (2022), no. 3, 1431–1446.

Chapter 4 consists of

- S. Iguchi, Y. Kajihara, and M. Shibayama, *Variational proof of the existence of periodic orbits in the spatial Hill problem and its constrained problems*, Jpn. J. Ind. Appl. Math., to appear.
- Y. Kajihara and M. Shibayama, *Variational proof of the existence of brake orbits in the planar 2-center problem*, Discrete Contin. Dyn. Syst. **39** (2019), no. 10, 5785–5797.

Chapter 5 consists of

- Y. Kajihara, E. Kin, and M. Shibayama, *Braids, metallic ratios and periodic solutions of the* $2n$*-body problem*, submitted.